

Copyright

by

Alyssa Jane Offutt

2014

**The Thesis Committee for Alyssa Jane Offutt
Certifies that this is the approved version of the following thesis:**

**The interaction of benthic oligochaetes, *T. tubifex*, with mercury
impacted sediments: An assessment of bioaccumulation and
biogeochemistry**

**APPROVED BY
SUPERVISING COMMITTEE:**

Supervisor:

Danny D. Reible

Lynn E. Katz

**The interaction of benthic oligochaetes, *T. tubifex*, with mercury
impacted sediments: An assessment of bioaccumulation and
biogeochemistry**

by

Alyssa Jane Offutt, B.S.C.E.

Thesis

Presented to the Faculty of the Graduate School of

The University of Texas at Austin

in Partial Fulfillment

of the Requirements

for the Degree of

Master of Science in Engineering

The University of Texas at Austin

May, 2014

Acknowledgements

I would like to thank my advisor Dr. Danny Reible for his help and for introducing me to the world of sediments; Dr. Lynn Katz for her support and guidance throughout my graduate school career; and the Reible Research Group, especially James Grundy and Ariette Schierz for patiently teaching me how to be scientist as well as an engineer. I would also like to thank my parents for their constant support and for enabling me to pursue my curiosity, my sister for challenging me and teaching me, and my friends from the EWRE department who provided a constant source of humor.

Abstract

The interaction of benthic oligochaetes, *T. tubifex*, with mercury impacted sediments: An assessment of bioaccumulation and biogeochemistry

Alyssa Jane Offutt, M.S.E.

The University of Texas at Austin, 2014

Supervisor: Danny D. Reible

Mercury is a pervasive environmental contaminant which is globally distributed in freshwater ecosystems. In order to assess the risk that mercury and methylmercury pose to public health through consumption and trophic level transfer, it is first necessary to understand the interactions and uptake that occurs between benthic organisms and mercury impacted sediments. Delineation of these interactions currently rely on correlating measurements of bulk sediment concentrations with bioaccumulation of either total mercury or methylmercury. However, it has been proposed that porewater concentrations, rather than sediment concentrations, should be used to predict uptake and bioavailability. Diffusive gradient in thin films (DGTs) have been proposed as a viable technique for porewater measurements to assess the bioavailable fractions of mercury. DGTs were compared to traditional bulk solid sampling to assess their capabilities for the prediction of total and methylmercury bioaccumulation in benthic oligochaetes, *T.*

tubifex. DGTs performed similarly to the bulk solids sampling approach in respect to their correlation with mercury bioaccumulation in the sediment matrix studied. Bioturbation was shown to impact microbial activity and redox profiles in the sediment which led to a decrease in porewater methylmercury concentrations in the uppermost surficial sediment depths. These results indicate that monitoring tools such as DGTs are necessary to better understand the fate of mercury at field scale contaminated sites.

Table of Contents

LIST OF TABLES	ix
LIST OF FIGURES	x
CHAPTER 1: INTRODUCTION	1
1.1 Justification of Research	1
1.2 Overview of Experimental Approach	3
1.3 Structure of Thesis	4
CHAPTER 2: LITERATURE REVIEW	5
2.1 Mercury in the Environment.....	5
2.1.1 Mercury sources.....	5
2.1.2 Cycling in Aqueous Environments	6
2.2 Bioavailability of Mercury for Microbial Methylation.....	7
2.3 Bioaccumulation in Macroorganisms	12
2.4 Traditional Sampling Mechanisms	17
2.5 Diffusive Gradient in Thin Films.....	19
2.6 Bioturbation	25
CHAPTER 3: EXPERIMENTAL APPROACH AND METHODS	29
3.1 Experimental Set-up.....	29
3.1.1 Sediment Source	29
3.1.2 Test Organism.....	30
3.1.3 Experimental Conditions	31
3.1.4 Established Mesocosms	33
3.2 Experimental Timeline.....	35
3.3 Sampling Employed.....	36
3.3.1 Bulk Sediment Coring.....	37
3.3.1.1 <i>Sediment Core Sampling</i>	37
3.3.1.2 <i>Sediment Core Analysis</i>	39
3.3.2 Diffusive Gradient in Thin Films.....	43
3.3.3 Voltammetry	45

3.3.4 <i>T. tubifex</i> Sampling and Processing	47
3.3.5 Overlying Water Dissolved Organic Carbon	49
3.4 Assessment of Results.....	49
CHAPTER 4: RESULTS AND ANALYSIS	52
4.1 Sediment Depositional Characteristics	52
4.2 Bioaccumulation Correlation	59
4.2.1 Overall Bioaccumulation	60
4.2.2 Correlation Across Depositional Environments	62
4.2.2.1 <i>Total Mercury Bioaccumulation</i>	63
4.2.2.2 <i>Methylmercury Bioaccumulation</i>	65
4.2.3.3 <i>The Role of Organic Matter in Bioaccumulation</i>	68
4.2.2.4 <i>Summary</i>	71
4.2.3 Correlation at the Depositional Level	74
4.2.3.1 <i>Total Mercury Bioaccumulation</i>	74
4.2.3.2 <i>Methylmercury Bioaccumulation</i>	77
4.2.3.3 <i>Summary</i>	82
4.3 Bioturbation	84
4.3.1 Zone of Oxygen Depletion.....	84
4.3.2 Impact on Metal Biogeochemistry.....	89
4.3.3 Impact on Porewater Methylmercury	97
CHAPTER 5: CONCLUSIONS.....	100
5.1 Conclusions.....	100
5.2 Recommendations for Future Work.....	102
APPENDIX.....	104
Appendix A.....	104
REFERENCES.....	105

List of Tables

Table 3.1: Mesocosms employed to study oligochaete interaction including date of construction, organism introduction, and destructive breakdown.	35
Table 4.1: Summary of relative total mercury and methylmercury concentrations in bulk solids and porewater in all three depositional environments.....	53
Table 4.2: Average total organic carbon (TOC) concentrations for all three depositional environments	56
Table 4.3: Lipid concentrations of a representative sample from each depositional environment and the <i>T. tubifex</i> culture	59
Table 4.4: The coefficients of determination for correlations of total mercury and methylmercury correlations across depositional environments, highlighted values represent negative correlations	73
Table 4.5: Coefficients of determination for correlation at the depositional level, with highlighted negative correlations.....	83

List of Figures

Figure 2.1: Piston structure of DGTs, used for slurry and overlying water sampling (Chess, 2010)	20
Figure 2.2: Profiler structure for DGTs, used for sampling throughout sediment depth (Chess, 2010)	20
Figure 2.3: Conceptual mercury concentration throughout the DGT layers (Zhang & Davison, 1995).....	22
Figure 2.4: Calibration of DGTs within sediment of the South River, VA (Chess, 2010)	24
Figure 2.5: Vertically stratified redox profile characteristic of freshwater sediments (Gao, Davis, & Tanji, 2003)	27
Figure 3.1: Conceptual model of mercury flux at relative river mile 3.5 of the South River, VA (South River Science Team, 2014a).....	30
Figure 3.2: Structure of flow-through mesocosms, “T-cells”, with approximately 8 cm sediment depth and 1.25 cm depth of overlying water (Johnson, 2009)	32
Figure 3.3: Bulk sediment coring employed in all mesocosms	38
Figure 3.4: Example calibration for CVAFS measured total mercury	40
Figure 3.5: Example calibration for CVAFS measured methylmercury	41
Figure 3.6: Example calibration curve for measurement of AVS	42
Figure 3.7: Example calibration curve for oxalate extracted ferrous iron	42
Figure 4.1: Relative concentrations of total mercury and methylmercury in bulk solids (mg/kg) and porewater (ng/L) in all three depositional environments.....	53

Figure 4.2: Fraction of methylmercury in bulk solids and porewater for all three depositional environments	56
Figure 4.3: Average acid volatile sulfides concentrations at each depth per depositional environment.....	57
Figure 4.4: Average ferrous iron concentrations at each depth per depositional environment	58
Figure 4.5: Relative total mercury and methylmercury concentrations in bulk solids and <i>T. tubifex</i>	61
Figure 4.6: Fraction of methylmercury in bulk solids, porewater, and <i>T. tubifex</i>	62
Figure 4.7: Total mercury bioaccumulation in <i>T. tubifex</i> with total mercury in porewater across mesocosms	64
Figure 4.8: Total mercury bioaccumulation in <i>T. tubifex</i> with total mercury in bulk solids across mesocosms.....	64
Figure 4.9: Methylmercury bioaccumulation in <i>T. tubifex</i> with methylmercury in porewater across mesocosms	66
Figure 4.10: Methylmercury bioaccumulation in <i>T. tubifex</i> with methylmercury in bulk solids across mesocosms.....	67
Figure 4.11: Methylmercury bioaccumulation in <i>T. tubifex</i> with total mercury in porewater across mesocosms	67
Figure 4.12: Methylmercury bioaccumulation in <i>T. tubifex</i> with total mercury in bulk solids across mesocosms.....	68
Figure 4.13: Total mercury bioaccumulation in <i>T. tubifex</i> with total mercury in bulk solids normalized to organic carbon across mesocosms.....	70
Figure 4.14: Methylmercury bioaccumulation in <i>T. tubifex</i> with methylmercury in bulk solids normalized to organic carbon across mesocosms.....	70

Figure 4.15: Methylmercury bioaccumulation in <i>T. tubifex</i> with total mercury in bulk solids normalized to organic carbon across mesocosms.....	71
Figure 4.16: Total mercury bioaccumulation in <i>T. tubifex</i> with bulk solids and porewater in the mid-channel deposit	75
Figure 4.17: Total mercury bioaccumulation in <i>T. tubifex</i> with bulk solids and porewater in the near-bank deposit	76
Figure 4.18: Total mercury bioaccumulation in <i>T. tubifex</i> with bulk solids and porewater in the bank deposit	77
Figure 4.19: Methylmercury bioaccumulation in <i>T. tubifex</i> with total mercury and methylmercury in bulk solids and porewater within the mid-channel deposit	78
Figure 4.20: Methylmercury bioaccumulation in <i>T. tubifex</i> with total mercury and methylmercury in bulk solids and porewater within the near-bank deposit	80
Figure 4.21: Methylmercury bioaccumulation in <i>T. tubifex</i> with total mercury and methylmercury in bulk solids and porewater within the bank deposit	81
Figure 4.22: Oxygen depletion in Mid-Channel Control 1 and Sample 1 at approximate Day 0 of organism introduction and approximate Day 28 of bioturbation.....	85
Figure 4.23: Oxygen depletion in Near-Bank Control 1 and Sample 1 and Sample 2 at approximate Day 0 of organism introduction and approximate Day 28 of bioturbation.....	87
Figure 4.24: Oxygen depletion in Bank Control 1 and Sample 1 at approximate Day 0 of organism introduction and approximate Day 28 of bioturbation	88

Figure 4.25: Averaged AVS concentrations per depth for comparison of control and bioturbated samples per depositional environment.....	90
Figure 4.26: Averaged ferrous iron concentrations per depth for comparison of control and bioturbated samples per depositional environment	91
Figure 4.27: Reducing profile of dissolved metals for Bank Sample 1 at approximated Day 0 of organism introduction and approximated Day 28 of bioturbation.....	93
Figure 4.28: Reducing profile of dissolved metals for Near-Bank Sample 1 at approximated Day 0 of organism introduction and approximated Day 28 of bioturbation.....	94
Figure 4.29: Reducing profile of dissolved metals for Near-Bank Sample 2 at approximated Day 0 of organism introduction and approximated Day 28 of bioturbation.....	95
Figure 4.30: Reducing profile of dissolved metals for Mid-Channel Sample 1 at approximated Day 0 of organism introduction and approximated Day 28 of bioturbation.....	96
Figure 4.31: Average methylmercury concentrations in porewater at each depth for bioturbated samples and controls.....	98

Chapter 1: Introduction

1.1 JUSTIFICATION OF RESEARCH

Mercury is a globally distributed, persistent environmental contaminant that has adverse impacts on all trophic levels. Anthropogenic and natural releases of mercury enter aquatic environments where the heavy metal is speciated into inorganic and organic forms capable of bioaccumulation. Of particular risk, is the organic form, methylmercury (MeHg), which is typically formed under reducing conditions in the underlying sediments. Methylmercury is a neurotoxin capable of passing through the blood-brain and placental barriers to cause neurologic damage as well as a variety of other serious health effects (Chemaly, 2002; Salonen et al., 1995). Due to its lipid solubility, methylmercury biomagnifies readily through trophic level transport, and this biomagnification has significant ramifications for public health (Chen et al., 2009; Morel, Kraepiel, Amyot, & Morel, 1998; Carl J Watras & Bloom, 1992). In order to minimize the risk of methylmercury exposure through human consumption of food, the FDA has set an action level of 1 ppm methylmercury in fish tissue and the EPA provides fish consumption advisories to limit mercury exposure (United States Food and Drug Administration, 2000).

A fundamental understanding of biotic uptake of mercury can be gleaned by evaluating the bioaccumulation that occurs at the initial trophic level (i.e., benthic organisms) within the sediment matrix. Traditional sampling methods to predict

bioaccumulation have relied on analysis of bulk solid total mercury (TotHg). However, bulk solids are not always good predictors of bioaccumulation due to strong binding mercury complexes in sediments which may decrease the availability of mercury for microbial methylation and biologic uptake (Lawrence & Mason, 2001). The measurement of dissolved mercury in interstitial porewater; however, may serve as a better indicator of the readily bioavailable and mobile fractions of mercury (Hsu-Kim, Kucharzyk, Zhang, & Deshusses, 2013; Zhang & Davison, 1995).

One technique for measuring available mercury in interstitial porewater is via diffusive gradient in thin films (DGTs). DGTs passively sample dissolved mercury in interstitial porewater in situ (Zhang & Davison, 1995). There are multiple benefits of this of passive sampling technique including lower detection limits and minimization of processing artifacts in ex-situ samples (Peijnenburg et al., 2014). This research is focused on evaluating the DGT passive sampling technique in order to assess bioaccumulation and risk associated with sediment matrices. However, to verify its potential, the performance of DGTs relative to traditional sampling methods must be assessed. Therefore, the objective of the first phase of this research is to compare the use of DGT passive samplers with bulk solid sampling for their ability to predict bioaccumulation of total mercury and methylmercury in benthic organisms.

While developing a more robust sampling technique was one of the primary objectives of this work, a second objective was to consider the impact of organisms on sediment biogeochemistry and mercury availability. Bioturbation, the perturbation and

mixing of sediments due to the activity of macroorganisms, can have profound effects on the reactions, redox profiles, and the diffusive fluxes of nutrients, contaminants, and byproducts in sediment columns (Binnerup, Jensen, Revsbech, Jensen, & Sørensen, 1992; Kristensen & Holmer, 2001; Navel, Mermillod-Blondin, Montuelle, Chauvet, & Marmonier, 2012). Very little work has been completed to evaluate the impact that macroorganism-induced mixing has on mercury fate and transport. The objective of this phase of the project was therefore to investigate the impact of oligochaetes (benthic worms) on mercury speciation and availability.

1.2 OVERVIEW OF EXPERIMENTAL APPROACH

In order to evaluate the objectives, benthic oligochaetes were subject to controlled exposures of mercury in laboratory mesocosms. Oligochaetes were chosen because they have intense interactions with surficial sediments (as deposit feeders) and can be found in high densities in contaminated sediment sites. Three sediment depositional environments were utilized and allowed to equilibrate prior to the addition of the oligochaetes. The oligochaetes were then introduced and subject to a 28-day bioaccumulation test in mesocosms. The redox profiles and mercury concentrations in the overlying water were monitored throughout the duration of the equilibration period and the bioaccumulation test. The remaining sampling techniques including depth-profiled bulk solids, depth-profiled porewater, biogeochemical, and organism bioaccumulation analyses were completed in the destructive sampling at the end of each mesocosm experiment.

1.3 STRUCTURE OF THESIS

The background on mercury cycling and speciation in the environment, the impact of biogeochemical factors on mercury speciation and availability, and the governing factors for mercury bioaccumulation in macroorganisms will be provided in Chapter 2, *Literature Review*. This section will also provide sufficient background and theory on the two major sampling techniques employed as well as the state of knowledge on the impact of bioturbation. This will be followed by Chapter 3, *Experimental Approach and Methods*, which will discuss the sampling techniques and materials used. Chapter 4, *Results and Analysis* will illustrate the relevant findings of the research and Chapter 5, *Conclusion*, will provide a synopsis of the ideas generated and recommendations for future work.

Chapter 2: Literature Review

2.1 MERCURY IN THE ENVIRONMENT

2.1.1 Mercury sources

Mercury is a widespread environmental contaminant that is emitted by anthropogenic and natural sources. Once volatile elemental mercury is released into the atmosphere, it is oxidized within the time scale of a year and is globally distributed in terrestrial and aquatic ecosystems due to wet deposition (Morel et al., 1998). It is estimated that 7,527 Mg of mercury are emitted annually (Pirrone et al., 2010). Of this, 5,207 Mg of mercury can be attributed to emission from natural sources and 2,320 Mg of can be attributed to anthropogenic sources (Pirrone et al., 2010). Natural mercury emissions span from volcanic activity, biomass burning, and degassing of mercury in saline and fresh water bodies (Morel et al., 1998). Anthropogenic emissions include fossil-fuel power plants, which provide the largest contribution to anthropogenic mercury emissions, in addition to metal production, mining, and waste handling (Pirrone et al., 2010). Once emitted, approximately 40% of atmospheric mercury is deposited into water bodies (Morel et al., 1998). Combined with terrestrial runoff and industrial and municipal point sources, the mercury load accumulates in aquatic environments where it has the potential to speciate and bioaccumulate, creating a line of contamination and public health risk.

2.1.2 Cycling in Aqueous Environments

Once present in aquatic ecosystems, mercury cycles through different speciation. Mercury is predominantly present in water in its inorganic ionic form, Hg(II) because oxidation and photoreduction decrease concentrations of the elemental mercury which is supersaturated relative to the air (Morel et al., 1998). This ion is then capable of complexing throughout the water column and sediment. Within the oxic freshwater column, mercury is most likely to be complexed with hydroxides and organic matter; however, in anoxic regions, including sediment, there is a broader potential for complexation particularly with sulfides and reactions forming the potent toxin, methylmercury (Morel et al., 1998).

Sediments often serve as sink for mercury within water bodies showing higher concentrations of ionic mercury accumulating near and within the sediment. Within the sediment matrix, ionic mercury will form thermodynamically favorable complexes with sulfides, iron, hydroxide, and organic matter (Morel et al., 1998). Complexes with sulfide and bisulfide will dominate in the sediment anoxic zones (Morel et al., 1998). Different complexation will impact the phase of the mercury by sorbing the mercury into the solid phase, or maintaining its dissolved nature in sediment interstitial porewater. Mercury sorbed onto the solid phase is thought to be relatively inert from a toxicological perspective; however, mercury within interstitial porewater is mobile and can be bioavailable to microbes for methylation (Hsu-Kim et al., 2013). Methylmercury, as previously discussed, is a highly bioaccumulative form of mercury linked to serious

health impacts (United Nations Environmental Programme, 2002). Its formation occurs in anaerobic and anoxic sediments through the microbial uptake of dissolved inorganic mercury and subsequent methylation, which will be discussed in depth in *Section 2.2*. The methylated mercury produced includes forms of monomethylmercury (MMHg), dimethylmercury (Me₂Hg), and ethylmercury (EtHg) (Morel et al., 1998). These organic species then complex and sorb to sediments or remain dissolved in porewater where they can diffuse into the overlying water column. The risks and potential for bioaccumulation associated with methylmercury highlight the necessity of understanding its formation in sediment matrices, and its fate in solids, porewater, and biota.

2.2 BIOAVAILABILITY OF MERCURY FOR MICROBIAL METHYLATION

The bioavailability of mercury to all trophic levels is dependent on mercury speciation and complexation. Although all forms of mercury can have adverse health effects upon exposure, when assessing risk, methylmercury is the predominant species of concern due to both its health implications and its capacity to bioaccumulate. Because of this relevance, it is necessary to understand the factors which govern methylmercury formation and rate. Mercury methylation is a microbially mediated process, and thus within this section, the factors which influence bioavailability of mercury to these microbes will be assessed.

In order to understand mercury bioavailability, it is necessary to first understand the mechanism of methylation. It is proposed that microbes in sediment methylate

mercury by utilizing a portion of the acetyl-CoA pathway (Choi, Chase, & Bartha, 1994; Parks et al., 2013). Therefore, microbes which methylate mercury must possess the acetyl-CoA biosynthetic pathway, although they may not rely solely on this process for microbial metabolism (Ekstrom, Morel, & Benoit, 2003). Traditionally, mercury methylation was attributed to sulfate-reducing and iron-reducing bacteria of the class *Deltaproteobacteria* (Choi et al., 1994; Ekstrom et al., 2003). However, recently, two genes, DND132_1056 and DND132_1057, and their inferred orthologs have been used to identify multiple phyla including methanogenic *Archea* and fermentative *Clostridia* of *Firmicutes*, which are capable of methylation (Gilmour et al., 2013; Parks et al., 2013). The identification of these species expands the environments and conditions in which mercury methylation can occur. While there is a broader diversity of known methylators, it should be noted that sulfate-reducing and iron-reducing bacteria maintain the highest methylation rates and tend to dominate systems in which they are present (Gilmour et al., 2013). For this reason, the factors influencing bioavailability for methylation will be considered mainly with respect to impact on these microbial guilds.

In order to methylate mercury, microbes uptake neutral mercury species which are often complexed with sulfur and hydrogen sulfides (Hsu-Kim et al., 2013; Jay et al., 2002). The mechanism of uptake is currently under debate. It has been argued that uptake is driven by either passive diffusion or active transport (Hsu-Kim et al., 2013; Schaefer et al., 2011). However, independent of the mode of uptake, conceptually, either mechanism is size exclusive. For mercury species to diffuse freely through the cell membrane or pass

through transport proteins, it is likely that these species must be dissolved or nanoparticulate (Hsu-Kim et al., 2013). These mercury forms can be found along with colloidal mercury in sediment interstitial porewater. Therefore, it is probable that the concentration of porewater neutral mercury species govern the capacity of mercury to be methylated (Hsu-Kim et al., 2013). This is especially relevant when considering the reactivity of mercury sulfide nanoparticles which likely increase uptake due to their surface area to volume ratios (Hsu-Kim et al., 2013).

As suspension or dissolution of mercury in porewater is a significant factor in availability of mercury for microbial uptake, the geochemical factors which impact this must be assessed. In aquatic systems, ionic mercury forms thermodynamically favorable complexes with sulfides, chlorides, iron, organic matter, and oxides (Morel et al., 1998). Several of these complexes bind mercury into the solid phase. In anoxic freshwater systems, ionic mercury sulfide complexes generally dominate, and thus the concentration and speciation of sulfur will influence methylation (Morel et al., 1998; Patton & Crecelius, 2001). When oxidized as sulfate, sulfur generally increases mercury methylation (Kampalath, Lin, & Jay, 2013). This is attributed to the metabolism of sulfate-reducing bacteria because metabolism and thus methylation will be boosted by the high concentrations of the required terminal electron acceptor, sulfate. However, the presence of sulfides also acts to inhibit methylation by complexation which binds the mercury into non-available solids or charged species (Kampalath et al., 2013). Iron, which is less dominant in most freshwater systems, can similarly impact methylation. The

capacity of ferrous iron to complex with mercury sulfides and mercury oxides is high which implies that it has the potential to sequester available mercury (Phillips & Lovely, 1987). In order to assess the potential for solutes present to complex and inhibit methylation, acid volatile sulfides (AVS) and oxalate extractable ferrous iron can be extracted from bulk sediment. These measures also demonstrate reduction occurring in sediment matrices. Acid volatile sulfides measure the sulfides capable of complexation which includes complexes with predominantly iron and manganese (De Jonge, Dreesen, De Paepe, Blust, & Bervoets, 2009). Conversely, oxalate extractable ferrous iron measures the iron present for complexation. Due to the dominance of sulfides in natural systems, acid volatile sulfides are often normalized to mercury concentrations to determine bioavailability. However, because mercury complexes with additional solutes including iron and organic matter, this requires that all aspects of geochemistry be assessed when determining availability (Peijnenburg et al., 2014).

As mentioned, total organic matter is an important biogeochemical factor in mercury availability. In general, higher concentrations of organic matter create more productive microbial activity, and in that, greater reducing conditions. This allows for guilds to more quickly establish within a sediment matrix and causes more rapid metabolism without hindering methylation (Hsu-Kim et al., 2013; Schartup, Mason, Balcom, Hollweg, & Chen, 2013). However, mercury species also have a high affinity for organic carbon which may complex and decrease bioavailability (Hsu-Kim et al., 2013). This can be linked to the size exclusion of microbial uptake as complexes with organic

matter create larger dissolved particles in addition to the precipitation of mercury sulfides (Hsu-Kim et al., 2013). Therefore, it can be determined that organic carbon can be a relevant factor in methylation and availability but is dependent on the specific matrix.

The establishment of reducing conditions is equally relevant in mercury methylation. As based on the microbial communities capable of methylation, reducing conditions must be established for these anaerobes to metabolize. This requires that the redox profile be established with zones favorable for iron and sulfate reducing bacteria (Johnson, 2009). Oxygen diffusion within the sediment does not only influence microbial survival, but also allows for oxidative demethylation of mercury (Bystrom, 2008). The impact of oxygen diffusion on methylation will be further addressed in the *Section 2.6*.

Finally, ambient sediment pH and temperature may also impact methylation of mercury and its availability. Although the breadth of microbes capable of methylation has expanded the range of environments capable of supporting methylation, pH and temperature still impact the availability of mercury species for methylation. First, pH is relevant due to its impact on complexation. At lower pH values, acidic conditions allow for greater mercury mobility and availability by releasing mercury complexes (Rosenberg, Nilsson, & Diaz, 2001). However, this pH must also remain within a range which is viable for methylating organisms; for example, sulfate-reducing bacteria are most productive in the of pH between 4-9.5 (Bystrom, 2008). Temperature, on the other hand, has direct impact on microbial productivity. In freshwater, low temperatures inhibit microbial activity and methylation, whereas at an optimum temperature 35°C, microbes

are highly productive methylators (Winfrey & Rudd, 2009). As based on temperature, methylation rates are highest in later summer and declines throughout the fall.

It can be determined that geochemical factors including solutes for complexation and reducing conditions as well as ambient pH and temperature can strongly impact mercury availability for methylation. Due to the relevance of these factors on mercury methylation, they will be evaluated within the context of this experiment. Mercury speciation and complexation in both sediment and porewater can also impact bioaccumulation of benthic organisms, and thus this bioavailability will be further assessed for macroorganisms.

2.3 BIOACCUMULATION IN MACROORGANISMS

In order to evaluate the role of contaminated sediment on mercury risk and transport of both inorganic and organic mercury, bioaccumulation in macroorganisms must be understood. This includes both concepts of food web transfers and bioaccumulation of benthic organisms due to sediment exposure.

The cycling of mercury within aquatic food webs is relatively well studied albeit not fully understood. Through consideration of pelagic and benthic food webs in freshwater and saline systems, several concepts appear to be ubiquitous. First, it is shown that while multiple forms of mercury can be present in organisms, it is methylmercury which has a large capacity to bioaccumulate and biomagnify between trophic levels. This can be seen when considering the ratio of methylmercury concentration to total mercury

concentration, or the percent of speciated methylmercury. In several studies, it is noted that as trophic levels increase, so does the percent methylmercury (Chen et al., 2009; Morel et al., 1998; Carl J Watras & Bloom, 1992). In two freshwater lakes, percent methylmercury was seen to increase from 13% in the lowest trophic level, phytoplankton, to 29% in the next trophic level, zooplankton, before reaching greater than 90% methylmercury in fish (Carl J Watras & Bloom, 1992). Similarly, a second study demonstrated that percentage of methylmercury increased by approximately an order of magnitude from algae to periphyton to macroinvertebrates (Žižek, Horvat, Gibičar, Fajon, & Toman, 2007). These trends demonstrate that trophic level governs relative methylmercury to total mercury concentrations with the lowest trophic levels dictating mercury availability for higher organisms (C. J. Watras et al., 1998). However, it should be noted that while the increase in percent methylmercury is relatively consistent, this does not necessarily mean that the overall methylmercury concentration increases as inorganic mercury often decreases in higher trophic levels (Chen et al., 2009; R. P. Mason, Laporte, & Andres, 2000).

It is proposed that methylmercury is more likely to bioaccumulate and magnify because it is more reactive than elemental and dimethylmercury, and thus has a greater capacity to be retained (Bystrom, 2008; Morel et al., 1998). In addition, due to the lipid solubility of methylmercury, it is capable of passing the blood-brain and placental barriers allowing for further reaction and accumulation (Chemaly, 2002). It is suspected that methylmercury mainly accumulates within tissues and also binds to protein-

sulfhydryl groups (R. P. Mason et al., 2000; United Nations Environmental Programme, 2002). It has been demonstrated that within certain species, the organs of greatest accumulation are the gut, liver, and head respectively (Dallinger, Prosi, Segner, & Back, 1987). Due to the reactivity of the species and its location of bioaccumulation, methylmercury has a long half-life within organisms and is absorbed into the body six times more easily than inorganic mercury (Environment Canada, 2013; United Nations Environmental Programme, 2002). This further provides a basis of mercury bioaccumulation and biomagnification between trophic levels.

Because mercury accumulation in higher trophic levels is governed by the lower trophic levels, it is important to understand the route of exposure to these initial organisms and understand the proxy ways to measure uptake. The relevant form of mercury exposure and lability are innately linked to the mechanism by which the organism encounters it within the environment. For benthic invertebrates, this exposure can be from sediment, porewater, the overlying water column, the benthic boundary layer, and burrow water as governed by consumption or dermal contact (Bouché, Habets, Biagianti-Risbourg, & Vernet, 2000; Parkerton et al., 2012). However, it can be noted that the route of exposure does not directly correlate with uptake. This was seen in Lawrence et. al (2001) which demonstrated that amphipod bioaccumulation and bulk sediment concentrations have a low correlation, with an R^2 of 0.12, and that sediment derived total mercury and methylmercury are insufficient to determine uptake (Lawrence & Mason, 2001). Other studies have evaluated rate of uptake in regards to various

exposures and have seen that in certain fish, rate of uptake from water is greater than that from sediment; however sediment contributes more to the total bioaccumulation (Dallinger et al., 1987). For this reason, while the route of exposure will determine factors in available mercury, it may not correlate to uptake, and other mechanisms will be required to measure the uptake occurring.

Depending on the predominant exposure route, various factors will influence availability. For instance, if porewater governed uptake, the presence and lability of mercury would be determined by complexation with sulfides, iron, and organic matter. Therefore the same factors which influence methylation potential will govern availability. However, biogeochemical factors can also influence bioaccumulation independent of the exposure. Low concentrations of organic matter generally correlate with higher bioaccumulation and vice versa (Chen et al., 2009; Lawrence & Mason, 2001; C. J. Watras et al., 1998). There are several potential reasons for this correlation. First, the organic matter present may complex with mercury and decrease bioavailability. However, complexes with inorganic mercury have supported bioaccumulation thus this is likely not the governing factor (Guthrie, Davis, Cherry, & Murray, 1979). Second, it is possible that greater organic matter leads to greater reducing conditions which produce sulfides that complex mercury (Chen et al., 2009). Yet, it has been seen that acid volatile sulfides do not impact bioaccumulation in benthic invertebrates as organisms still bioaccumulate metals in the presence of high concentrations of complexed sulfides (De Jonge et al., 2009). Lastly, the most significant impact that organic matter has is likely

linked to consumption by the organism itself. It has been observed that organic matter negatively correlates with ingestion rate and body size for deposit feeders and denitrivores (Cammen, 1980). This is likely due to the diminished need for organisms to process large volumes sediment because sufficient organic matter is present, and is supported by the observations that dissolved organic matter governs bioavailability at lower trophic levels (C. J. Watras et al., 1998).

The test organism used in this study, *Tubifex tubifex*, is a sub-surface deposit feeder and thus experiences all of the previously mentioned routes of exposure (Bouché et al., 2000). Therefore, it is possible that either bulk solids or porewater govern bioaccumulation, as slightly acidic gut conditions will cause solid mercury to be more labile, but the organism also has sufficient dermal contact with porewater. When considering bioaccumulation of other metals in the *T. tubifex* species, it can be seen that a maximum of 9% of Cd and 52% of Zn bioaccumulation is derived from sediments, with dissolved metals in porewater contributing to the remaining portion of exposure (Redeker, Bervoets, & Blust, 2004). While this value varies between metals, it is likely that porewater will also be a relevant factor in *T. tubifex* uptake of mercury, which will be assessed within this research. It is also possible that porewater will be capable of predicting any uptake from solids.

A 28-day test with *T. tubifex* was chosen because high bioaccumulation can be completed within this span of time. *T. tubifex* have a high tolerance for metals and thus will not reach lethal endpoints in the sediment conditions (Vidal & Horne, 2003). In fact,

T. tubifex are capable of developing a tolerance to mercury which persists for three generations after exposure (Vidal & Horne, 2003). An additional benefit of using *T. tubifex*, is that studies have shown that this organism bioaccumulates quickly. For cadmium, bioaccumulation begins to occur as early as 96 hours into exposure (Bouché et al., 2000). In addition, in copper sub-lethal toxicity testing, it was shown that 28-day tests achieve similar survival rates as 6 month testing (Pasteris, Vecchi, Reynoldson, & Bonomi, 2003). Finally, in other benthic species, bioaccumulation of mercury is seen to equilibrate around 20-28 days (Amirbahman et al., 2013). Therefore, it is reasoned that a 28-day bioaccumulation test is sufficient to study *T. tubifex*, as bioaccumulation should reach equilibrium with either porewater or bulk sediment concentration within this time frame and this duration aligns with standards of bioaccumulation tests (American Society for Testing and Materials International, 2010).

2.4 TRADITIONAL SAMPLING MECHANISMS

Two different media can be sampled in order to determine mercury concentrations in sediment systems. These include bulk sediment sampling and sampling of interstitial porewater. Within these both techniques, total mercury is determined as the lump sum of mercury species, and methylmercury is measured in order to determine the fraction of mercury which is most bioavailable. Both bulk soil sampling and porewater sampling assess different properties of the mercury impacted matrix and have various benefits. Bulk solids sampling generally involves the removal of cores which allows for analysis of cumulative total mercury and methylmercury from the mercurial solids phases and

porewater phase. Bulk solids sampling is commonly used due to several benefits. Primarily, bulk solids are simple to sample. As concentrations are higher in the solid phase, detection limits can be higher and therefore sample contamination is less of a concern, and samples can be tested with commonly used instrumentation. Additional benefits occur through the sampling of cores, as this provides the possibility to complete further geochemical analysis on the sediment sample. However, while bulk solid concentrations are accepted as a monitoring technique and are widely used, they may not be the most applicable when assessing bioavailability due to the biogeochemical influences discussed in *Section 2.2*. Therefore, it can be more beneficial to assess the available mercury within porewater.

Sampling of interstitial porewater can be either active or passive. Active sampling includes the use of centrifugation, sediment filtration, whole core squeezing, and displacement, whereas passive sampling includes porewater peepers, Teflon sheets, diffusive gradient in thin film samplers, and diffusion equilibration in thin films (R. Mason et al., 1998; Peijnenburg et al., 2014). The use of active sampling presents several challenges including insufficient sample volume and difficult sampling techniques which allow for a large range of error (R. Mason et al., 1998). In addition, the disruption of sediment which occurs with active sampling can allow for compaction and loss of porewater which would not produce representative results (R. Mason et al., 1998). Due to the challenges associated with active sampling, passive sampling is becoming the preferred method of measuring concentrations in porewater (Peijnenburg et al., 2014).

Passive sampling techniques are able to determine representative concentrations in porewater *in situ* without disturbing the sediment column. For many of the sampling techniques, the length of deployment allows samplers to achieve lower detection limits and minimize any temporal variability through time averaging (Peijnenburg et al., 2014). Within these samplers, several are capable of selective binding in order to better assess mercury speciation. When selective binding is preferred, it is beneficial to use diffusive equilibrium in thin films (DETs) or diffusive gradient in thin films (DGT). While DETs are useful for high ambient mercury concentrations, DGTs are particularly beneficial in a range of sediment matrices (Peijnenburg et al., 2014).

2.5 DIFFUSIVE GRADIENT IN THIN FILMS

DGTs allow for passive sampling with low detection limits and no influence of ionic strength (Zhang & Davison, 1995). They minimize temporal variability from varying flow rate and allow for high resolution of concentrations at depth through limited time exposure as they quantify dissolved metals via kinetics (Zhang & Davison, 1995). DGTs were developed by Davison and Zhang in 1995 to measure labile dissolved metals of cadmium, iron, manganese, and copper in fresh and saltwater. They have since been optimized for measurement of labile dissolved mercury as well. The metallic ions measured within samplers are then used to estimate the concentration of trace metals in the bulk solution. DGTs are constructed in three basic layers. The outermost layer is comprised of a 0.45 μm filter, the middle layer is a diffusive gel, and the innermost layer is a resin that is designed to be an infinite sink for mercury over limited exposures. This

basic structure can be seen in Figure 2.1 and Figure 2.2 as a piston design for measurement of overlying water and slurry concentrations and as a profile design for measurements throughout the sediment depth, respectively.

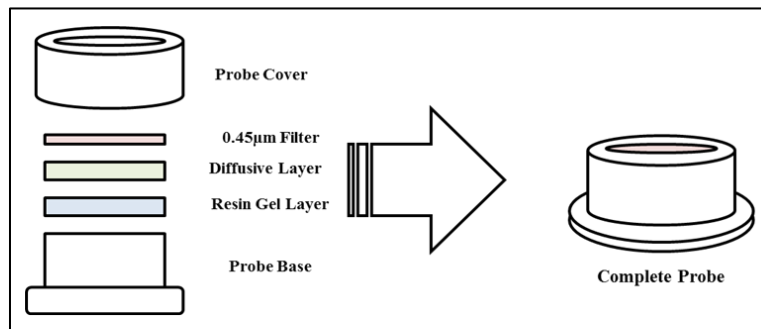


Figure 2.1: Piston structure of DGTs, used for slurry and overlying water sampling (Chess, 2010)

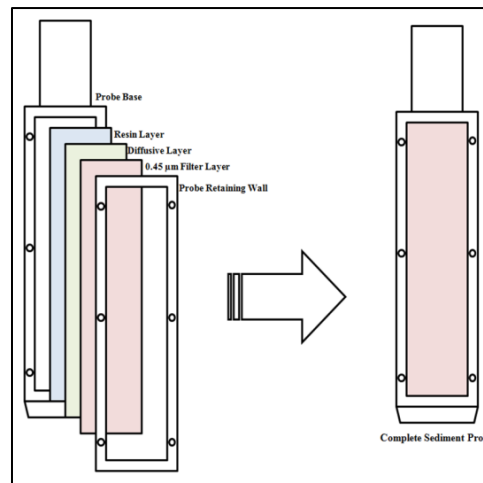


Figure 2.2: Profiler structure for DGTs, used for sampling throughout sediment depth (Chess, 2010)

DGTs are based off of Fick's first law of diffusion, with the diffusive gel governing flux of ions into the sampler. A representation of the concentration gradient

throughout the diffusive layer can be seen in Figure 2.3. It can be seen from Figure 2.3 that ionic concentration is depleted at the resin layer due to rapid binding with the resin; this generates a steady-state linear diffusion gradient (Zhang & Davison, 1995). Therefore, any excess of metals in bulk solution will not impede the measurement of concentration. The equation of flux used for determination of bulk concentrations by DGTs can be seen in Equation 2.1 and Equation 2.2.

$$M = DC_b t A / \Delta g \quad (\text{Equation 2.1})$$

$$C_b = M \Delta g / D t A \quad (\text{Equation 2.2})$$

Where M = mass of metal adsorbed (M),

C_b = concentration of the metal ion in bulk solution ($M L^{-3}$),

D = diffusion coefficient in the gel ($L^2 T^{-1}$),

t = length of deployment (T),

A = exposure area of the device to the bulk solution (L^2),

Δg = thickness of the diffusive layer (L) (Davison & Zhang, 1995).

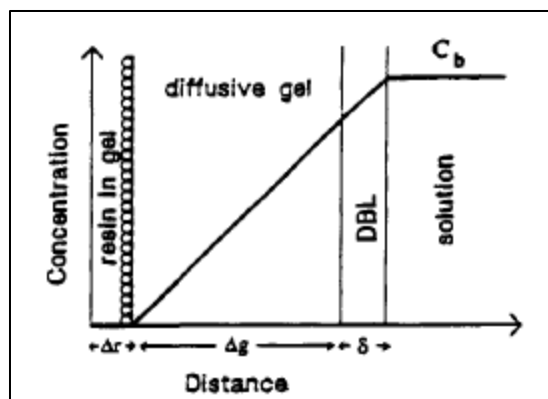


Figure 2.3: Conceptual mercury concentration throughout the DGT layers (Zhang & Davison, 1995)

The type of diffusion of metal ions throughout the gel is expected to be purely molecular diffusion (Zhang & Davison, 1995). Therefore, particle differentiation due to reactivity and size influenced diffusion will be governed by the type of gel utilized. The original DGT fabrication by Davison and Zhang suggested the use of a polyacrylamide hydrogel diffusive layer; however, for mercury, an agarose diffusive layer has since been adapted to prevent any interferences or binding with amine groups (Divis et al., 2009; Zhang & Davison, 1995). The agarose gel has a pore size of 20 nm or greater and be comprised of 98% water from hydration (Zhang & Davison, 1999). This pore size and water concentration allows for relatively free diffusion of particles 20 nm in diameter or smaller, while partially impeding and slowing diffusion of larger molecules (Zhang & Davison, 1995). The dissolved ions and nanoparticles within this diameter range are thought to be similar to the particle size available for uptake and methylation by microorganisms (Zhang & Davison, 1995). In addition to the diffusive gel, the resin layer

of DGTs has also been optimized for use in measurement of mercury. 3-Mercaptopropyl-Functionalized silica resin beads have replaced the initial Chelex-100 ion resin beads due to their greater affinity for mercury (Olivier Clarisse & Hintlemann, 2006).

As diffusion governs uptake within DGTs it is important to understand the factors which influence diffusion, prior to deployment of samplers. For each sediment matrix, the diffusive coefficient must be determined and optimized to minimize any interference from the impact of the double layer. The change of flow patterns at the sampler-bulk solution interface may hinder diffusion and thus underestimate dissolved concentrations (Zhang & Davison, 1995). This is especially relevant in low flow conditions and thus must be considered in low flow or variable flow systems (Zhang & Davison, 1995). Temperature also impacts the diffusion, as the diffusion coefficient is a function of free diffusion within the bulk water solution. As temperature changes, so does the water viscosity, and thus Equation 2.3 must be utilized to adjust the diffusion coefficient at any temperature deviation from 25°C (Zhang & Davison, 1995).

$$\log D_t = \frac{1.37023(t-25)+8.36 \times 10^{-4}(t-25)^2}{109+t} + \log \frac{D_{25}(273+t)}{298} \quad (\text{Equation 2.3})$$

Where D_t = diffusion coefficient at a given temperature t ($L^2 T^{-1}$),
 D_{25} = diffusion coefficient of ions in water at 25 °C ($L^2 T^{-1}$),
 t = temperature (°C).

For the sediment matrix assessed within this research, the South River, VA, previous work has been completed in order to calibrate the diffusion coefficient. This

calibration can be seen in Figure 2.4 (Chess, 2010). From the shape of this curve it was determined that the diffusive agrose layer does indeed control uptake and thus the effects of the diffusive boundary layer and slow diffusion from colloidal mater are negliglbe, ultimately simplifying the analysis completed in this research (Chess, 2010).

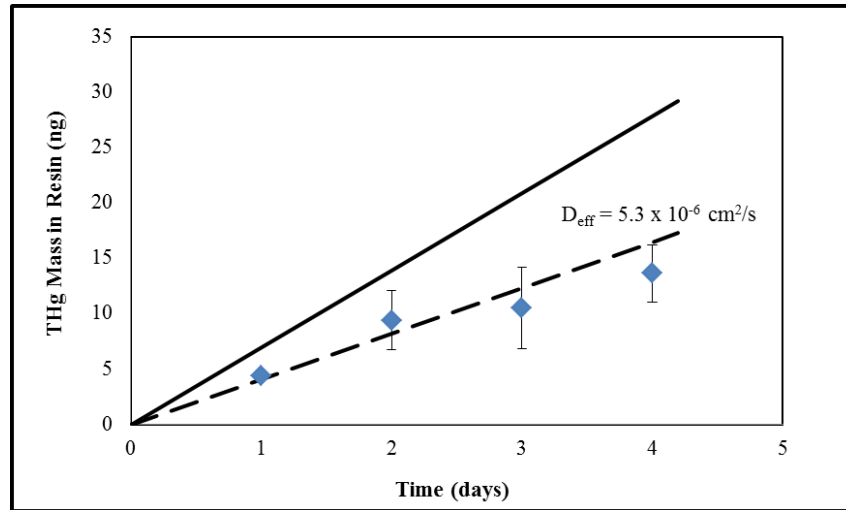


Figure 2.4: Calibration of DGTs within sediment of the South River, VA (Chess, 2010)

As diffusion through the DGT is based on available particle characteristics, it is expected that the uptake by the passive samplers will correlate to the uptake of mercury by microbes for methylation and thus serve to predict bioavailability in sediments (Zhang & Davison, 1995). However, it is also possible that mercury measured by DGTs will be indicative of mercury which is also bioavailable to macroorganisms. Several studies have considered this link between DGT passive sampling with mercury bioavailability. Liu et al. (2012) assessed a correlation between methylmercury within DGT measured porewater with methylmercury uptake by rice plants and found a significant correlation ($R=0.853$)

largely attributed to the rice paddy mode of uptake. Other studies have considered the relationship of DGTs used over an extended duration, thus applied similar to DETs, with bioaccumulation in saline systems. Clarisse et. al. (2013) was able to determine a correlation of prolonged DGT exposures with clam accumulation of methylmercury with a R^2 of 0.89, whereas Amirbahman et. al. (2014) found a correlation range of R^2 of 0.57 to 0.97 for total mercury and methylmercury between DGTs and various benthic organisms (Amirbahman et al., 2013; O. Clarisse, Lotufo, Hintelmann, & Best, 2012). These results are promising; however, while DGTs act as an infinite sink under limited exposures, they will ultimately reach resin capacity (Zhang & Davison, 1995). Therefore, it would be preferable to complete correlation studies with a limited DGT exposure to more accurately gauge flux of porewater mercury with bioaccumulation in organisms, as will be completed within this research.

2.6 BIOTURBATION

Sediment matrices influence organism bioaccumulation, and, in tandem, are influenced by the organisms due to bioturbation. Bioturbation is the mixing, processing, burrowing, and irrigating of sediment as completed by benthic infaunals (Rosenberg et al., 2001). The species *T. tubifex* contributes to sediment bioturbation as sub-surface deposit feeders by processing and transporting sediment through consumption and creating burrows throughout the upper sediment layers. Therefore, their activity within this research will be used to assess the impacts of bioturbation. Bioturbation has varying effects on sediment; however it is most consistently linked to an introduction of oxygen.

Through burrowing and irrigating, preferential pathways are created between the sediment water interface and lower depths. This allows for diffusion of oxygen to lower regions of sediment profile which is one of the greatest factors influencing sediment biogeochemistry (Navel et al., 2012).

The presence of oxygen at lower depths has multiple impacts. Notably, the presence of oxygen disturbs the stratified redox profile established in sediments as it introduces a terminal electron acceptor in regions where oxygen had previously been depleted. A traditional sediment redox profile as based on the depletion of terminal electron acceptors with depth can be seen in Figure 2.5. A bioturbation study has determined that anywhere between 64% and 81% of oxygen consumption is attributed to oxygen introduced by bioturbation (Binnerup et al., 1992). Naturally, this impacts the microbial community. The introduction of oxygen to different depths will vertically homogenize microorganism species while causing heterogeneity on the horizontal plane. Often, this bioturbation and thus oxygen introduction increases bacterial production and abundance (Van De Bund, Goedkoop, & Johnson, 1994). However, for the given test organism, *T. tubifex*, which derives a portion of its energy demand from sediment bacteria, it is seen that bioturbation does not increase abundance but can increase bacterial production by a factor of 1.4 (Van De Bund et al., 1994). This increase may be due to the physical disturbance causing a greater availability of substrates, but may also be linked to the introduction of oxygen which would allow aerobic organisms to survive and utilize their greater thermodynamic capacity to create biomass. Similar oxygen

stimulation of microbial communities has been linked with greater metabolic activity as correlated with an 30% increase in leaf-litter breakdown (Navel et al., 2012).

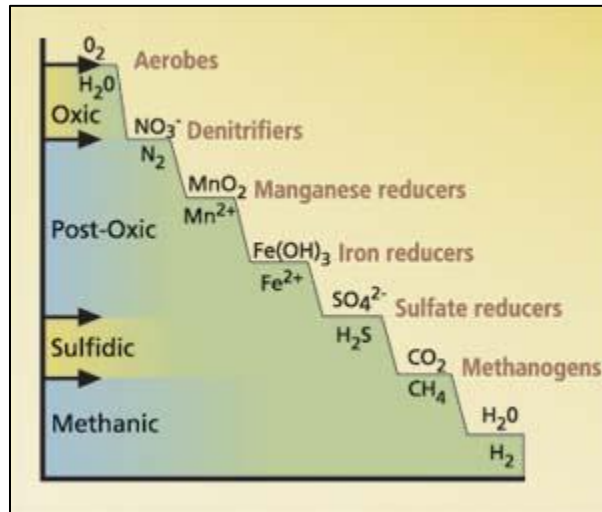


Figure 2.5: Vertically stratified redox profile characteristic of freshwater sediments (Gao, Davis, & Tanji, 2003)

The diffusion of oxygen also abiotically alters carbon within sediment systems. It has been demonstrated that inconsistent oxygen exposure, as occurs with bioturbation, is superior at more quickly oxidizing organic matter than direct exposure of oxygen (Kristensen & Holmer, 2001). This allows for greater carbon decomposition and ultimately greater availability of organic matter in bioturbated systems after initial leaching of labile organic matter (Kristensen & Holmer, 2001). In addition to carbon degradation, denitrification is significantly impacted by the activity of bioturbators as only 29-62% of nitrification is due to diffusion, with the remaining attributed to the introduction of solutes through bioturbation (Binnerup et al., 1992). This ultimately alters

the redox profile near the sediment-water interface and may impact the nitrogen available to microbes for synthesis of biomass.

However, while the degradation of carbon and nitrification are impacted by bioturbation, biogeochemistry through the transport of solutes across the sediment water interface is also affected. Bioturbation has been seen to enhance the exchange of TCO_2 , dissolved organic carbon, and iron(II) across the sediment water interface, especially in the upper centimeters (i.e. 15-20 cm) of sediment (Gribsholt & Kristensen, 2002). In addition, by introducing oxygen, organisms help to mobilize reduced compounds which then diffuse out of sediments (Gribsholt & Kristensen, 2002). This can decrease availability of NH_3^+ , PO_4^{3-} , and DOC in bioturbated sediments (Navel et al., 2012). These processes may also lead to greater homogenization of solutes between sediment.

Each of these biogeochemical shifts can have an interesting impact on mercury fate and transport. While the impact of bioturbation has not been directly assessed for mercury, it is likely that its alterations to biogeochemistry will impact methylation potential and mercury sequestration. This will be addressed within the second objective of this research.

Chapter 3: Experimental Approach and Methods

3.1 EXPERIMENTAL SET-UP

3.1.1 Sediment Source

The sediment studied was from three depositional environments at relative river mile 11.8 of the South River, VA. This sediment has a legacy of contamination from a rayon production industrial point source which lasted from the 1920s to 1950 located 11.8 miles upstream of the sediment location (South River Science Team, 2014b). The three depositional environments include a bank deposit, characterized by finer sediment containing detritus, a near-bank deposit, that is within the channel itself and also characterized by high fines content, and a mid-channel deposit which is characterized by coarser sediment, more comparable to gravel.

A conceptual model was generated for the South River as seen in Figure 3.1. It can be seen that from this conceptual model that bank erosion contributes the most significant flux into the stream followed by the flux from legacy sediments. Within the stream itself, the coarse channel bed deposit, or the mid-channel deposit, contributes a larger percentage of flux than the fine grained deposits, including the near-bank and bank deposit. This may be attributed to the greater distribution of coarse grain sediment within the stream. Differences in the mercury speciation within these different deposits will be considered in this research.

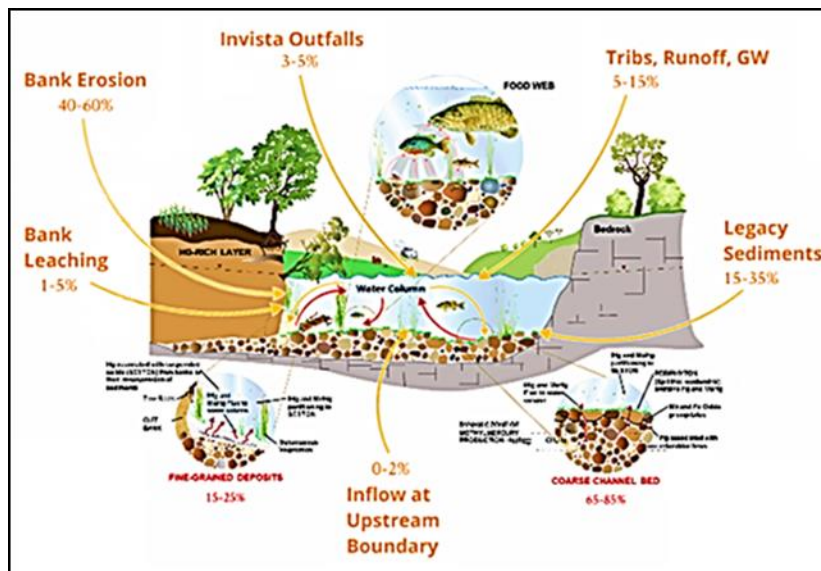


Figure 3.1: Conceptual model of mercury flux at relative river mile 3.5 of the South River, VA (South River Science Team, 2014a)

Sediments were obtained from the South River, VA in June 2013 and immediately shipped to the University of Texas at Austin where they were stored in a 4°C dark environment. Mesocosms were constructed within seven months of obtaining the sediment.

3.1.2 Test Organism

The benthic oligochaete, *T. tubifex* was selected as the test organism for the assessment of bioavailability and bioturbation. *T. tubifex* was selected due to its ability to uptake mercury through multiple exposure routes as a sub-surface deposit feeder and its heavy metal tolerance. Prior to the addition of *T. tubifex* into the mesocosms, the culture was maintained in a static mixture of potting soil and artificial pond water. The solution

was aerated and the culture was fed approximately 5 cm³ of Gerber[®] oatmeal once a week. The organisms were removed from the culture by taking small sections of the potting soil and extracting each *T. tubifex* with a needle pointed syringe. These organisms were then placed in a Petri dish filled with artificial pond water and were allowed to depurate in this chamber for 24 hours prior to deployment. The organisms were maintained in a 20°C environment to equilibrate to the experimental temperature for several hours prior to mesocosm introduction. Three-hundred *T. tubifex* were placed into each mesocosm with an expectation that the culture would double every two weeks and thus create approximately 1200 *T. tubifex*/sample. A 28-day bioaccumulation test was selected for the exposure period based on previous studies of *T. tubifex* and mercury bioaccumulation (*see Section 2.3*).

3.1.3 Experimental Conditions

In order to assess bioavailability and bioturbation, controlled exposures to mercury were established in flow-through mesocosms referred to as “T-cells”. This mesocosms structure can be seen in Figure 3.2. The use of flow-through mesocosms is beneficial for several reasons. First, the sediment depth within the mesocosms allows for a redox profile of approximately 8 cm to be established, thus presenting the range of microbial guilds and reducing conditions relevant to mercury speciation. Second, the flow through mesocosms also provide beneficial conditions for organisms as the constant flux of overlying water provides a source of oxygen to and removes waste which can

contribute to detrimental biological oxygen demand (BOD) (American Society for Testing and Materials International, 2010).

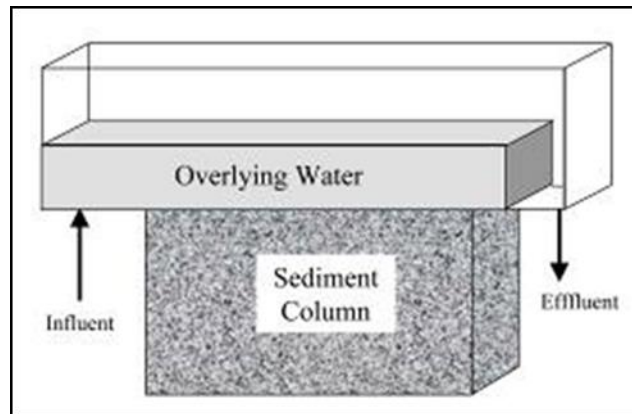


Figure 3.2: Structure of flow-through mesocosms, “T-cells”, with approximately 8 cm sediment depth and 1.25 cm depth of overlying water (Johnson, 2009)

The constant influent water supply consisted of aerated artificial pond water. The concentrations of the salts used to mix each batch of artificial pond water can be seen in Appendix A. This pond water was utilized in order to maintain a sufficient ionic strength in order to prevent additional stress on the organisms. The flow rate was maintained at approximately 2mL/min, with a residence time of 75 minutes, for the duration of the bioaccumulation experiment. The flow rate was maintained at a lower flow rate of 1 mL/min during the stabilization period.

To maintain consistent exposure conditions, the mesocosms were kept within a controlled temperature chamber of 20°C. This temperature was selected for two main reasons. First, it mimics the ambient conditions of the South River, VA, as 20°C is the

average temperature of the stream in spring, the season when microbial populations within the stream are most productive (Chess, 2010). Thus, these conditions provide a more conservative analysis of methylation. To encourage survival of the test organism, the 20°C conditions were also maintained to in order lower toxicity of mercury to *T. tubifex* (Rathore & Khangarot, 2003). This promotes a more accurate bioaccumulation experiment as survival is required throughout the test. The mesocosms were also maintained in a mostly dark environment for the duration of the experiment by covering the open mesocosm top with tin foil. This served to prevent any aerial deposition of microorganisms, while also maintaining a darker condition more indicative to the sediment conditions within the stream.

3.1.4 Established Mesocosms

Fourteen mesocosms were established in total. Nine of the mesocosms were constructed to contain the focus oligochaete, *T. tubifex*. These include three replicates of each depositional environment including the bank, near-bank, and mid-channel deposits. Due to the large grain size of the mid-channel deposit, it was empirically determined to be unable to sustain *T. tubifex* life. To test the mid-channel deposit, a 1 cm potting soil cap was placed on top of each of the mid-channel mesocosms which contained *T. tubifex*. In addition to the nine mesocosms containing *T. tubifex*, five controls were established. These include a control for each depositional environment which contained no added *T. tubifex*. For the mid-channel deposit, two control mesocosms were created, one with and one without the 1 cm potting soil cap in order to determine the impact of this cap on

biogeochemistry and mercury speciation. The fifth control was constructed with autoclaved near-bank sediment. This was created in order to gain a greater understanding of the establishment of reducing conditions while also removing any additional bioturbation that would be associated with native macroorganisms present from the sediment collection. The sediment was autoclaved at 250°F for 30 minutes for two cycles to eliminate the activity of native organisms (Tuttnauer Autoclave Model 6690 SP-1A).

When constructing the mesocosms, the samples were homogenized and any large detritus or rocks were removed. This was completed to provide greater consistency in the mesocosms. The mesocosms were filled using acid washed spatulas and were leveled prior to the addition of any artificial pond water. Approximately $8.9 \times 10^{-4} \text{ m}^3$ of sediment was added to each mesocosm, and no packing was employed to prevent any differences in settling. A summary of the mesocosm conditions and identifying nomenclature can be seen in Table 3.1. This also includes the dates of construction, introduction of organisms, and breakdown.

Table 3.1: Mesocosms employed to study oligochaete interaction including date of construction, organism introduction, and destructive breakdown.

Sample Name	Depositional Environment	Sample Type	Date of Construction	Date of <i>T.tubifex</i> Introduction	Date of Destructive Breakdown
11.8-G-C1	Mid-Channel	Control	6/10/2013	N/A	9/24/2013
11.8-G-C2	Mid-Channel	Control with 1 cm potting soil	8/14/2013	N/A	9/24/2013
11.8-G-S1	Mid-Channel	<i>T.tubifex</i> with 1 cm potting soil	6/10/2013	8/27/2013	9/24/2013
11.8-G-S2	Mid-Channel	<i>T.tubifex</i> with 1 cm potting soil	1/9/2014	2/20/2014	3/20/2014
11.8-G-S3	Mid-Channel	<i>T.tubifex</i>	1/9/2014	2/21/2014	3/21/2014
11.8-F-C1	Near-Bank	Control	6/10/2013	N/A	9/5/2013
11.8-F-C2	Near-Bank	Autoclaved Control	8/8/2013	N/A	2/1/2014
11.8-F-S1	Near-Bank	<i>T.tubifex</i>	6/10/2013	8/8/2013	9/5/2013
11.8-F-S2	Near-Bank	<i>T.tubifex</i>	6/10/2013	8/8/2013	9/5/2013
11.8-F-S3	Near-Bank	<i>T.tubifex</i>	1/9/2014	2/17/2014	3/17/2014
11.8-B-C1	Bank	Control	6/10/2013	N/A	9/5/2013
11.8-B-S1	Bank	<i>T.tubifex</i>	6/10/2013	8/8/2013	9/5/2013
11.8-B-S2	Bank	<i>T.tubifex</i>	1/9/2014	2/18/2014	3/18/2014
11.8-B-S3	Bank	<i>T.tubifex</i>	1/9/2014	2/19/2014	3/19/2014

3.2 EXPERIMENTAL TIMELINE

The experiment was completed in three main phases: an equilibration period, a bioaccumulation exposure period, and destructive breakdown of the mesocosms. Within each phase different sampling techniques were employed.

The equilibration period immediately followed construction to allow the mesocosms to stabilize and establish relatively constant reducing profiles. Within this period, the overlying water concentrations of dissolved total mercury and methylmercury, and the establishment of the voltammetric mesocosm redox profiles were constantly monitored. The duration of this phase lasted for approximately 2 months for the initial experiment run, and approximately 1.5 months for the second experimental run. The

shortened time was based on analysis of the quickly established redox profiles within the initial experiment set.

At 1.5-2 months, the bioaccumulation phase was initiated by the addition of *T. tubifex* into the sample mesocosms. The control mesocosms were simultaneously maintained in the same environment and experienced the same sampling intervals. During the 28-day bioaccumulation period, the DGT measured dissolved overlying water total mercury and methylmercury concentrations and reducing profiles were monitored.

Finally, during the destructive breakdown phase, the majority of sampling was completed. Approximately three to four days prior to destructive breakdown, voltammetry was employed in each mesocosm. The DGTs were then deployed for a 2-3 day exposure. The morning of destructive breakdown, the DGTs were extracted, and immediately following, cores were taken from each mesocosm. Finally, each section of sediment was rifled through to locate *T. tubifex*. The organisms were removed and samples from this experiment were processed and analyzed in the following months.

3.3 SAMPLING EMPLOYED

Multiple sampling techniques were employed during the duration of this experiment. These included techniques to sample total mercury and methylmercury concentrations, to determine reducing conditions, and to analyze biogeochemistry. Additionally, analysis was completed to characterize the lipid concentration and moisture content of *T. tubifex*. The methodology consisted of bulk sediment core sampling, DGT

sampling, voltammetry, and *T. tubifex* sampling. All chemicals used in sampling and analysis were ACS grade and all acids used were trace metal grade. Mercury analysis was completed in a Class-100 clean room (Servicor-CPI) which was constructed with all non-metal components.

3.3.1 Bulk Sediment Coring

3.3.1.1 Sediment Core Sampling

In order to assess bulk solids for total mercury and methylmercury concentrations, in addition to many biogeochemical factors, bulk sediment cores were collected at the end of the 28-day bioaccumulation experiment. Four cores were taken from each mesocosm as seen in Figure 3.3. The cores were sampled by using 100 mL graduated cylinders that had been adapted by removing the upper most section to create a level circle while also drilling a hole in the base of the cylinder. The graduated cylinders were then placed upside down into the sediment, and pressure was applied at the upper most holes in order to create suction. The samples were slowly raised from the sediment, capped and taped with vinyl tape prior to being frozen until analysis. In the absence of sufficient graduated cylinders, 50 mL centrifuge tubes were also used by removing the tapered end at the bottom, and capping the tube to create suction. This was employed for approximately 12 cores.

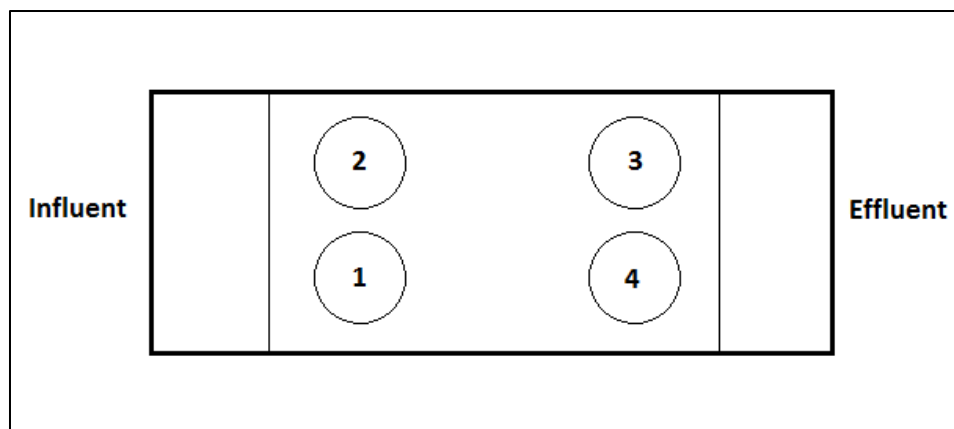


Figure 3.3: Bulk sediment coring employed in all mesocosms

The cores were processed while frozen, in order to preserve chemical properties, and separated into 1 cm section by a razor blade. From each 1 cm segment, samples were quickly removed for methylmercury analysis and returned to the freezer to avoid any thawing. The remaining sections were transferred into an anaerobic chamber which maintains an environment of 97% $N_{2(g)}$ and 3% $H_{2(g)}$ atmosphere (Coy Laboratory Products Inc.). These samples were allowed to thaw and were then homogenized and sectioned by mass into samples for total mercury, acid volatile sulfides, iron sulfides, total organic carbon, and moisture content. The approximate density of each segmented core was also measured and determined based on total mass and approximate volume. In order to provide sufficient sediment mass for these analyses, two cores were blended for each sample providing two replicates overall. For the bank samples, near-bank samples, and Mid-Channel Samples 2 and 3, the influent cores and the effluent cores were blended (Cores 1-2, and 3-4). This allows for consideration of any spatial distribution over the

length of the mesocosm, its largest parameter. For the Mid-Channel Controls 1 and 2 and Sample 1, cores were blended on either side of the mesocosm (Cores 2-3, and 1-4), its smaller parameter. If the samples were not immediately processed through the analysis in *Section 3.2.1.2*, they were stored in the freezer until processing. For the initial sampling event the entire depth of the core was studied. For the second sampling set, the first 4 cm were sampled for simplicity.

3.3.1.2 Sediment Core Analysis

The sediment cores were assessed for total mercury and methylmercury. Total mercury was extracted from the sediments by completing an aqua regia digestion (10 mL HCl and 3 mL HNO₃) which was diluted in Millipore water 24 hours after the acid addition (Bloom, Preus, Katon, & Hiltner, 2003). Samples were stored at room temperature until analysis. Prior to analysis, samples were digested at room temperature overnight in 2% BrCl and then were analyzed following EPA Method 1631 (Oxidation, Purge and Trap, and Cold Vapor Atomic Fluorescence Spectroscopy (CVAFS)), with additional dual pre-concentration (Tekran 2600) (United States Environmental Protection Agency, 2002). Dilution blanks and spike checks were utilized to assure functionality. Calibration standards were prepared and run the morning of analysis to produce standard curves as seen in Figure 3.4.

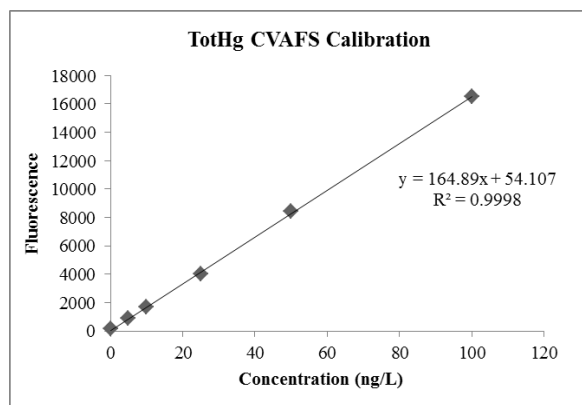


Figure 3.4: Example calibration for CVAFS measured total mercury

Bulk methylmercury was extracted immediately after thawing and digestion using USGS Method 5A-7 of organic extraction and aqueous ethylation (DeWild, Olund, Olson, & Tate, 2004). Estuarine reference material (ERM-CC580, RTC analytical) and dilution blanks were additionally extracted with every 20 samples. The samples were then stored at 4°C and analyzed within 24 hours of extraction. Samples were analyzed using EPA Method 1630 (Distillation, Aqueous Ethylation, Purge and Trap, and Cold Vapor Atomic Fluorescence Spectroscopy) both on manual and automatic instrumentation (Tekran 2600, Brooksrand Merx Model III) (United States Environmental Protection Agency, 2001). Blanks and spikes were used to monitor functionality of the instrument. Calibration standards were prepared and run the morning of analysis to produce the standard curves. An example calibration curve can be seen in Figure 3.5.

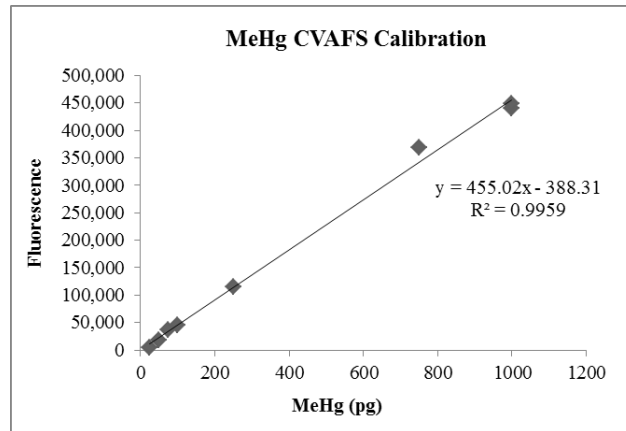


Figure 3.5: Example calibration for CVAFS measured methylmercury

Acid volatile sulfides were measured using the diffusion method (Hsieh, Chung, Tsau, & Sue, 2002). Samples were analyzed twenty-four hours after the addition of the acid, and a calibration curve was prepared in deaerated sulfide antioxidant buffer during each day of analysis. An example calibration curve can be seen in Figure 3.6. Ferrous iron was measured through oxalate extracts (Phillips & Lovely, 1987). A calibration curve was also prepared during each analysis. The example calibration curve can be seen in Figure 3.7.

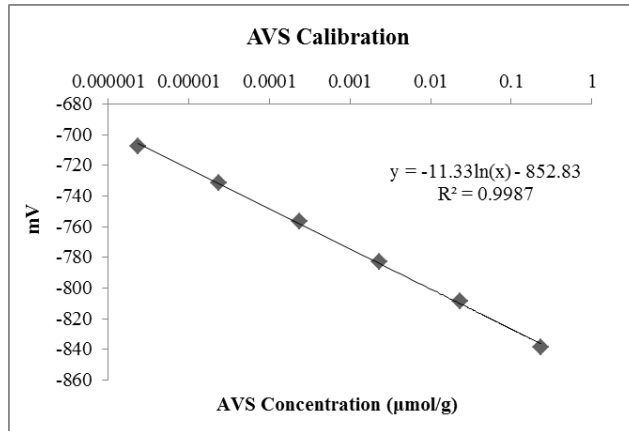


Figure 3.6: Example calibration curve for measurement of AVS

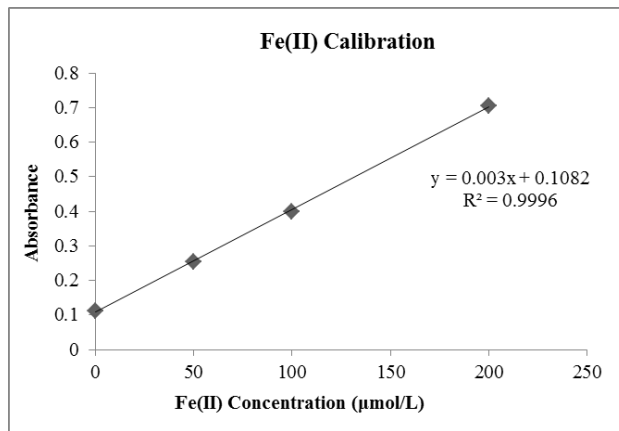


Figure 3.7: Example calibration curve for oxalate extracted ferrous iron

The total organic carbon (TOC) sediment sample was utilized to measure moisture content. Wet mass was measured the day of sampling and the samples were dried in a 105°C oven for 24 hours until dry weight was measured. Ten representative total organic carbon samples were then shipped on ice to the Lower Colorado River Authority laboratory for analysis.

3.3.2 Diffusive Gradient in Thin Films

The DGTs were fabricated within a laboratory fume hood maintained exclusively for DGT fabrication. The resin gel was prepared by the procedure indicated in Zhang and Davison (1995). The polyacrylamide gel solution was prepared by mixing aqueous solutions of 15% of 40% acrylamide/Bis solution 37.5:1 (Bio-Rad Laboratories, Inc) and 0.3% patented cross-linker (DGT research Ltd.). One gram of 3-Mercaptopropyl-Functionalized resin beads, 30 μL of ammonium persulfate (Bio-Rad Laboratories, Inc.), which was prepared within hours of gel casting, and 7.5 μL of N, N', N'-tetramethylethylenediamine (TEMED) (Bio-Rad Laboratories, Inc.) were used with 5 mL of the polyacrylamide gel solution.¹ The resin gel was cast, allowed to set, and then hydrated for 24 hours in 0.1 M NaNO_3 . The diffusive gel was cast using a boiled solution of 0.15 g agarose per 10 mL of Millipore water. Upon cooling to room temperature (30 minutes) the gel was removed from the casting plates. Immediately following, the resin gel and diffusive gels were cut to fit and constructed on DGT profiler and piston bodies as purchased from Research Ltd.

After construction, the DGTs were stored at 4°C in two sealed containers containing a slight amount of 0.1 M NaNO_3 or Millipore water. The samplers were then deaerated in a 0.1 M NaNO_3 solution for at least 8 hours prior to deployment in order to prime the samplers for uptake. After deaeration, the samplers were immediately deployed

¹ For the Bank Control and Sample 1, in addition to the Near-Bank Control 1, and Samples 1 and 2, no cross-linker was used in the polyacrylamide gel solution. This should have no effect on uptake.

or brought into the anaerobic chamber for separation into sealed containers (Coy Laboratory Products Inc.). The samplers were deployed into the mesocosms with minimal exposure to oxygen and remained within the mesocosm for a range of 2-3 days. Profile DGTs were gently pushed into the sediment within the center of each mesocosm, and overlying water piston samples were either allowed to float on the overlying water, were placed at the sediment water interface, or were suspended in the solution using wire. When removed, the samples were rinsed with Millipore water, stored in sealed containers at 4°C, and were digested within 5 days for total mercury and methylmercury.

Upon digestion, the DGTs were sectioned using an acid washed cutting board and Teflon coated razor blades. Total mercury samples were digested in 3 mL HCl and maintained in a dark environment for 24 hours at room temperature before the digestate was pulled off and stored in new vials in 4°C until analysis. For analysis, samples were then diluted in 2% BrCl at room temperature and analyzed using EPA Method 1631 with additional dual pre-concentration (Tekran 2600) (United States Environmental Protection Agency, 2002). The methylmercury samples were digested in 15 mL of 13.1 mM thiourea and 0.1 M HCl for 24 hours in a dark environment at room temperature. The digestate was then removed and stored in new vials prior to being frozen until analysis. Several 500 pg methylmercury spikes were prepared on the date of digestate removal and were stored in similar conditions in order to assess recovery after freezing. Samples were analyzed within 6 months of sample digestion by utilizing EPA Method 1630 both on

manual and automatic instrumentation (Tekran 2600, Brooksrand Merx Model III) (United States Environmental Protection Agency, 2001).

Piston DGT bodies were used for periodic measurement overlying water mercury samples. One piston was used in each mesocosm and was sectioned in half for one total and one methylmercury sample. Three profiler DGT bodies were used in each mesocosm prior to the destructive breakdown in order to establish depth profiles. The profiler DGTs were sectioned in half for total mercury and methylmercury, in addition to samples being sectioned into 2 cm in depth segments starting at the sediment water interface. The depth of the overlying water was also sectioned, which generally spanned 1 cm above the sediment water interface.

For quality control, resin blanks were often utilized in addition to deaeration blanks which were constructed and deaerated in the same conditions as the samplers. These were digested in the same manner in order to assess any background total mercury and methylmercury. Between uses, DGT profiler and piston bodies underwent two soap baths and an HCl acid wash.

3.3.3 Voltammetry

Voltammetry was employed within the mesocosms in order to determine concentration of dissolved oxygen and redox metals at each 0.5 cm depth resolution using an automatic manipulator (Analytical Instrument Systems). The voltammetric microelectrodes utilized were capable of measuring dissolved oxygen and dissolved

metals including manganese (Mn^{2+}), ferrous and ferric iron (Fe^{2+} and Fe^{3+}), hydrogen sulfide (HS^-), and iodide (I^-) (Brendel & Luther, 1995). The microelectrodes were constructed in the laboratory using the method proposed by Brendel and Luther (1995) with 100 μm diameter wire held within a peek structure. Prior to each use, electrodes were polished, plated using 0.1 M mercury, and polarized at 9V for 90s. Based on the microelectrode response, one to three microelectrodes were selected for each sample, and triplicate scans were used per electrode at each depth. The electrodes were generally centered within the mesocosm for analysis. Electrodes were polished in the same manner as previous experiments by the same researcher and calibrated at a single time point. Between each sampling event, the electrodes were only lightly polished to minimize any inconsistency in electrode response. The electrodes were calibrated for manganese, and the deviation of the electrode response from the value presented by Brendel and Luther (1995) was adjusted for in calibration of the remaining dissolved metals and oxygen. The electrode calibrations for the remaining metals in addition to scan parameters and detection limits were also taken from Brendel and Luther (1995). Voltammetry was employed in samples approximately every 3 weeks during the equilibration period, and was additionally run at approximately Bioaccumulation Day 0 and immediately prior to DGT profiler deployment at destructive mesocosm breakdown.

Linear sweep voltammetry was used to measure dissolved oxygen and square wave voltammetry was utilized to measure dissolved metals. Linear sweep voltammetry was employed until visual determination that oxygen had depleted and then square wave

voltammetry was employed. In several instances, dissolved metals were present even with oxygen present. In these situations, both voltammetry sweeps were employed. For select samples, ORP and pH were also measured at each depth. ORP was gauged using a platinum electrode, and pH was gauged using a pH probe that was calibrated using standard solutions of pH 4, 7, and 11.

3.3.4 *T. tubifex* Sampling and Processing

To begin the bioaccumulation experiment, the *T. tubifex* were extracted individually with a needle pointed syringe from the culture, counted into sets of 300 and allowed to depurate in artificial pond water for 24 hours prior to deployment. At this time, three hundred worms were also depurated, separated, and frozen to serve as the Day 0 sample set. Upon destructive breakdown of the mesocosms, the worms were again individually extracted and allowed to depurate in artificial pond water for 24 hours. After depuration, the worms were separated into sets of 20-30, any remaining particles were carefully removed from their exteriors, and the worms were placed in vials and frozen until analysis. The holding period for the worm samples ranged from 1-2 months.

Three replicates from each mesocosm and from the Day 0 sample were digested for total mercury. The samples were digested in 5 mL of HNO₃ and HCl (3:7 ratio) as scaled from EPA Method 1631 Appendix due to the small sample size (United States Environmental Protection Agency, 2001a). During digestion, digestion spikes and blanks were run to assess any background and sample loss. Samples were then stored at 4°C

prior to analysis. For analysis, samples were diluted in 2% BrCl at room temperature and analyzed using EPA Method 1631 with additional dual pre-concentration (Tekran 2600) (United States Environmental Protection Agency, 2002). Three replicates from each sample set were also analyzed for methylmercury. This analysis was completed using the acid leaching technique developed by Hintelmann and Nguyen (Hintelmann & Nguyen, 2005). Sample blanks and spikes were also digested. The samples were then analyzed using EPA Method 1630 both on manual and automatic instrumentation (Tekran 2600, Brooksrand Merx Model III) (United States Environmental Protection Agency, 2001). A lower flow rate had to be amended to this analysis in order to account for foaming of the samples that would have contaminated the traps had the full flow rate been used.

One sample from each mesocosm and Day 0 analysis were utilized to study lipids concentration with a Herbes modified Bligh/Dyer method of total lipid extraction and purification (Bligh & Dyer, 1959; Herbes & Allen, 1983). A cholesterol standard with 10 mg/mL lipid content (Sigma Cod liver oil fatty acid methyl esters) was utilized to assess recovery. Finally, moisture content of the *T. tubifex* within each mesocosm was determined by utilizing three replicates of a 1-3 *T. tubifex* sample size and measuring the wet weight of the sample in addition to the dry weight after 24 hours of heating in a 105°C oven.

3.3.5 Overlying Water Dissolved Organic Carbon

Initially dissolved organic carbon (DOC) was also sampled using acid washed glass syringes and a 0.45 μm filter at every 2 weeks. These samples were then stored in amber vials and preserved with 2 mL HNO_3 in 4°C. Unfortunately due to the lack of organic carbon instrument functionality, the samples were held for too long and thus were compromised and not analyzed.

3.4 ASSESSMENT OF RESULTS

In order to gauge successful results, several methods were used. For the analysis of bioaccumulation prediction, the first four centimeters of bulk solids and porewater derived mercury were averaged to be compared to the bioaccumulation within the *T. tubifex*. The mercury concentrations within this zone were averaged because the organisms were mobile within the mesocosm, and thus they were potentially exposed to mercury throughout this depth. The depth of 4 cm was selected as it was visually determined to be the depth of *T. tubifex* exposure. This was noted by observation of bioturbated pathways on the side of the mesocosm. This depth was thought to be a conservative exposure range, as bioturbation appeared to vary between 2-4 cm. This follows with previously studied *T. tubifex* bioturbation in which 93% of the organisms were found within the uppermost 5 cm of sediment (Navel et al., 2012).

Bioaccumulation will be compared to both DGT and bulk solid sampling techniques and linear correlations will be determined. These correlations will be

developed for bioturbation across depositional environments and within each depositional environment. The applicability of either sampling technique will be primarily based on analysis of the correlations across depositional environments. Correlation within each depositional environment will be evaluated in order to minimize the impact of biogeochemistry and allow for further interpretation of results. Successful correlations will be evaluated based on if the correlation with bioaccumulation is positive relative to ambient mercury concentrations in addition to consideration of the coefficient of determination (R^2). The coefficient of determination is frequently used in prediction of bioaccumulation and therefore will allow for a clearer comparison with previous literature (Amirbahman et al., 2013; O. Clarisse et al., 2012; Lawrence & Mason, 2001). Finally, the role of organic matter in bioaccumulation will be evaluated by normalizing bulk solid concentrations to average organic carbon concentrations across depositional environments. The correlation will be similarly evaluated and compared to the other cross-depositional bioaccumulation correlations.

Bioturbation will be evaluated by considering biogeochemical trends including oxygen depletion, and reducing conditions as seen through acid volatile sulfides, ferrous iron, and redox profiles. This will then be tied to mercury through the evaluation of methylmercury present within porewater. Oxygen depletion will be evaluated by looking at the rate of depletion between vertical concentrations at an approximated Day 0 of organism addition and an approximated Day 28 of bioturbation. The controls and the samples containing *T. tubifex* will be visually compared in order to eliminate the impacts

of electrode sensitivity between sampling events. Acid volatile sulfides and ferrous iron will be evaluated by comparing the bioturbated samples and controls by using relative depth profiled concentrations between the two sets to identify any trends. These will be compared within each depositional environment to elucidate depositional dependent concentrations, and will serve as a proxy for active reduction. The redox profile of dissolved metals will similarly compare sampling at Day 0 and Day 28 to determine any shifts in the dissolved metals redox zonation and stabilization. Finally, methylmercury in porewater will be compared between the bioturbated samples and controls at each depth. This will demonstrate any specific impacts on mercury methylation within the zone of bioturbation.

Chapter 4: Results and Analysis

4.1 SEDIMENT DEPOSITIONAL CHARACTERISTICS

For greater understanding of the correlation and bioturbation results, it is first necessary to understand the characteristics of the depositional environments studied. This will provide context throughout the analysis. The mid-channel, near-bank, and bank deposits have varying geochemistry which influences the interactions of the organisms with the sediment. These depositional environments also have varying total mercury and methylmercury concentrations in both the bulk solids and porewater which can have an overall impact on availability.

The average total mercury and methylmercury concentrations throughout the depths of all sediment mesocosms can be seen in Figure 4.1.² This is further summarized in Table 4.1. Due to variability throughout the mesocosms, any trends observed from Figure 4.1 are not statistically conclusive; however, observations can be made. The total mercury in bulk solids are relevant to assess because this is the mercury which can diffuse into porewater and then become methylated. Although geochemical factors will impact the ratios of mercury in all other forms, bulk solids serve as the initial mercury source. As seen in Figure 4.1, the bank deposits appear to have the highest total mercury in bulk solids followed by the near-bank, and mid-channel deposits. However, these concentrations are fairly similar throughout depositional environment, implying that they

² Near-Bank Control 2 was excluded from comparison in the depositional characteristics due to the potential thermal alterations to the original sediment chemistry.

are within an active receiving area of mercury impacted sediments as seen in the South River conceptual model in *Section 3.1*. The difference between the mid-channel and bank and near-bank deposits can be largely attributed to the characteristics of the particles. The mid-channel sediment is a coarser deposit which is more comparable to gravel, and thus is less likely to sorb mercury than the bank and near-bank deposits.

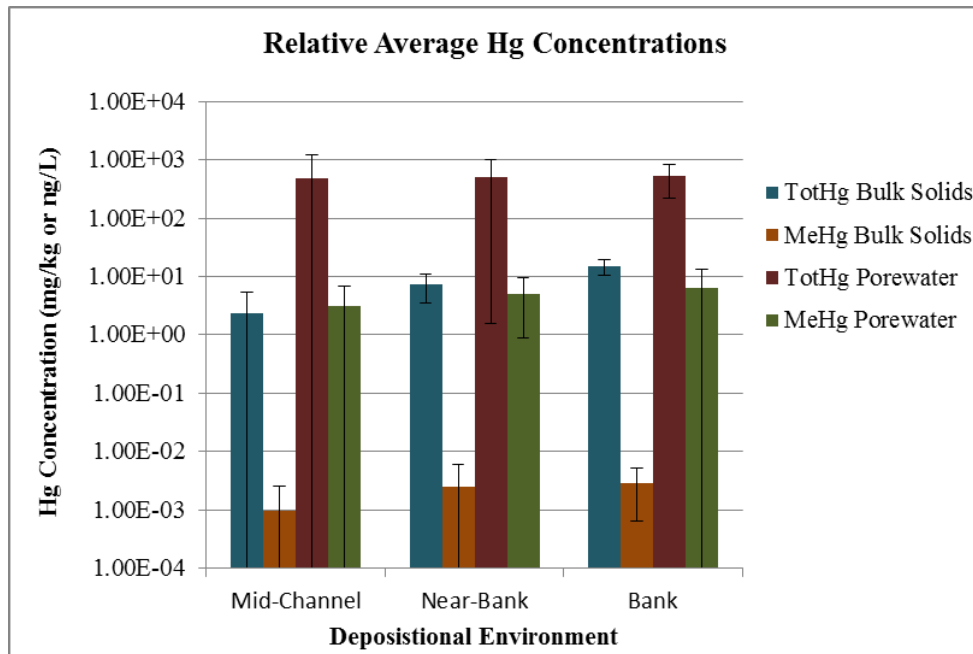


Figure 4.1: Relative concentrations of total mercury and methylmercury in bulk solids (mg/kg) and porewater (ng/L) in all three depositional environments

Table 4.1: Summary of relative total mercury and methylmercury concentrations in bulk solids and porewater in all three depositional environments

Sample	TotHg Bulk Solids		MeHg Bulk Solids		TotHg Porewater (DGTs)		MeHg Porewater (DGTs)	
	Average (mg/kg)	Standard Deviation (mg/kg)	Average (mg/kg)	Standard Deviation (mg/kg)	Average (ng/L)	Standard Deviation (ng/L)	Average (ng/L)	Standard Deviation (ng/L)
Mid-Channel	2.389E+00	2.937E+00	9.586E-04	1.671E-03	4.892E+02	7.001E+02	3.178E+00	3.753E+00
Near-Bank	7.174E+00	3.583E+00	2.531E-03	3.407E-03	5.005E+02	4.990E+02	5.137E+00	4.230E+00
Bank	1.493E+01	4.323E+00	2.966E-03	2.328E-03	5.169E+02	2.930E+02	6.454E+00	6.814E+00

The bank deposit appears to have the highest concentrations of methylmercury in bulk solids as well as the highest concentrations of total mercury and methylmercury in porewater. The near-bank deposit and mid-channel deposit sequentially follow in methylmercury bulk solids and total mercury and methylmercury porewater concentrations. Although differences between the samples are not large, the general trend of increased concentrations in the bank is largely attributed to the total mercury contained within the bulk solids, as it is linked to the overall concentrations of total porewater mercury, and through that process it increases methylmercury in porewater and bulk solids. However, while the relationship between methylmercury concentrations in porewater and bulk solids may be ranked similarly to total mercury in regards to depositional environment, the variations between the samples show different relative values. Therefore, methylmercury is not solely linked to the total mercury concentration in bulk solids.

This can be further evaluated by considering the ratio of methylmercury to total mercury (%MeHg) as seen in Figure 4.2 for porewater and bulk solids. Percent methylmercury is a quasi-first order rate of methylation, with higher percentages correlating to a greater rate of methylation. As can be seen in Figure 4.2, the near-bank sediments appear to have the highest methylmercury percentage relative to the other depositional environments although there is little statistical difference between the depositional environments. This is likely due to the total organic carbon concentrations of the sediment which directly impact microbial productivity. The average concentrations of

total organic carbon for each depositional environment (Table 4.2) indicate that organic carbon is highest in the bank deposit followed by the near-bank deposit, and is lowest in the mid-channel deposit of which the total organic carbon was below detection limits. For the resulting analyses, the detection limit was utilized for the mid-channel total organic carbon concentration in order to serve as a conservative estimate. The somewhat similar organic carbon concentrations in the bank and near-bank deposits can be used to explain the percent methylmercury in the near-bank versus the bank deposits. Both organic carbon concentrations should facilitate a microbially active community which has high methylmercury production. However, the total mercury is lower in the near-bank deposit, and thus the methylmercury production linked to carbon is greater relative to total mercury. Therefore, while overall total mercury in sediments governs mercury capable of methylation, geochemical factors such as carbon play a significant role in the relative ratios of methylated mercury. It can also be seen in Figure 4.2 that the percent methylmercury is two orders of magnitude greater in porewater than in bulk solids, demonstrating that methylmercury is less strongly sorbing to sediment.

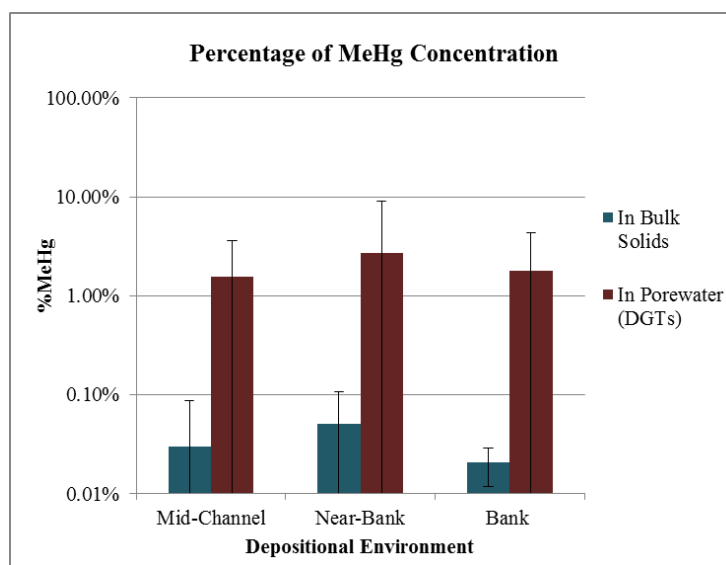


Figure 4.2: Fraction of methylmercury in bulk solids and porewater for all three depositional environments

Table 4.2: Average total organic carbon (TOC) concentrations for all three depositional environments³

Sample	Average (mg/kg)	Standard Deviation (mg/kg)
Mid-Channel	1500	0.00E+00
Near-Bank	18155	9.32E+03
Bank	31103	1.08E+04

Due to the potential relevance of geochemical factors in mercury availability and methylation, it is also important to assess acid volatile sulfides and ferrous iron throughout the sediment depth. While these values vary among mesocosms, the averages of each depositional environment can be seen in Figure 4.3 for acid volatile sulfides and Figure 4.4 for ferrous iron. In general, the near-bank deposit has the highest acid volatile

³ Mid-channel TOC concentrations were below detection limits, and thus the value given for a conservative TOC estimate is the detection limit.

sulfide concentration, followed by the bank and mid-channel deposits. These results demonstrate that methylation will likely occur in the upper 3 cm of the sediment due to the apparent acid volatile sulfide peaks, and suggest that greater reduction is occurring within the near-bank deposit. For ferrous iron, the bank sediments have the highest concentrations in the upper centimeters of the sediment profile but also similar concentrations in the near-bank and mid-channel deposits at lower depths. Since ferrous iron is fairly similar between all deposits, this demonstrates that partial reduction is occurring throughout the sediment profiles.

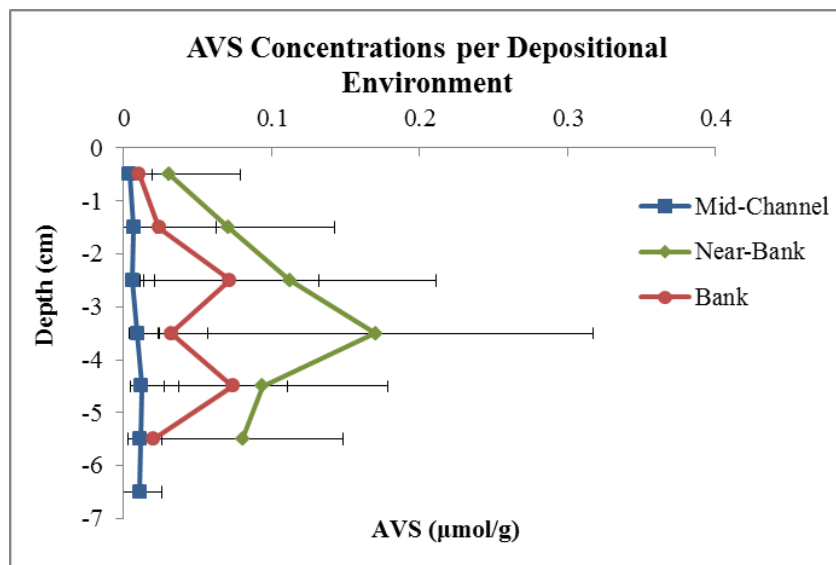


Figure 4.3: Average acid volatile sulfides concentrations at each depth per depositional environment

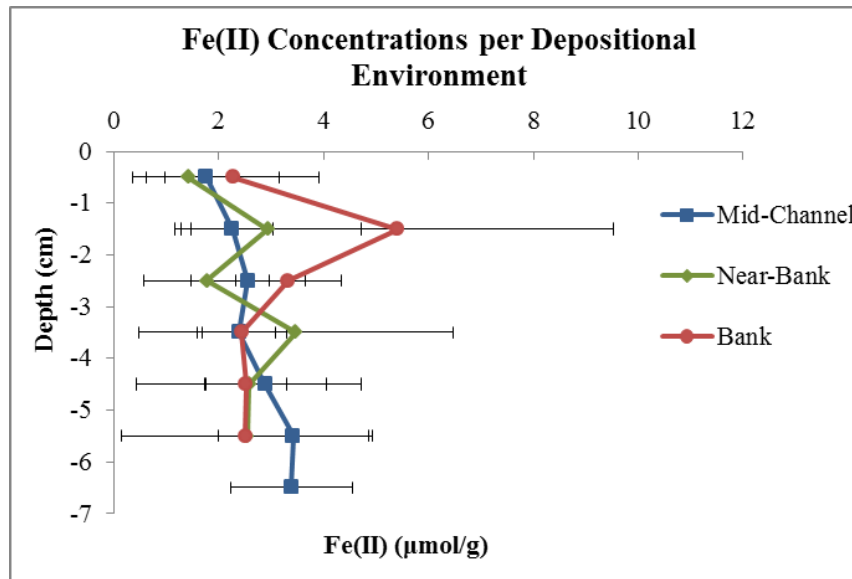


Figure 4.4: Average ferrous iron concentrations at each depth per depositional environment

However, for both acid volatile sulfides and ferrous iron, the concentrations in all depositional environments are within the lower range of the calibration curve, with the acid volatile sulfides of the mid-channel deposit near the detection limit. Due to the low concentrations of acid volatile sulfides and ferrous iron, this suggests that only mild reduction is occurring within the sediments which may contribute to lower methylmercury concentrations. In addition, the low concentrations of acid volatile sulfides may also suggest that solid phase mercury is not sorbed to an appreciable extent to insoluble sulfides and may be more bioavailable through complexation with oxides.

4.2 BIOACCUMULATION CORRELATION

The bioaccumulation of total mercury and methylmercury can be correlated with the upper 4 cm of sediment and porewater concentrations. This range was determined empirically to be the main zone of *T. tubifex* exposure. Often in bioaccumulation studies, concentrations are normalized to lipid concentrations within each sample. However, results show an overall consistency in lipid concentrations, and thus they will not be considered within the correlations assessed. The similarity in lipid concentrations can be seen for one representative sample set of each depositional environment in Table 4.3.

Table 4.3: Lipid concentrations of a representative sample from each depositional environment and the *T. tubifex* culture

Sample Name	Lipids (g/g wet weight)
Mid-Channel Sample 1	0.0197
Near-Bank Sample 2	0.0216
Bank Sample 1	0.0276
Day 0 (from culture)	0.0264

To evaluate correlations, total mercury bioaccumulation will be compared to total mercury concentrations in porewater and bulk solids. Methylmercury bioaccumulation will be compared to methylmercury concentrations in porewater and bulk solids in addition to total mercury concentrations in porewater and bulk solids. Methylmercury is compared to a wider breadth of samples because methylation is influenced by the total mercury available.

Bioaccumulation will be evaluated in several contexts. First of all, the overall bioaccumulation will be assessed to determine that total mercury and methylmercury are bioaccumulating relative to ambient conditions. The amount of methylmercury bioaccumulation relative to total mercury bioaccumulation will also be evaluated to determine if correlations are feasible. Next, the bioaccumulation correlation will be considered across depositional environments. This will be the main assessment of both techniques' capacity to broadly predict bioaccumulation. Finally, for further depth of analysis, bioaccumulation will be considered within each depositional environment in order to eliminate any external biogeochemical or physical influences on DGT measured porewater and bulk solid sampling.

4.2.1 Overall Bioaccumulation

The total mercury and methylmercury bioaccumulation in *T. tubifex* can be compared directly to bulk sediments due to the similar units utilized. It can be seen in Figure 4.5 that both total mercury and methylmercury concentrate in the organisms by one-two orders of magnitude relative to ambient sediment concentrations. As total mercury and methylmercury concentrations in bulk solids are greater than concentrations in porewater, it can be assumed that total mercury and methylmercury are bioaccumulating relative to porewater concentrations as well. This validates that bioaccumulation of both total mercury and methylmercury is occurring, and thus correlations can be assessed.

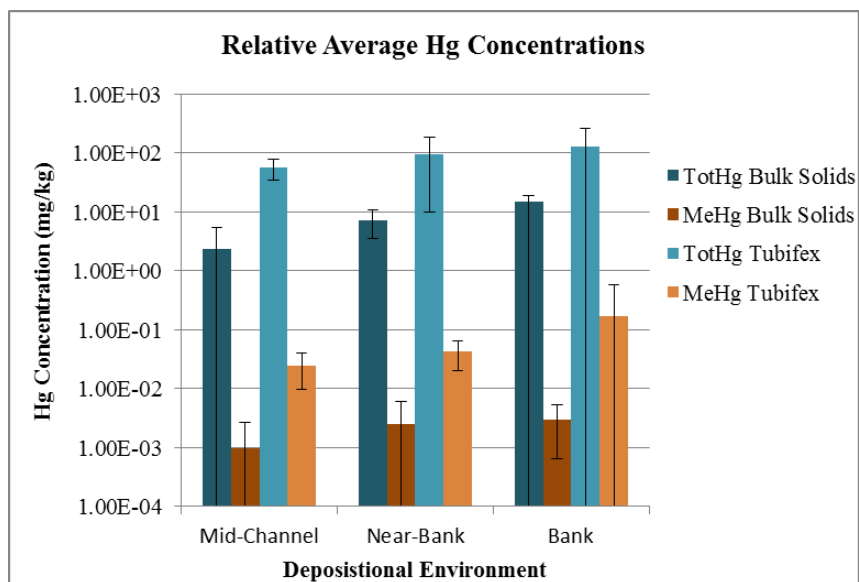


Figure 4.5: Relative total mercury and methylmercury concentrations in bulk solids and *T. tubifex*

Similar to the analysis of bulk solids and porewater, the percent methylmercury which accumulates in the organisms can also be considered. This can be seen relative to bulk sediment and porewater in Figure 4.6. It can be noted that there is only a small fraction of methylmercury relative to total mercury which has bioaccumulated within the *T. tubifex*, as the percent methylmercury ranges from 0.07% to 0.10% with large standard deviations. Due to this low methylmercury fraction within a small sample size, in addition to potential demethylation of mercury from the *T. tubifex* depuration, it can be assumed that methylmercury will be variable and it will not be easy to correlate methylmercury porewater or bulk sediment. Therefore, the majority of the analysis will focus on the potential for total mercury DGT measured porewater and bulk solid sampling to gauge bioavailability of total mercury to *T. tubifex*.

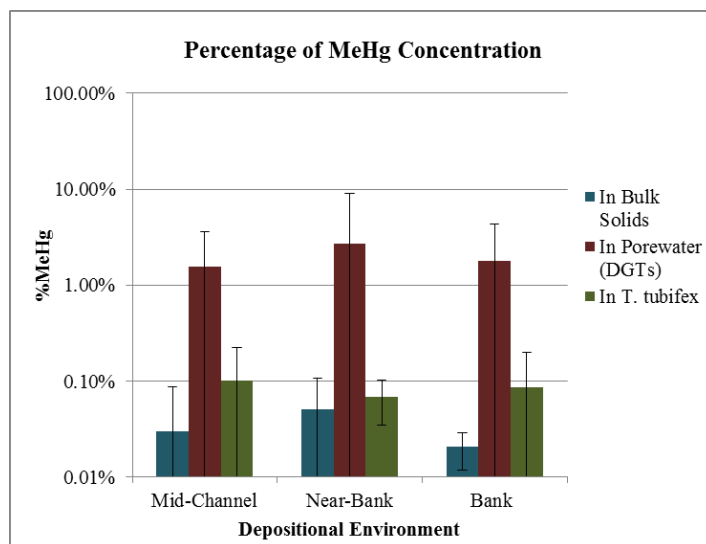


Figure 4.6: Fraction of methylmercury in bulk solids, porewater, and *T. tubifex*

4.2.2 Correlation Across Depositional Environments

The robust capacity of both DGTs and bulk solids to predict bioaccumulation must be considered because field sites will have variable environments. Application across depositional environments will most accurately depict the capacity of both sampling techniques to estimate bioaccumulation. In addition to the direct comparison of bioaccumulation with porewater and bulk solids, bulk solid concentrations were also normalized to organic carbon to account for any influences of organic matter. If biogeochemical factors do not directly impact bioaccumulation, it is expected that sampling of porewater and bulk solids should positively correlate with bioaccumulation. This was evaluated for both sampling techniques. For all analysis within this section, due

to variable concentrations relative to the sample mean, Bank Sample 3 was discarded as an outlier.

4.2.2.1 Total Mercury Bioaccumulation

The bioaccumulation of total mercury as correlated to porewater mercury can be seen in Figure 4.7 with each discrete point representing averaged concentrations in a mesocosm. It can be seen that there is a positive correlation with DGT measured total mercury in porewater, and that the coefficient of determination suggests that this correlation describes approximately 50% of the variability. The total mercury bioaccumulation in organisms versus bulk solids can be seen in Figure 4.8. This also shows a positive correlation, with a slightly higher coefficient of determination. However, given the variability within each mesocosm, the difference in coefficient of determination is insignificant, and this demonstrates a similar capacity of DGT measured porewater to estimate bioaccumulation. Therefore, DGTs may serve as beneficial method to predict total mercury bioaccumulation in a breadth of environments; however, this variability in the data is too large to be definitive.

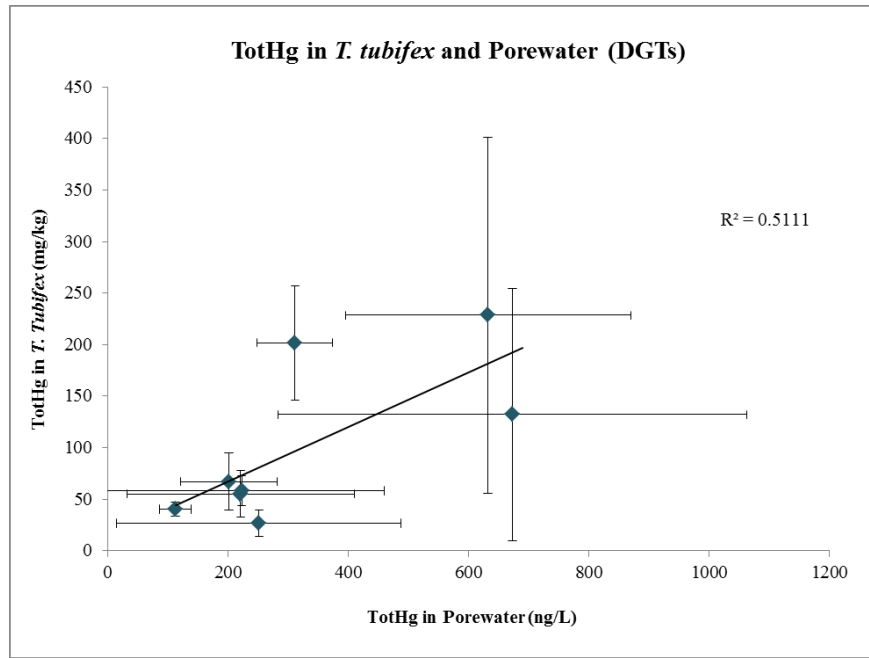


Figure 4.7: Total mercury bioaccumulation in *T. tubifex* with total mercury in porewater across mesocosms

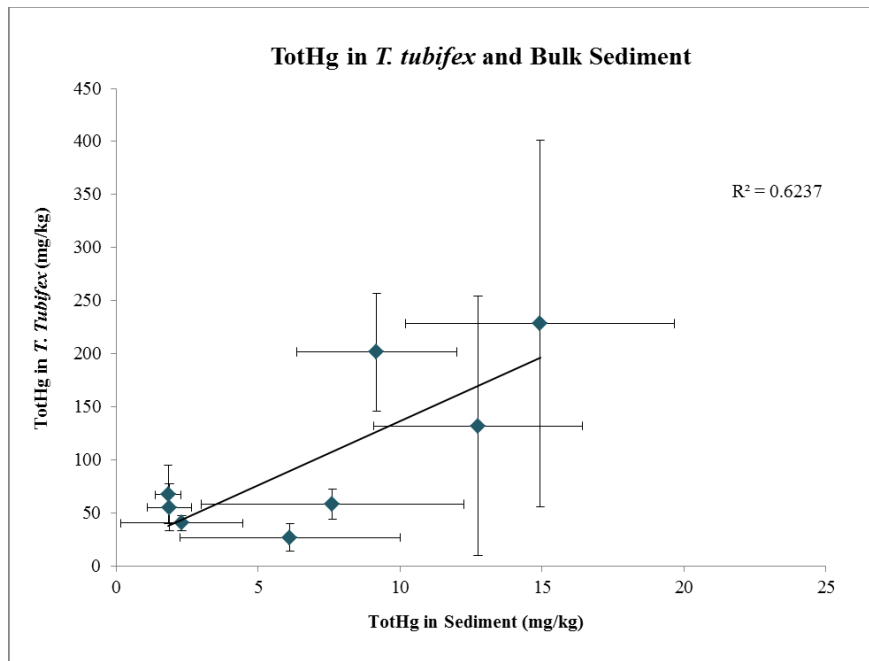


Figure 4.8: Total mercury bioaccumulation in *T. tubifex* with total mercury in bulk solids across mesocosms

4.2.2.2 Methylmercury Bioaccumulation

Correlations with methylmercury bioaccumulation were also evaluated, and as expected a weaker correlation was evident due to low relative bioaccumulation. The relationship between methylmercury bioaccumulation and methylmercury in porewater and bulk solids can be seen in Figure 4.9 and Figure 4.10, respectively. The correlation between methylmercury bioaccumulation and total mercury in porewater and bulk solids can also be seen in Figure 4.11 and Figure 4.12, respectively. In all four comparisons, the correlation is positive, suggesting that while the methylmercury bioaccumulation is not entirely clear, it is represented in varying degrees by total mercury and methylmercury in DGTs and bulk sediment. Again, however, the variability is too high to draw definitive conclusions.

It appears that both total mercury porewater and bulk solids are superior at predicting methylmercury bioaccumulation. Again, although the coefficient of determination is slightly higher for bulk solid correlation, given the variability within the samples, this is not significant. The correlation of methylmercury with total mercury in porewater and bulk solids is logical. As total mercury in porewater governs the mercury available for methylation, it is likely that it would correlate to methylmercury in porewater and solids which are then uptaken by *T. tubifex*. Total mercury on bulk solids also correlates to this available porewater total mercury due to the limited influences of complexation with insoluble sulfides in these depositional environments, as seen by the low concentrations of acid volatile sulfides in *Section 4.2.1*.

Within this sampling, the graphical distribution suggests that there are similar trends between the correlation of methylmercury bioaccumulation with total mercury in porewater and in methylmercury bioaccumulation with methylmercury in bulk solids. If variability were reduced, this could imply that DGT measured total mercury in porewater is also correlated with the methylmercury produced and sorbed onto bulk solids. As this would fit the model of methylation, this strengthens the theory that DGTs measure the microbial available fraction of mercury.

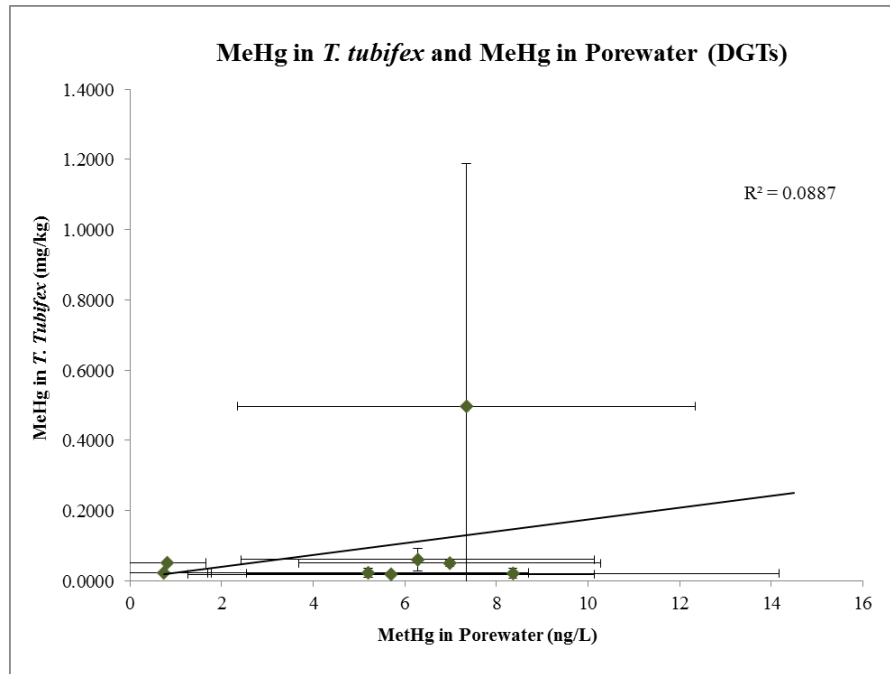


Figure 4.9: Methylmercury bioaccumulation in *T. tubifex* with methylmercury in porewater across mesocosms

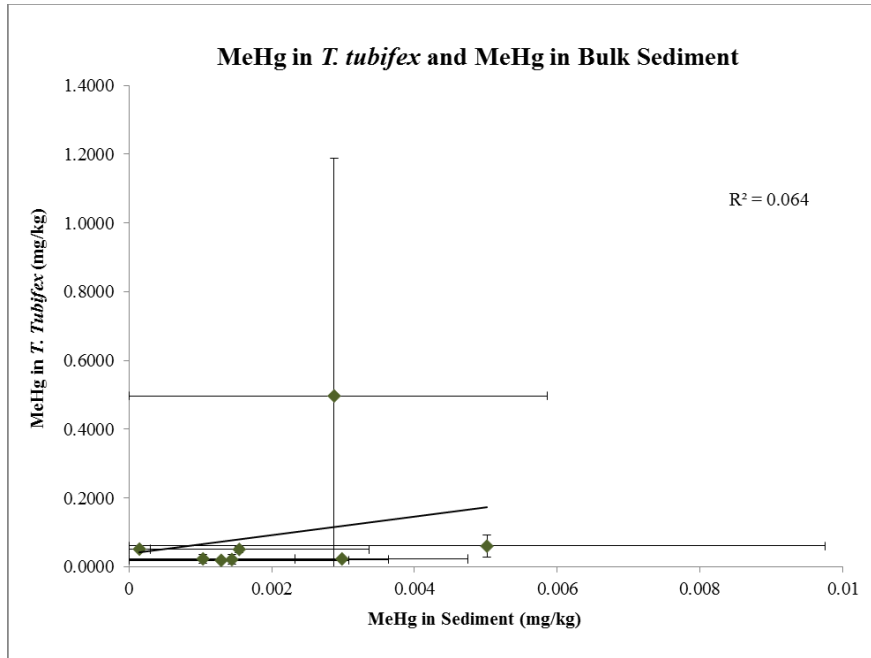


Figure 4.10: Methylmercury bioaccumulation in *T. tubifex* with methylmercury in bulk solids across mesocosms

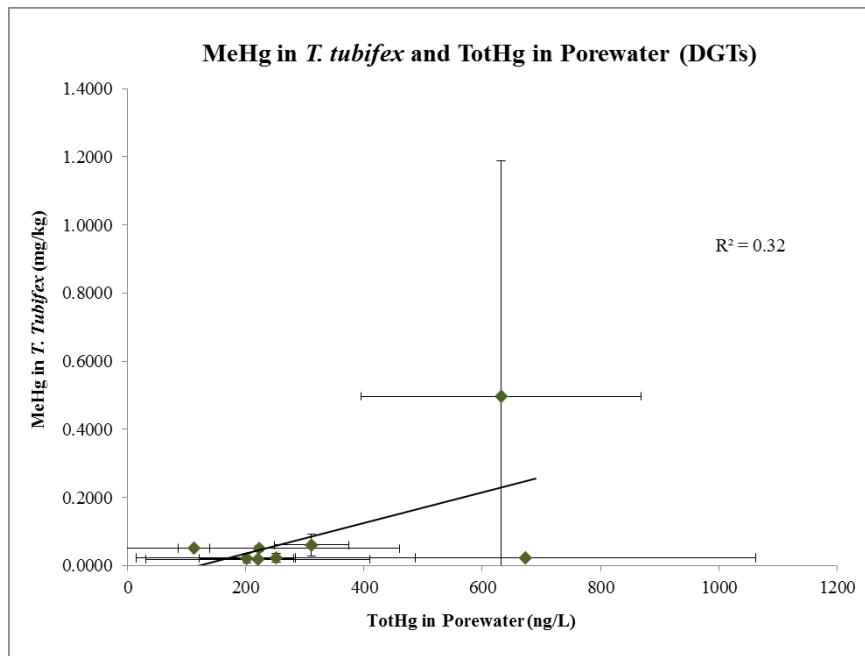


Figure 4.11: Methylmercury bioaccumulation in *T. tubifex* with total mercury in porewater across mesocosms

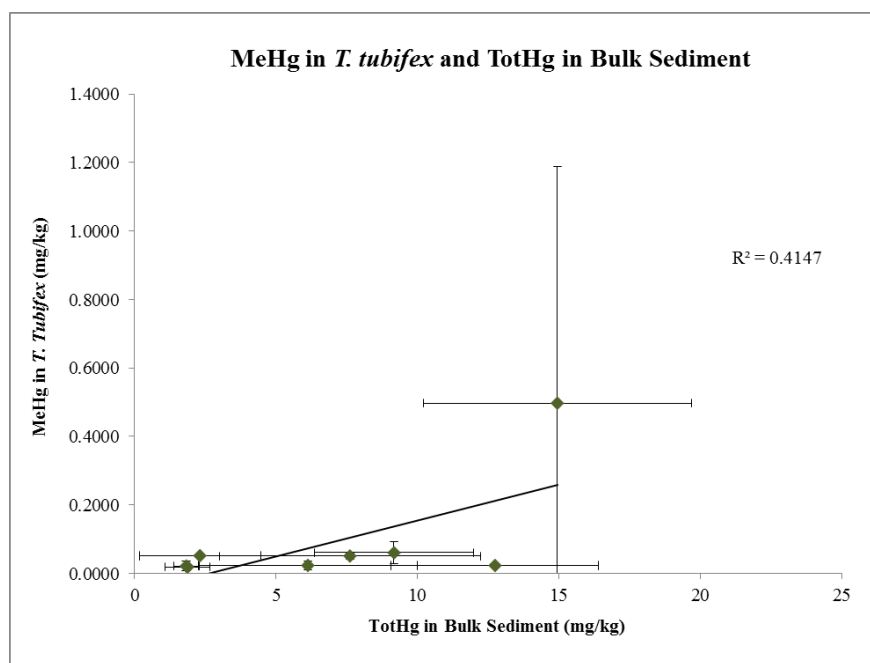


Figure 4.12: Methylmercury bioaccumulation in *T. tubifex* with total mercury in bulk solids across mesocosms

4.2.3.3 The Role of Organic Matter in Bioaccumulation

Finally, the role of organic carbon can be considered in correlation with bioaccumulation. The total mercury bioaccumulation correlated with total mercury in bulk solids normalized by organic carbon can be seen in Figure 4.13. The methylmercury bioaccumulation correlated with methylmercury and total mercury normalized by organic carbon can be seen in Figure 4.14 and Figure 4.15, respectively. It is expected that if organic carbon played a role in bioaccumulation, as expected for *T. tubifex*, that normalizing by organic carbon would create a positive correlation with a superior coefficient of determination. This is especially applicable within these depositional

environments due to the large range of organic carbon between the mid-channel deposit and the bank and near-bank deposits. However, as seen in Figures 4.12-4.14, the correlations between bioaccumulation and organic carbon normalized bulk solids are negative. This is most likely attributed to the particle distribution in the mid-channel deposit. Because the particles within the mid-channel deposit are coarse, there are few particles of a diameter which the *T. tubifex* can consume. This is the reason that a potting soil cap had to be added to the mid-channel deposit mesocosms. Due to this, bioaccumulation is linked only to the smallest particle size which is not necessarily represented by the organic carbon within the entire sample. Therefore, organic carbon may still play a role in bioaccumulation; however, due to the depositional environments used within this study, there is not a good correlation with normalizing bulk solids by organic carbon. This also illustrates a deficiency in use of bulk solids for measurements. As it is well established that organic matter has a role in bioaccumulation within benthic organisms, in many sediment matrices it is necessary to determine organic carbon concentrations in addition to the bulk solid concentrations (Chen et al., 2009; Lawrence & Mason, 2001; C. J. Watras et al., 1998). However, given the challenges of accurately measuring the consumable organic carbon within certain depositional environments, this would reduce the capacity of bulk solids to predict bioaccumulation. The uptake by DGTs; however, would not be influenced by organic carbon as complexation with dissolved particles will slow diffusion of mercury and thus would likely correlate with the low bioaccumulation seen.

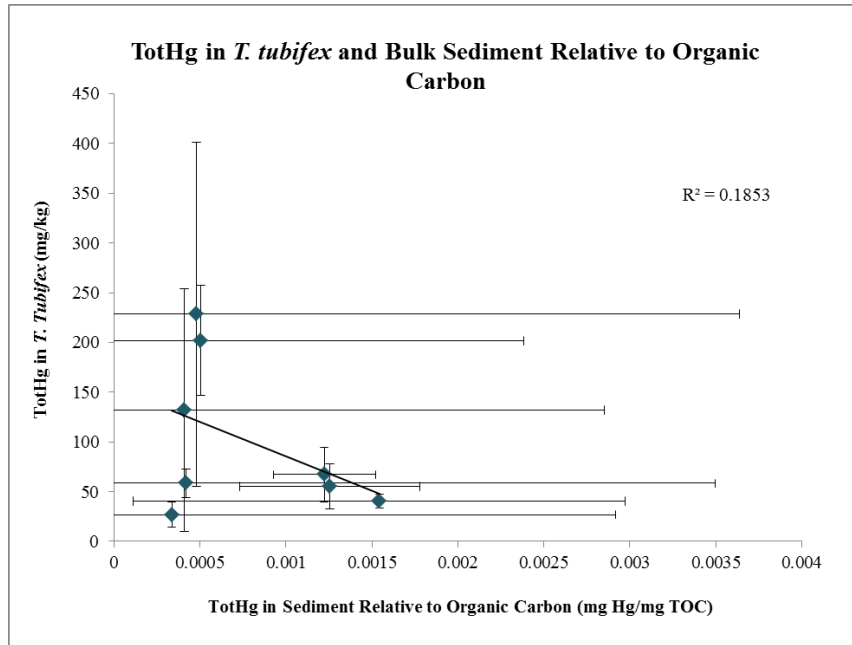


Figure 4.13: Total mercury bioaccumulation in *T. tubifex* with total mercury in bulk solids normalized to organic carbon across mesocosms

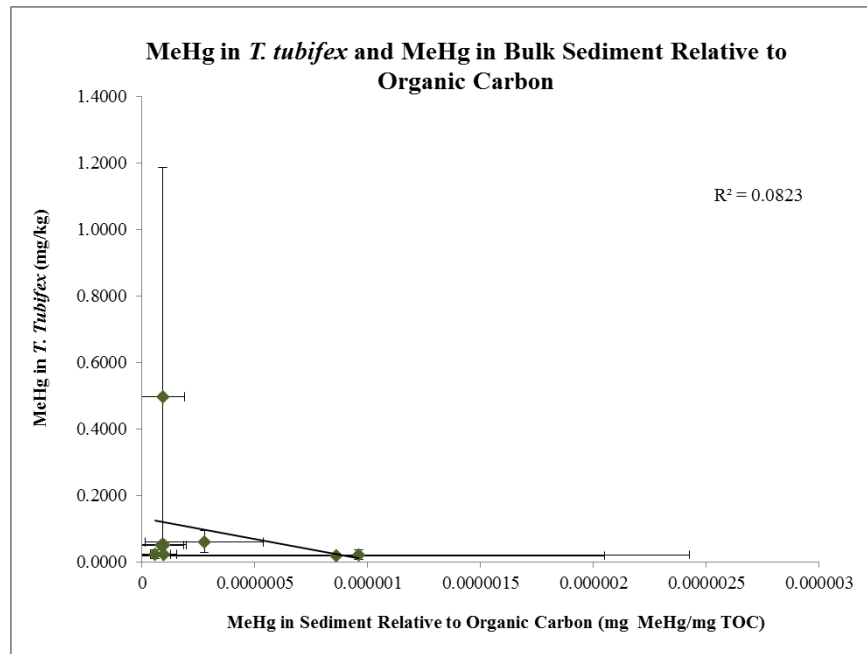


Figure 4.14: Methylmercury bioaccumulation in *T. tubifex* with methylmercury in bulk solids normalized to organic carbon across mesocosms

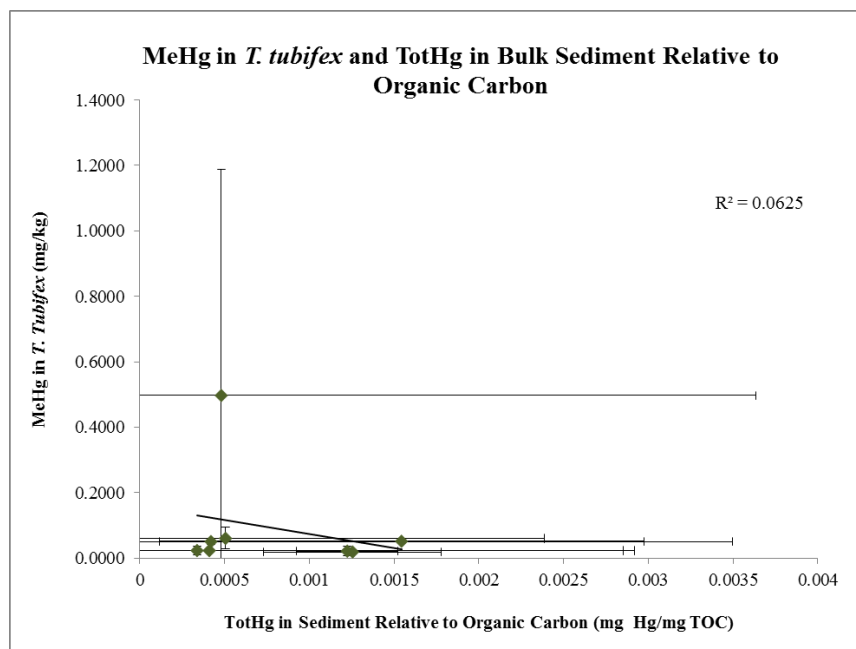


Figure 4.15: Methylmercury bioaccumulation in *T. tubifex* with total mercury in bulk solids normalized to organic carbon across mesocosms

4.2.2.4 Summary

The coefficients of determination for the bioaccumulation across depositional environments can be seen in Table 4.4. Within this table, negative correlations are highlighted and demonstrate that these correlations cannot be used to predict bioaccumulation. For this sediment matrix, it was demonstrated that both DGT measured total mercury in porewater and bulk solid measurements of total mercury provide reasonable correlations to bioaccumulation with some variability in the data. Both methods performed similarly within this context. The methylmercury, as a low fraction of the *T. tubifex* body burden, was more difficult to correlate.

It was expected that the bioaccumulation correlations would be improved by normalizing bulk solids concentrations by the organic carbon within each depositional environment. However, within this matrix the organic carbon normalization created a poorer correlation. Although this deviation from expectations was largely attributed to difficulties in measuring the organic carbon available to the organism as based on particle size, this has negative implications for the use of bulk solid measurements in other sediment matrices. If organic carbon plays a large role in bioaccumulation, bulk solids may need to be normalized by organic carbon in order to provide a logical correlation. Yet, this is not feasible if available organic carbon cannot be measured.

In addition, within this sediment matrix, total mercury on bulk solids correlated with methylmercury bioaccumulation. However, this correlation is likely unique to this specific sediment matrix due to the low reduction and low concentration of acid volatile sulfides seen within the depositional environments which allowed the mercury associated with solids to be more bioavailable. Therefore, it can be concluded that DGT measured total mercury in porewater is as reasonable a means to predict bioaccumulation; however, the capacity of bulk solid measured total mercury can only be concluded to be a functional predictor of bioaccumulation within this sediment matrix.

Table 4.4: The coefficients of determination for correlations of total mercury and methylmercury correlations across depositional environments, highlighted values represent negative correlations

Bioaccumulation	TotHg in Porewater (DGTs)	TotHg in Bulk Solids	TotHg in Bulk Solids Relative to TOC	MeHg in Porewater (DGTs)	MeHg in Sediment Bulk Solids	MeHg in Bulk Solids Relative to TOC
TotHg Tubifex	0.5111	0.6237	0.1853			
MeHg Tubifex	0.3200	0.4170	0.0625	0.0887	0.0640	0.0823

It could be considered that variability in the data would serve as a comparison of the DGT and bulk solid sampling types. However, this is not applicable due to the conceptual variation in the samples. It can be seen in all Figures 4.7 and Figure 4.11 that porewater total mercury as measured by DGTs has a greater standard deviation, relative to the mean, than bulk solid total mercury. This is because porewater concentrations vary by depth as attributed to the spatially varied chemistry. Bulk solid total mercury, on the other hand, should not vary significantly within the depth studied, especially as the samples were homogenized prior to mesocosm construction. As the samples being considered (0-4 cm) are depth averaged, this leads to an innate variability in porewater but not bulk solids. Therefore, for total mercury, the scatter cannot help to validate or invalidate either sampling technique. For methylmercury, relative standard deviations are similar between porewater and bulk solids as both sample types will vary by depth.

4.2.3 Correlation at the Depositional Level

In order to eliminate the influence of biogeochemical factors including organic carbon and physical factors such as particle distribution on bioaccumulation, the capacity for bioaccumulation prediction can be further assessed within each depositional environment. This section will consider the mid-channel, near-bank, and bank samples separately. Because within each depositional environment, only available mercury concentrations should impact bioaccumulation, for a correlation to be viable it must be positively correlated. Similar to *Section 4.2.2*, it is expected that methylmercury will be more difficult to correlate.

4.2.3.1 Total Mercury Bioaccumulation

Within the mid-channel deposit, total mercury bioaccumulation can be considered relative to the total mercury concentrations in DGT measured porewater and bulk sediment. It can be seen in Figure 4.16, that bioaccumulative correlation with porewater is positively correlated, whereas it is negatively correlated with bulk solids. Although the coefficient of determination is greater for bulk sediment, only the correlation with DGT measured porewater is logical, and thus the bulk solids total mercury do not serve as a viable estimator of total mercury bioaccumulation in the mid-channel deposit.

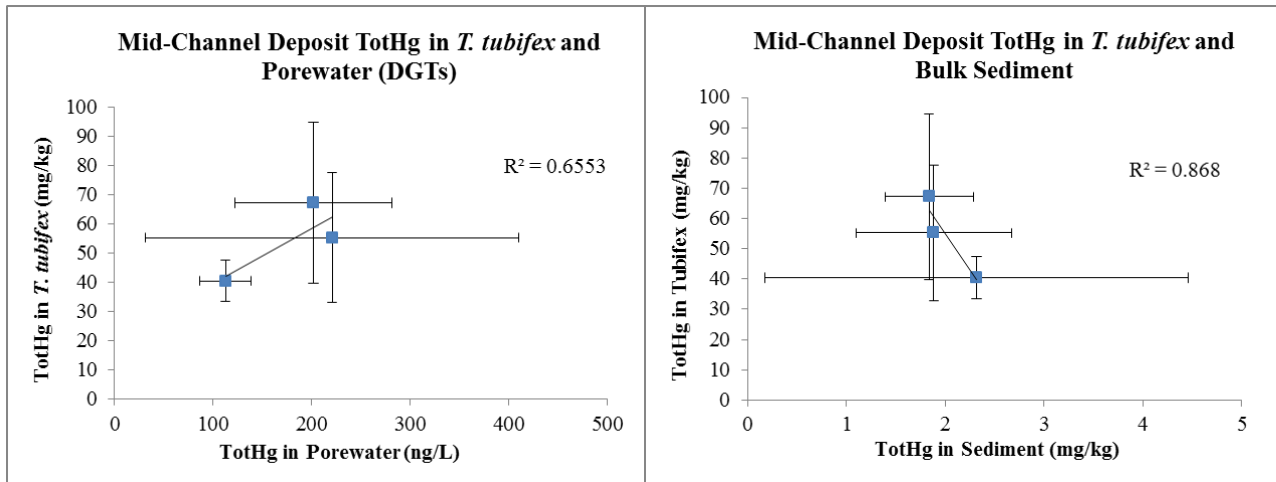


Figure 4.16: Total mercury bioaccumulation in *T. tubifex* with bulk solids and porewater in the mid-channel deposit

A similar comparison can be considered for near-bank sediment as seen in Figure 4.17. In this depositional environment it can be seen that both DGT measured porewater and bulk sediment yield similar positive correlations with total mercury bioaccumulation. Both correlations have similar coefficients of determination, and thus both sampling techniques function to predict bioaccumulation within the near-bank deposit. However, the slopes of the regression lines for this data is very steep in both cases which suggests that it may not be possible to apply this correlation, especially at low concentrations.

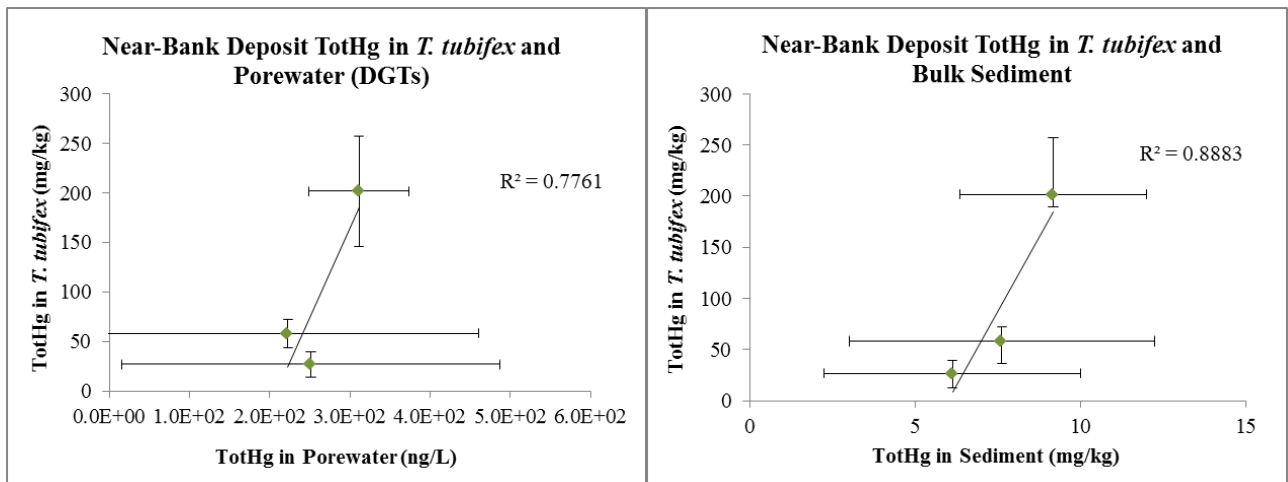


Figure 4.17: Total mercury bioaccumulation in *T. tubifex* with bulk solids and porewater in the near-bank deposit

Finally for the bank deposit, both sampling techniques can be compared as seen in Figure 4.18. For the bank deposit, only total mercury in sediment is positively correlated with a low coefficient of determination. However, when considering the total mercury correlation with porewater, it can be seen that all samples lie within a similar porewater range, and thus the negative correlation is likely attributed to variability in the bank bioaccumulation samples. From analysis of this variation, it is likely that the bioaccumulation in Bank Sample 3 is an outlier relative to the mean and skews this analysis towards a negative trend. Due to its variation as a sample, Bank Sample 3 was removed from the analysis in Section 4.2.2. However, because of the variability within this mesocosm, it is also difficult to conclude the applicability of either sampling technique.

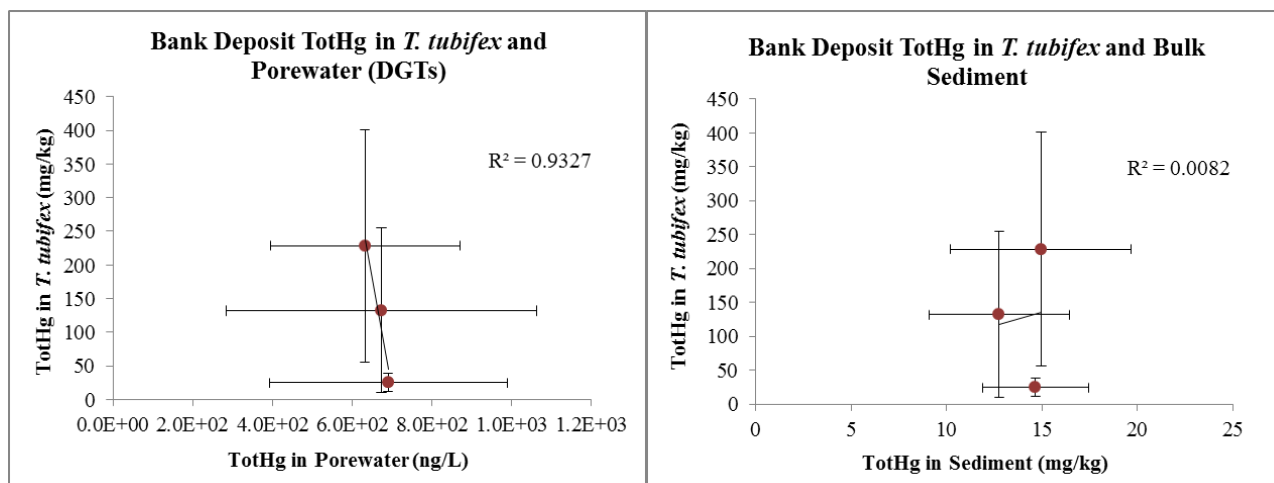


Figure 4.18: Total mercury bioaccumulation in *T. tubifex* with bulk solids and porewater in the bank deposit

4.2.3.2 Methylmercury Bioaccumulation

Methylmercury bioaccumulation was also analyzed. The bioaccumulation of methylmercury relative to total mercury and methylmercury in porewater and bulk solids in the mid-channel deposit can be seen in Figure 4.19. It can be seen in this figure that only bioaccumulation with total mercury in bulk solids is positively correlated. This correlation has a high coefficient of determination and thus is a good correlation; however as the slope is steep this correlation may not function at lower concentrations. Similar to observations in *Section 4.2.2*, this correlation was not expected. Additionally similar to the cross-depositional correlation, within this set, the methylmercury bioaccumulation correlation with total mercury in the porewater and the methylmercury bioaccumulation correlation with methylmercury on bulk solids appear very similar. Conversely, the correlation of methylmercury bioaccumulation with total mercury in porewater does not follow cross-depositional trends. However, this negative correlation

may be explained by consideration of *T. tubifex*. Concentrations are higher in porewater under more reducing zones where oxygen is depleted; however, *T. tubifex* require oxygen for respiration. If the DGTs are measuring zones of high reduction, this may be at a depth to which the organism avoids and is not actively exposed. Therefore, if high reduction is seen in porewater, the zone of exposure may need to be reassessed before conclusions can be drawn about correlation.

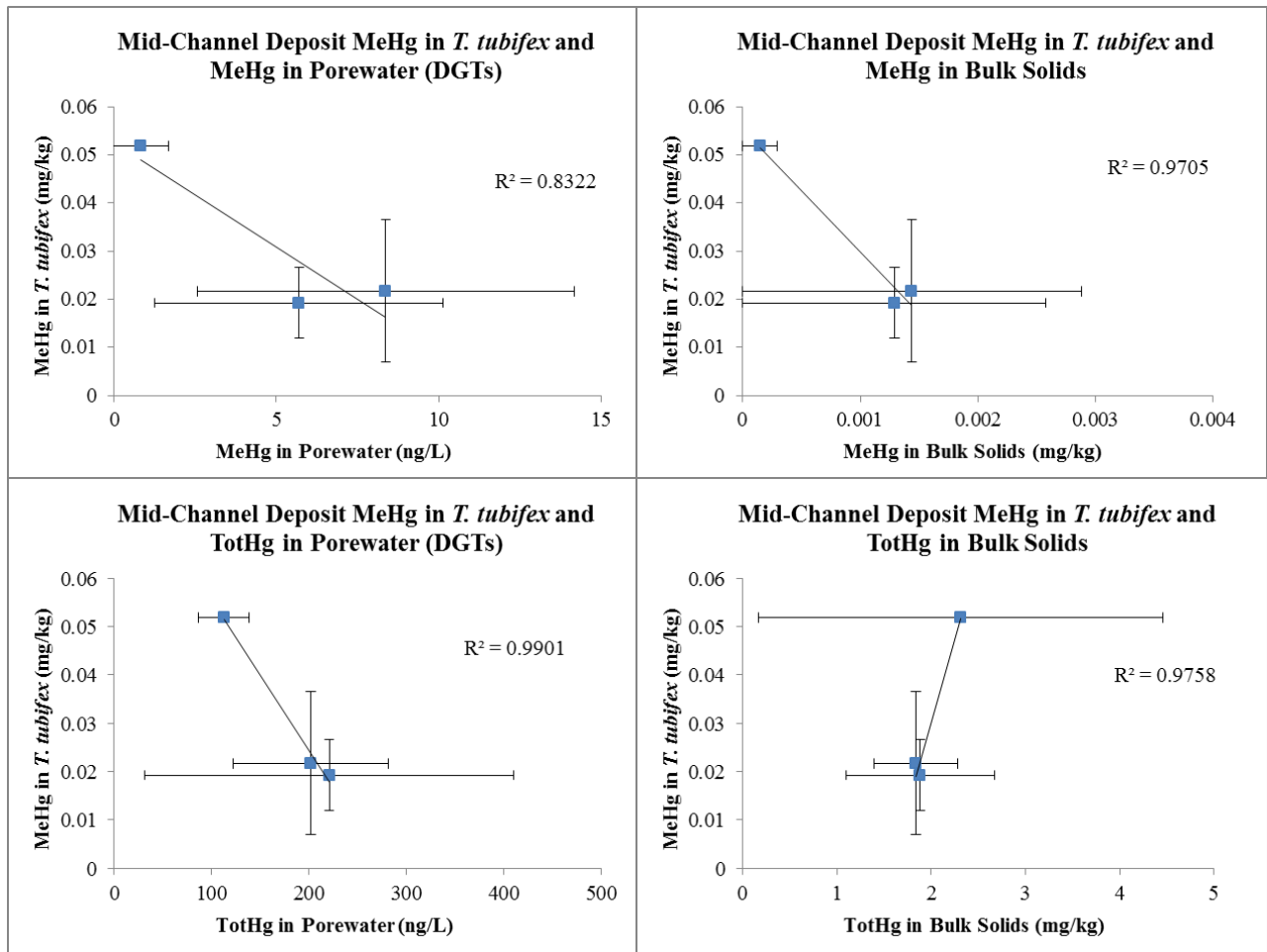


Figure 4.19: Methylmercury bioaccumulation in *T. tubifex* with total mercury and methylmercury in bulk solids and porewater within the mid-channel deposit

The methylmercury bioaccumulation within the near-bank deposit was analyzed as seen in Figure 4.20. For the near-bank deposit, both methylmercury in porewater and bulk solids positively correlate with relatively high coefficients of determination. Methylmercury bioaccumulation also positively correlates with total mercury in porewater and total mercury in bulk solids with a clearer correlation to bulk solids. Although a good correlation was not expected from methylmercury bioaccumulation data, it is logical that there are clear correlations with methylmercury in porewater and methylmercury in bulk solids as presented in *Section 4.2.3.3*. This may be represented only in the near-bank sediment due to various factors. It is possible that the methylmercury data was better of higher quality and correlated better due to the productivity of the near-bank sample, with a higher percentage methylmercury in both the porewater and the bulk solids. This may also be attributed to the particle size consumed by the organism. Within the near-bank sediment, the *T. tubifex* community appeared healthy based on body size and density, and this likely because the all of the organic matter present was at a particle size accessible to the organism. This may also have contributed to a reduced variability in bioaccumulation and body burden. However, this is speculative.

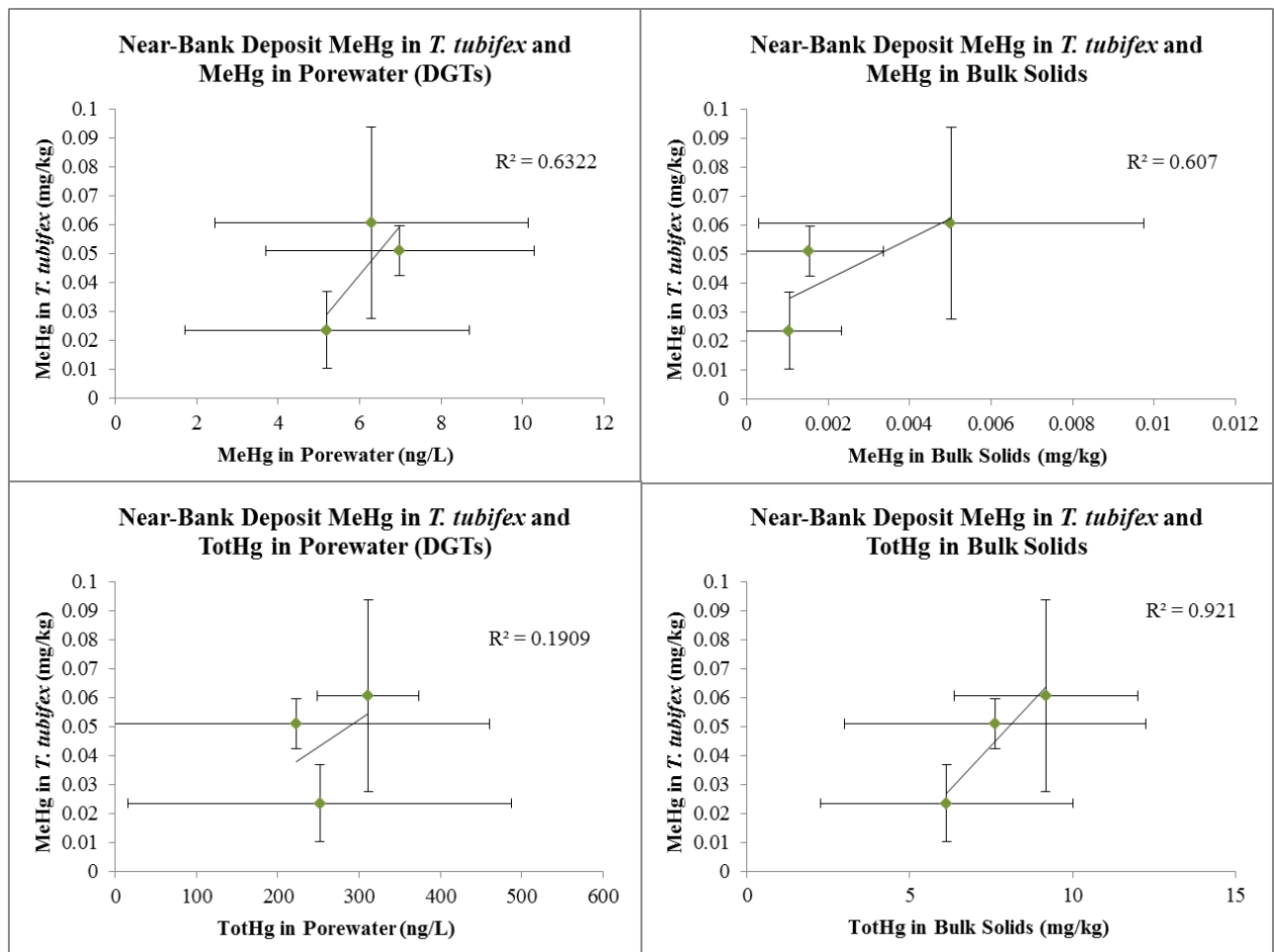


Figure 4.20: Methylmercury bioaccumulation in *T. tubifex* with total mercury and methylmercury in bulk solids and porewater within the near-bank deposit

Finally, the methylmercury bioaccumulation within the bank was evaluated as seen in Figure 4.21. The bioaccumulation within the bank sediment demonstrates the greatest inconsistency and is likely linked to variability in bioaccumulation. Due to this inconsistency, as well as an attempt to minimize variation between total mercury and methylmercury analyses, Bank Sample 3 was discarded as an outlier in cross-depositional methylmercury bioaccumulation. From Figure 4.21 it is seen that only total mercury in

bulk solids is positively correlated with methylmercury bioaccumulation which may be linked to variability in the sampling or an inaccurate depth of exposure. Again, comparison of the shape of the methylmercury bioaccumulation correlation with methylmercury in bulk solids to the methylmercury bioaccumulation correlation with total mercury in porewater demonstrates that the graphs have a similar shape which strengthens the relationship between these two measurements.

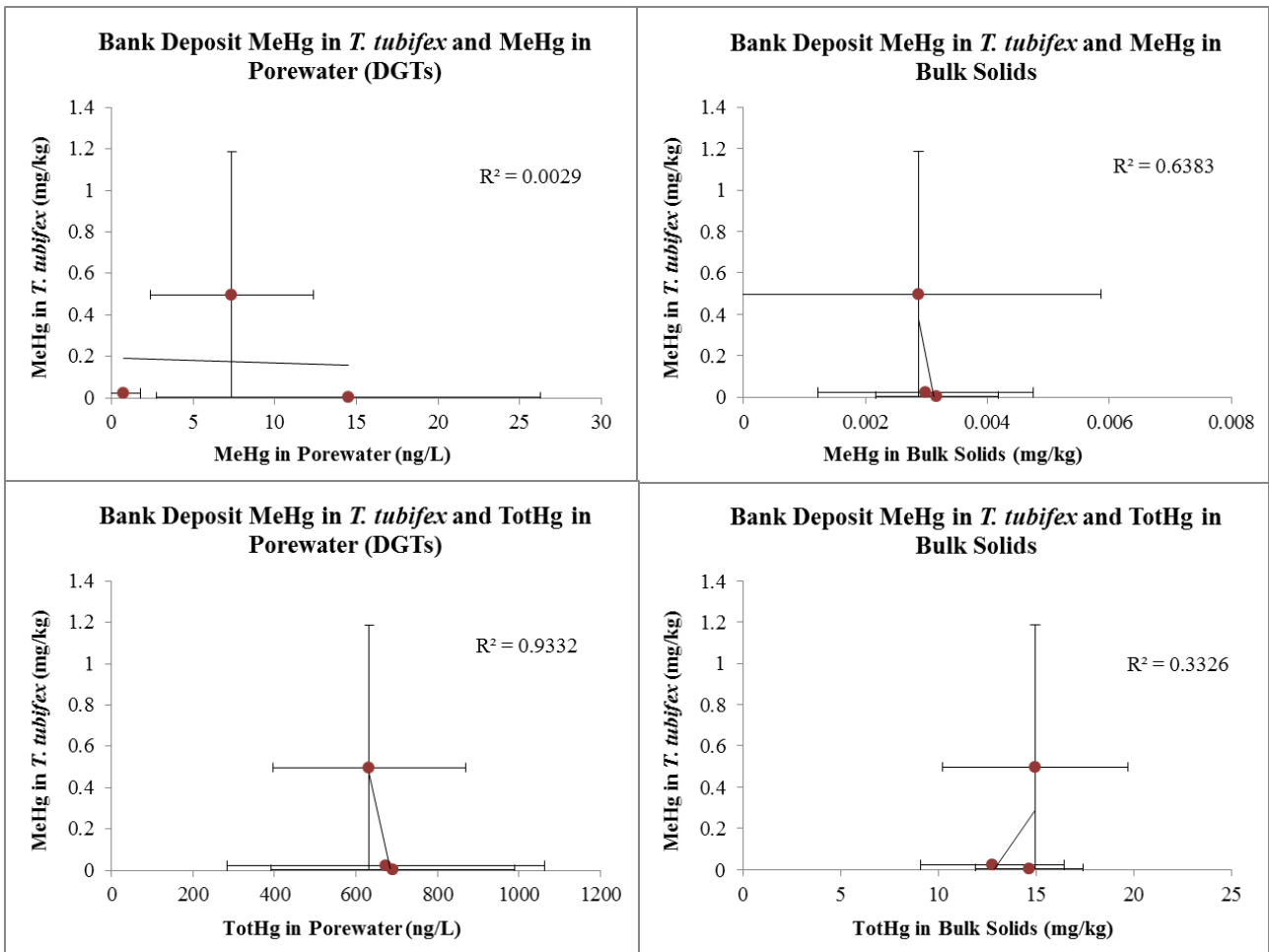


Figure 4.21: Methylmercury bioaccumulation in *T. tubifex* with total mercury and methylmercury in bulk solids and porewater within the bank deposit

4.2.3.3 Summary

The summary of coefficients of determination can be seen in Table 4.5. Negative correlations are highlighted within the table as insufficient correlations for prediction of bioaccumulation. The small variability of values within each depositional environment and large variability within the measurements complicated correlation analysis and thus while multiple points were illustrated through this analysis, cross-depositional correlation is a more accurate depiction of the capacity of DGTs and bulk solids to predict bioaccumulation.

However, it was consistently seen that DGT measured total mercury in porewater has a potential for predicting total mercury bioaccumulation. This follows with the cross-depositional correlation and shows that this sampler also has application in homogenous depositional environments. For methylmercury bioaccumulation, correlation is scattered due to the relatively low bioaccumulation in the organisms. In certain applications, DGT measured methylmercury and total mercury are capable of predicting bioaccumulation; however, in other depositional environments, only total mercury in bulk solids allow for correlation to occur. Similar to cross-depositional correlation, bulk solid measured total mercury was capable of predicting total mercury and methylmercury bioaccumulation in most environments. Again, it is expected that the low reduction and complexation with sulfides allowed for a more direct correlation between total mercury on bulk solids and methylmercury bioaccumulation.

The methylmercury bioaccumulation further validates the capacity of DGTs to measure the microbial bioavailable fraction of total mercury in porewater. As seen in the mid-channel deposit, the bank-deposit, and the cross-depositional correlation, there was a clear similarity in shape of correlation between methylmercury bioaccumulation with total mercury in porewater and methylmercury in bulk solids. This is logical as porewater total mercury governs availability of mercury to microbes for methylation, and thus total mercury in porewater should be similar to methylmercury which sorbs on to solids. The fact that DGTs were capable of representing this connection strengthens the conceptual use of the passive sampler, and thus independent of its link to bioaccumulation, it does demonstrate microbial mercury bioavailability.

Table 4.5: Coefficients of determination for correlation at the depositional level, with highlighted negative correlations

Depositional Environment	Bioaccumulation	TotHg in Porewater (DGTs)	TotHg in Bulk Solids	MeHg in Porewater (DGTs)	MeHg in Sediment Bulk Solids
Mid-Channel	TotHg Tubifex	0.6553	0.8680		
	MeHg Tubifex	0.9901	0.9758	0.8322	0.9705
Near-Bank	TotHg Tubifex	0.7761	0.8883		
	MeHg Tubifex	0.1909	0.9210	0.6322	0.6070
Bank	TotHg Tubifex	0.9327	0.0082		
	MeHg Tubifex	0.9332	0.3326	0.0029	0.6383

4.3 BIOTURBATION

In order to assess potential geochemical impacts of bioturbation, and its influence on mercury fate and transport, sample mesocosms, containing *T. tubifex*, were compared to control mesocosms which were devoid of any external organism additions. When applicable, temporal changes within the sample mesocosms were also compared to determine the direct variability attributed to bioturbation. To provide an understanding of the impact of bioturbation, sediment reduction and complexation are considered. These are also evaluated for their influence on mercury bioavailability.

4.3.1 Zone of Oxygen Depletion

A means to gauge microbial activity and subsequent reduction is to determine the zone of oxygen depletion within the sediment depth profile. A more active microbial community will deplete oxygen quickly, and the community will become comprised of anaerobes including species capable of methylating mercury. By using voltammetric microelectrodes, this approximate zone of oxygen depletion and rate of depletion over vertical depth can be observed. This provides a means to compare any changes in the mesocosm reduction from the point of *T. tubifex* introduction to approximately 28-days of *T. tubifex* bioturbation.⁴ To assess oxygen depletion, the three depositional environments are considered from the first sampling event. These include one control and at least one sample containing *T. tubifex* from each environment. Only one sampling

⁴ The voltammetry employed was approximated to Day 0 of *T. tubifex* introduction and Day 28. However, the range of voltammetry sampling was +/-4 days from these dates.

event was considered within this analysis to minimize any variability in electrode sensitivity.

The mid-channel deposit can first be considered for oxygen depletion in Control 1 and Sample 1 as seen in Figure 4.22. In both mesocosms, the rate (or slope) of oxygen diffusion is consistent between the approximated Day 0 and Day 28. In addition, the shape of the curves between the control and sample are very similar, independent of the relative oxygen concentrations at each depth. This suggests that oxygen depletion does not vary between the control and sample mesocosm, and thus for the mid-channel deposit, bioturbation has little impact on oxygen depletion and thus sediment reduction.

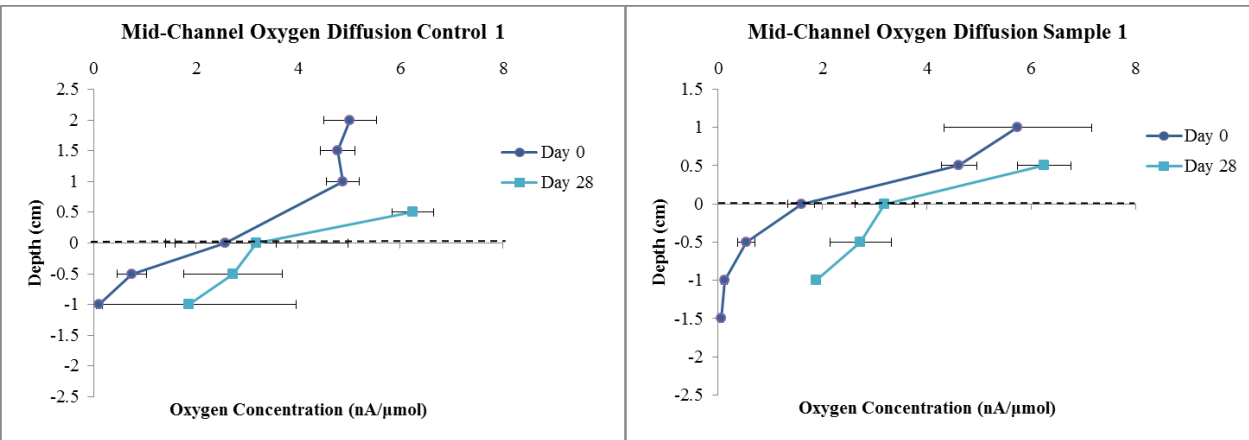


Figure 4.22: Oxygen depletion in Mid-Channel Control 1 and Sample 1 at approximate Day 0 of organism introduction and approximate Day 28 of bioturbation

For the near-bank deposit, on the other hand, there is a greater variation between Control 1 with Sample 1 and 2 as seen in Figure 4.23. From Control 1, it can be seen that the slopes, or rate of diffusion between approximate Day 0 and Day 28 are similar. This

suggests that similar oxygen depletion was occurring independent of time. However, for Sample 1 and 2, there are greater rates of oxygen depletion at Day 28. This suggests that bioturbation is causing similar or greater microbial reduction within the near-bank sediment.

It can be noted for Sample 2, that the diffusion of oxygen is lower at Day 28 than at Day 0. However, due to bulging of sediment within both Sample 1 and Sample 2, this caused the sediment-water interface to rise within the mesocosm and eliminated approximately a half a centimeter of overlying water, thus facilitating oxygen diffusion within the mesocosm. This may have allowed the oxygen to be present at a half a centimeter deeper; however, once again by considering the slope of oxygen depletion, it is seen that depletion is occurring similarly to or more rapidly in mesocosms containing *T. tubifex*.

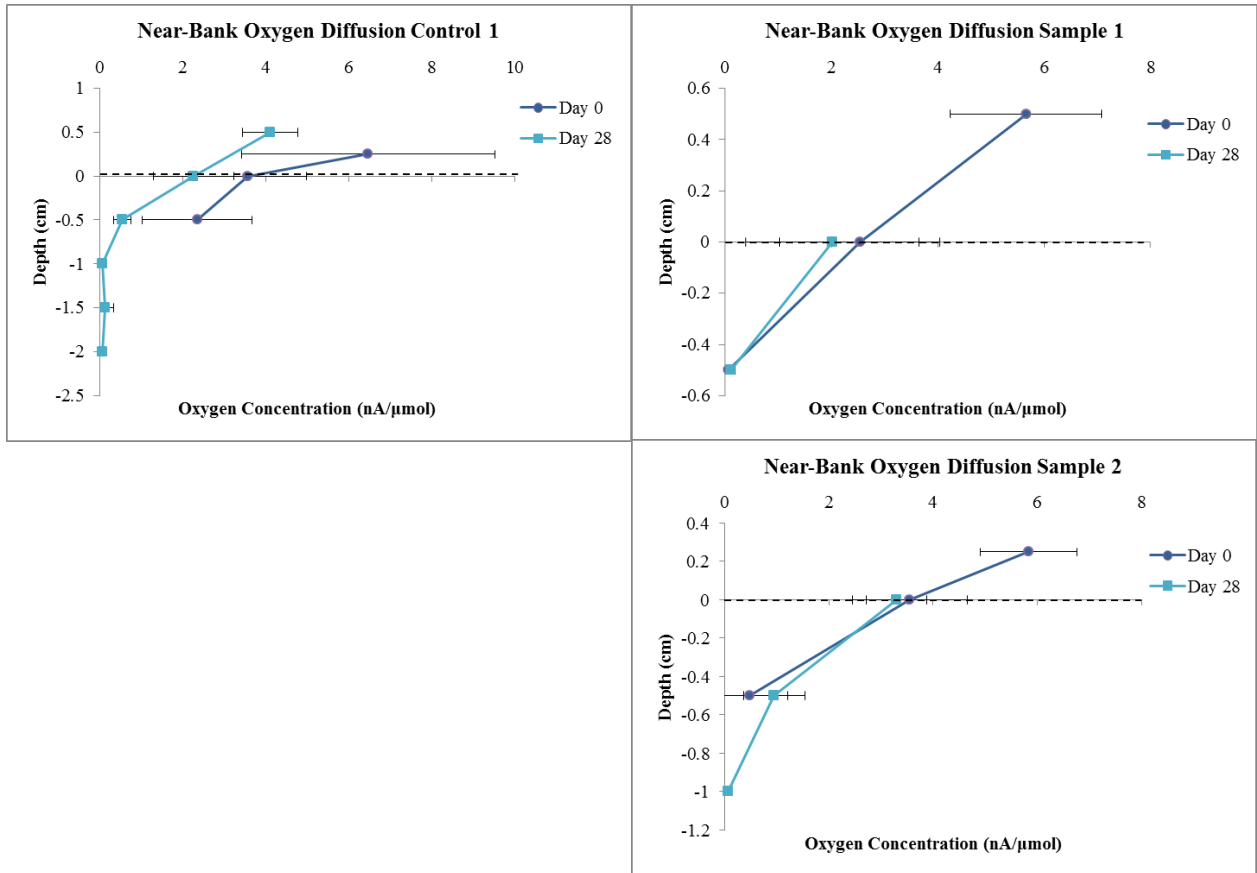


Figure 4.23: Oxygen depletion in Near-Bank Control 1 and Sample 1 and Sample 2 at approximate Day 0 of organism introduction and approximate Day 28 of bioturbation

Finally, the bank deposit can be considered as seen in Figure 4.24. Within the control it can be seen that oxygen appears to be consumed less rapidly after 28 days relative to Day 0. However, for Sample 1, oxygen is depleted within the first centimeter. Therefore, as the bioturbated sample is different from the control, it can be seen that bioturbation within the sample is causing a greater oxygen depletion in the bank deposit.

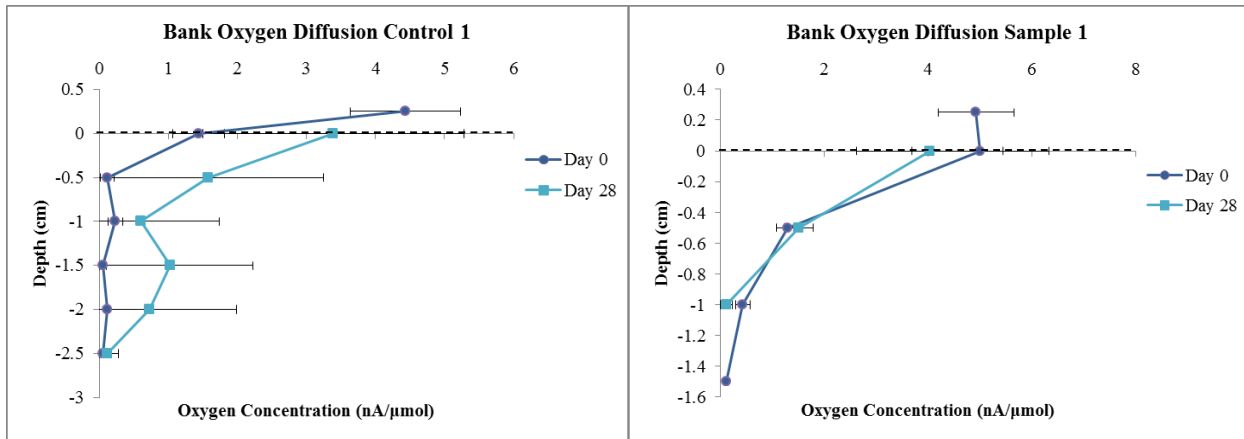


Figure 4.24: Oxygen depletion in Bank Control 1 and Sample 1 at approximate Day 0 of organism introduction and approximate Day 28 of bioturbation

Oxygen appears to deplete more rapidly in the near-bank and bank bioturbated samples relative to the controls and initial conditions (exposure Day 0). This suggests that in the near-bank and bank samples, bioturbation is increasing microbial activity and initial reduction. This is logical as previous studies have demonstrated that bioturbation, through the facilitation of inconsistent oxygen flux and the diffusion of solutes, increases the oxidation of organic matter and thus promotes microbial activity (Kristensen & Holmer, 2001; Navel et al., 2012).

On the other hand, bioturbation appears to have little impact on the mid-channel deposits. This is likely due to the particle distribution within the sediment. The mid-channel deposit has coarser sediment and lower productivity allowing for deeper oxygen diffusion than the other depositional environments. Because of this, it is possible that the *T. tubifex* have a smaller impact as the zone of bioturbation is more comparable to the

inherent zone of oxygen diffusion. This is similarly seen in previous analysis of *T. tubifex*, which demonstrate that the organism has a lower geochemical impact on coarse sediment (Navel et al., 2012). Overall, however, the oxygen depletion data is limited to a 0.5 cm a sampling interval which prevents a comprehensive analysis within the small zone of oxygen diffusion. Therefore, from this data it is not conclusive that bioturbation is stimulating microbial activity and other factors must be assessed.

4.3.2 Impact on Metal Biogeochemistry

To assess the impact that the organisms have on the geochemistry of metals, the proxy indicators of reduction and complexation, acid volatile sulfides and ferrous iron, were analyzed. These samples are indicative of the mesocosm conditions due to 28-days of bioturbation. Dissolved metals within the redox profiles were also analyzed to compare any shifts in the profile over the 28-day period. The depth profile of the average acid volatile sulfide concentrations of the bioturbated samples and the controls of the depositional environments can be seen in Figure 4.25. It can be noted that for both the mid-channel and bank deposit, acid volatile samples are lower in bioturbated samples relative to those of the control. The near-bank deposit, on the other hand, has elevated averaged acid volatile sulfide concentrations in the bioturbated samples relative to the control. Acid volatile sulfides are indicative of the reduction occurring. Within greater reducing conditions, there is a greater availability of sulfides and more potential for complexation with acid volatile sulfides (Chapman, Wang, Janssen, Persoone, & Allen, 1998). Therefore, it is expected from analysis of only acid volatile sulfides that reduction

is decreasing in the mid-channel and bank deposits, whereas it is potentially increasing in the near-bank deposit. However, as mentioned previously, the concentrations of acid volatile sulfides are relatively low within the South River mesocosms relative to other sediment deposits, and therefore any trends are not solely conclusive.

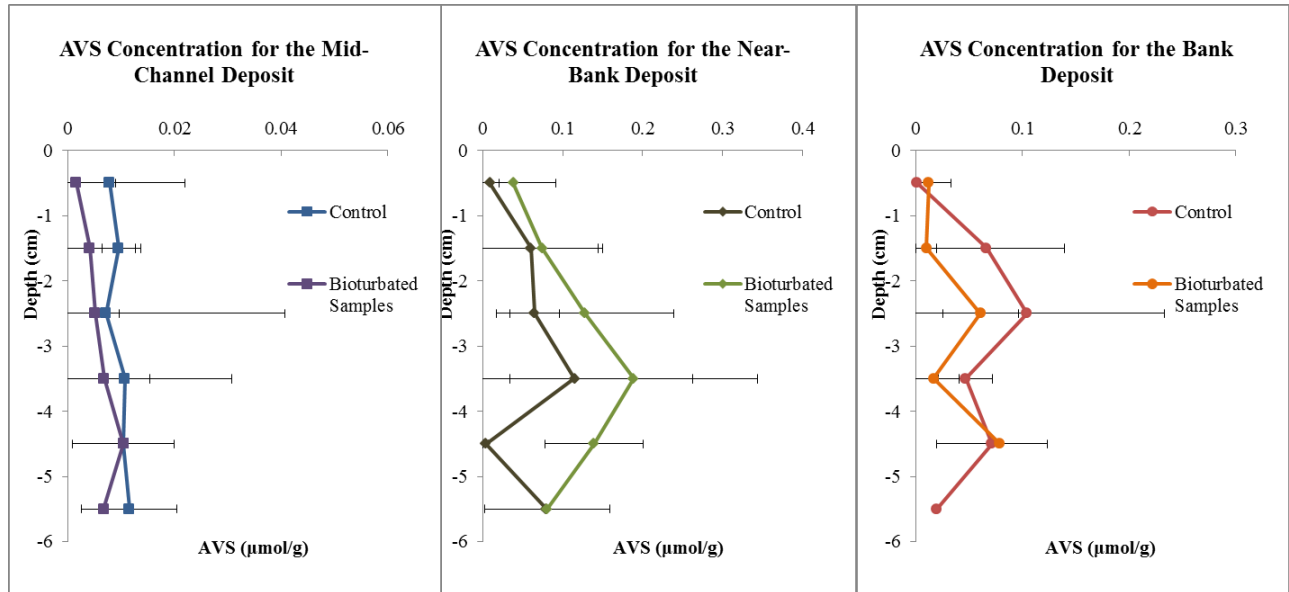


Figure 4.25: Averaged AVS concentrations per depth for comparison of control and bioturbated samples per depositional environment

To strengthen the analysis of reduction occurring, an additional proxy, extractable ferrous iron, can be evaluated as seen in Figure 4.26. Within this figure, the averaged depth profiles are compared between the bioturbated samples and the controls of each sediment deposit. From this, it can generally be seen that the ferrous iron concentrations in the bioturbated samples are less than or comparable to those within the controls, with only Bank Sample 3 serving as an outlier. Due to its variation from the other samples,

Bank Sample 3 is presented separately in Figure 4.26. This consistency suggests that less reduction is occurring throughout all three depositional environments in the bioturbated sediments as opposed to the controls. This supports the observations of acid volatile sulfides in the mid-channel and bank deposits while contradicting that of the near-bank deposit. Therefore, a deeper analysis is required to conclusively understand the impact of bioturbation by the *T. tubifex* on the reducing condition of the mesocosms.

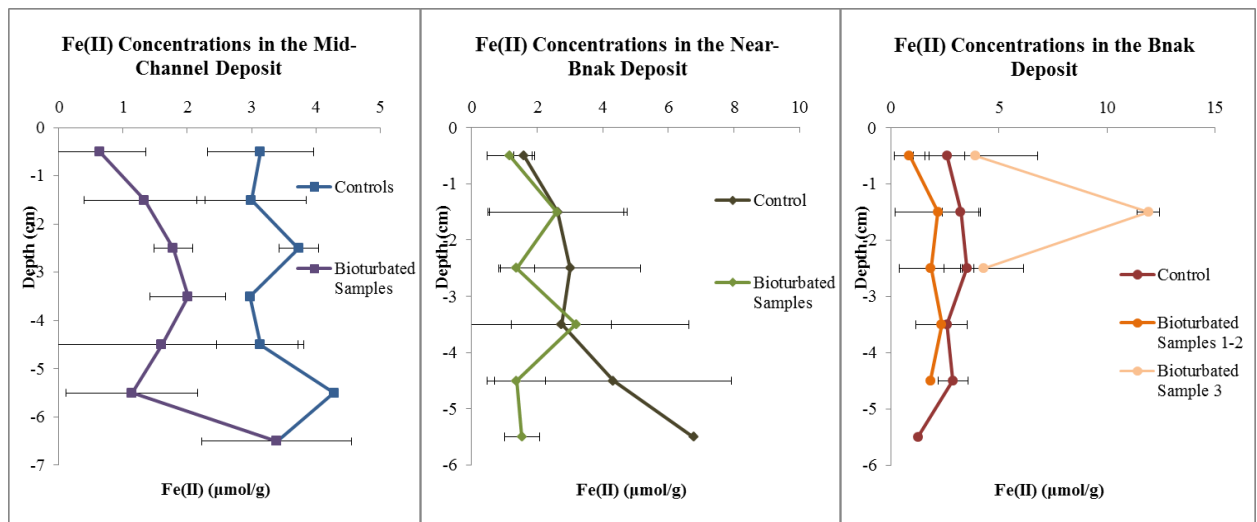


Figure 4.26: Averaged ferrous iron concentrations per depth for comparison of control and bioturbated samples per depositional environment

This analysis was completed through comparison of the voltammetric redox profiles of the depositional environments between approximated Day 0 of organism addition, and approximated Day 28 of bioturbation. These profiles can be seen in Figures 4.27-4.30 for the bank, near-bank, and mid-channel deposits respectively.

It can be seen that for the bank deposit, in Bank Sample 1 of Figure 4.27, that there is an upward shift in the reduction of manganese (Mn^{2+}), which includes the presence of manganese within the overlying water column. However, at the same time, the presence of hydrogen sulfide (HS^-) is not detected at Day 28. This follows with the trends of both the more rapid oxygen depletion and the decrease in reduction from the extracted solids relative to the control. If the microbial community is stimulated and more productive, due to bioturbation, this will cause the zone of reduction to shift upward, as seen in the trends of dissolved manganese. However, if the mesocosm is overall less reduced, this will alter the presence and zones of more reduced metals including hydrogen sulfide. Therefore, this suggests that while reduction is occurring more rapidly, the overall reduction is decreased, and the zones of mercury relevant reduction (sulfate and iron reduction) are shifted downward. The presence of manganese within the overlying water column is surprising and reduction is likely mainly occurring within the sediment environment. However, bioturbation has been demonstrated to increase the diffusion of mobile solutes across the sediment-water interface (Gribsholt & Kristensen, 2002). Therefore, this suggests that solute flux, specifically of reduced manganese, may be occurring within the bank mesocosm in addition to increased reduction at the sediment-water interface.

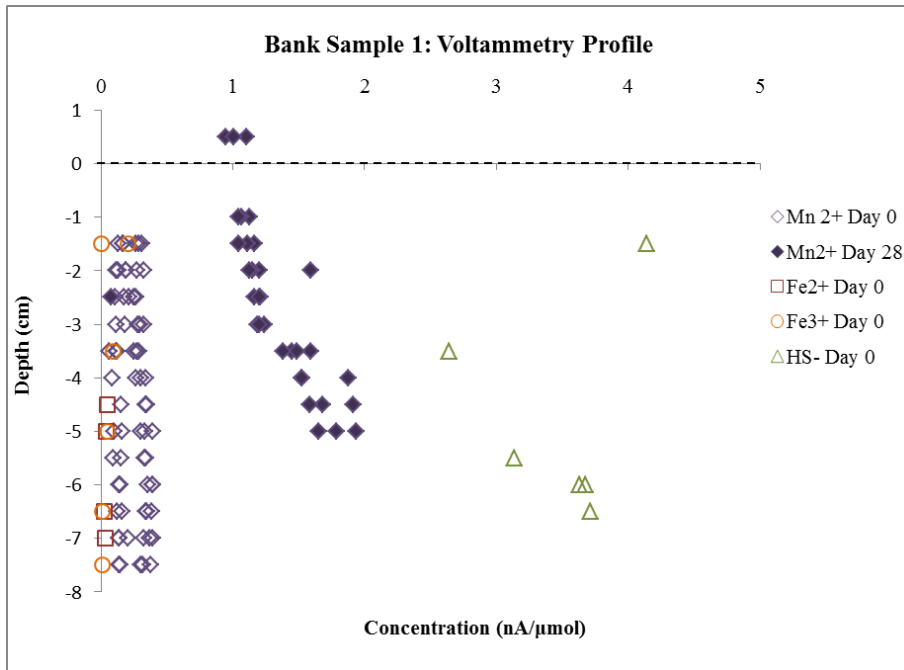


Figure 4.27: Reducing profile of dissolved metals for Bank Sample 1 at approximated Day 0 of organism introduction and approximated Day 28 of bioturbation

The shift in reducing zones can similarly be seen in the Near-Bank Sample 1 and 2 reducing profiles in Figure 4.28 and Figure 4.29, respectively. Within the Near-Bank Sample 1, similar to Bank Sample 1, after bioturbation, the zone of manganese reduction is shifted upward, whereas the presence of dissolved hydrogen sulfide is not detected at 28 days. For Near-Bank Sample 2, the presence of hydrogen sulfide is detected after bioturbation, however its zone of existence is shifted downward from its location at Day 0. For both mesocosms, the shift in reducing conditions supports the observation of extracted ferrous iron, which suggests that less reduction is occurring in the bioturbated

samples within the upper sediment depths. However, the zone of reduction is generally shifting upward with manganese similarly supports the trends seen in oxygen depletion.

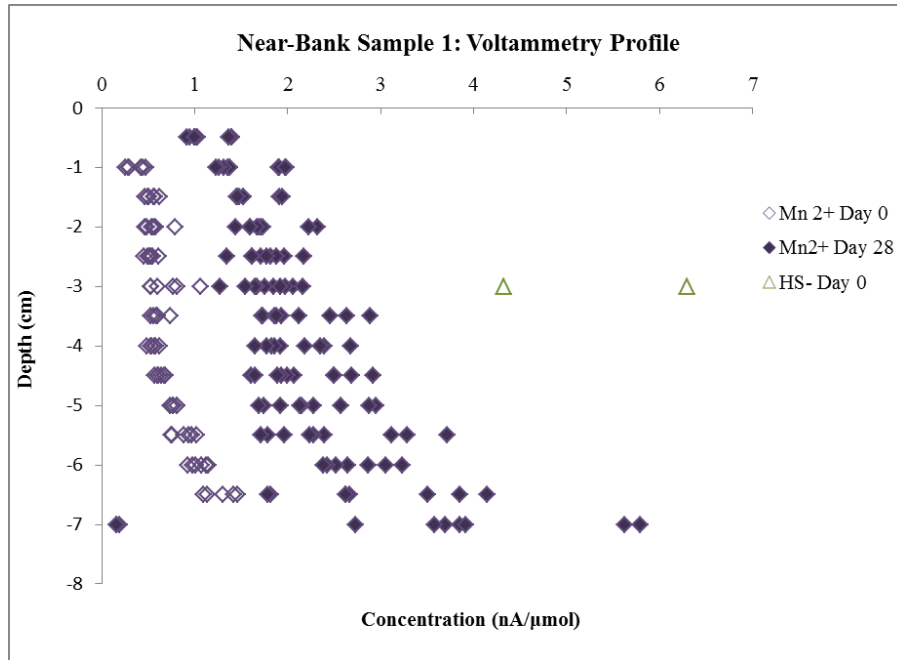


Figure 4.28: Reducing profile of dissolved metals for Near-Bank Sample 1 at approximated Day 0 of organism introduction and approximated Day 28 of bioturbation

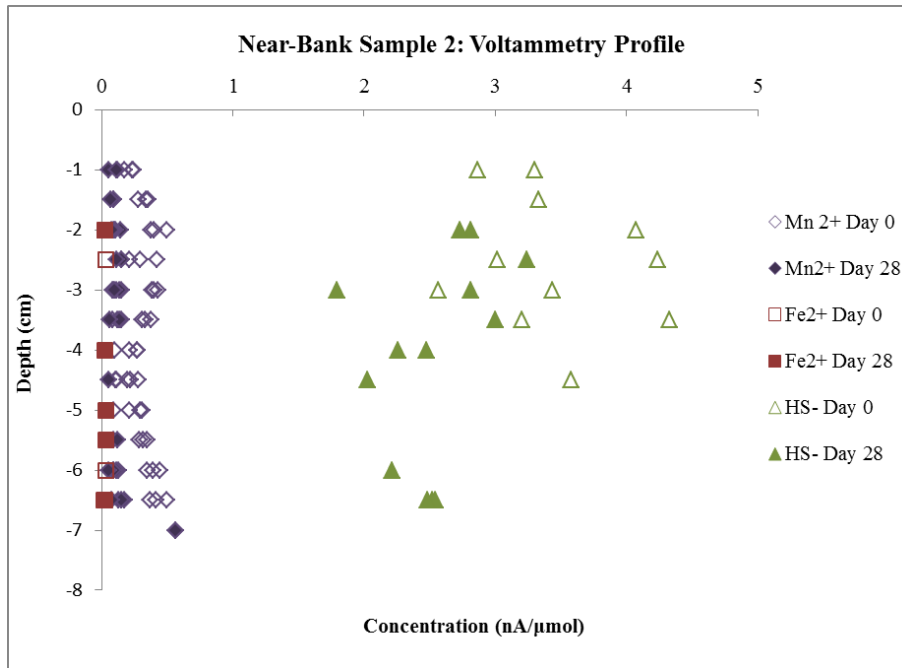


Figure 4.29: Reducing profile of dissolved metals for Near-Bank Sample 2 at approximated Day 0 of organism introduction and approximated Day 28 of bioturbation

Finally, the redox profile of the mid-channel deposit can be evaluated as seen in Figure 4.30. It can be seen that within the mid-channel deposit, there similarly is a shift in the presence of hydrogen sulfide and subsequent sulfate reduction; however there is no substantial change in the reduction of manganese. Therefore, for the mid-channel bank deposit, the similar decrease in reduction is visible, however the alteration of reduction in the most surficial sediment is constant, as seen similar to the oxygen depletion, for the mid-channel deposit does not appear to have a large change within the ambient zone of oxygen diffusion.

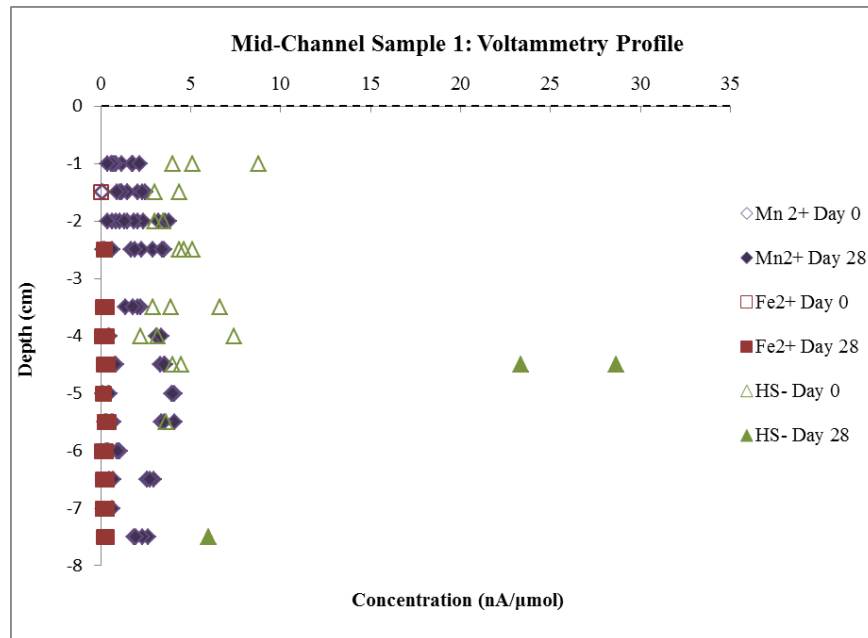


Figure 4.30: Reducing profile of dissolved metals for Mid-Channel Sample 1 at approximated Day 0 of organism introduction and approximated Day 28 of bioturbation

Therefore, the bank and near-bank deposits have a more productive microbial community due to bioturbation, but overall have less reduction and a downward shift in the zones of relevant reduction for mercury methylation. This can logically be facilitated by bioturbation, as the oxygen diffusion will help to stimulate microbial activity and thus allow for more rapid reduction in zones of facultative anaerobes which can exist in the occasional presence of oxygen (including manganese and iron reducing guilds). However, microbial communities which are strictly anaerobic (sulfate reducers), and thus cannot survive the presence of oxygen, would need to shift their existence beyond the bioturbation zone of influence with oxygen diffusion. Therefore, for the bank and near-

bank sediment, while bioturbation is increasing microbial productivity in the surficial layers, the introduction of oxygen facilitated by bioturbation to lower depths is causing an overall lower reduction and shift in the location of sulfate reduction. The mid-channel deposit is similarly influenced by oxygen diffusion in overall reduction and zonation of sulfate reduction; however, at the upper surficial depths, the role of bioturbation has little impact on productivity as attributed to the ambient oxygen diffusion linked to the particle composition within the deposit.

4.3.3 Impact on Porewater Methylmercury

Sediment complexation, reduction, and solute diffusivity are most likely to impact concentrations of mercury within porewater. Specifically, due to the direct relationship with reduction, methylmercury in porewater is most likely to be impacted by these influences of bioturbation. It is important to understand this interaction because methylmercury is also tied to the greatest risk within sediment matrices and therefore its fate and transport must be understood. The average methylmercury concentrations in porewater can be seen at each depth by comparing the bioturbated sample mesocosms with the controls in Figure 4.31. For both the near-bank and bank deposits, methylmercury is lower in the porewater of the bioturbated samples within the 0-4 cm zone of bioturbation. However, this relationship dissipates past the bioturbated region. The mid-channel deposit, on the other hand, does not have a similar relationship between the control and the bioturbated samples, as often, the methylmercury concentration is higher in the bioturbated samples.

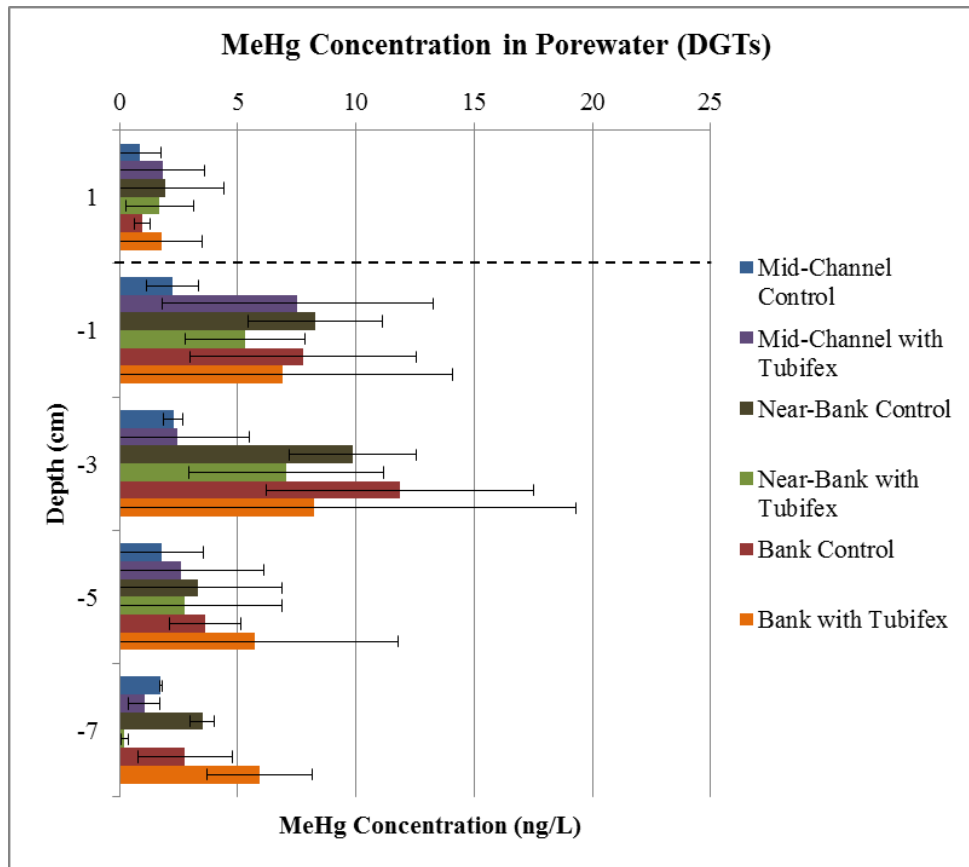


Figure 4.31: Average methylmercury concentrations in porewater at each depth for bioturbated samples and controls

From this relationship, there is clearly a link with bioturbation in the near-bank and bank deposits and methylmercury in porewater. This can be explained by several factors. In *Section 4.3.2*, the oxygen diffusion attributed to bioturbation causes lower reduction to occur within sediment, and also shifts downward the zone of sulfate reduction and often iron reduction. This subsequently shifts the zone of methylation downward, and therefore would limit methylmercury production within the upper centimeters of sediment. It is also possible that solute transfer between the sediment-

water interface is additionally impacting methylmercury, by allowing for a greater diffusion of this mercury species into the overlying water body. If this is the case, this will have significant implications for mercury fate and transport and will require further research.

The mid-channel deposit, however, does not experience this decrease in methylation. Although the zone of reduction shifted for sulfate reduction, it is possible that the lack of stimulation of microbial activity prevented any drastic change in the porewater methylation profile of the mid-channel deposit. It is also possible that the low ambient acid volatile sulfide and ferrous iron concentrations did not significantly complex with the total mercury within this deposit, and thus did not prevent methylation of mercury within the porewater. Finally, iron reduction can occur within suboxic sediment, and thus methylation within this depositional environment may be dominated by iron reducing bacteria. However, although the understanding of methylation in the mid-deposit is not entirely clear, it can be concluded that bioturbation has a direct impact on the presence methylmercury in the near-bank and bank deposits, while it has little influence on methylation of mercury within the mid-channel deposit.

Chapter 5: Conclusions

5.1 CONCLUSIONS

Mercury is a widely distributed and challenging environmental contaminant due to its complex interactions within aquatic and sediment matrices and its capacity to bioaccumulate. In order to address fate and transport of mercury, and assess risk of mercury through biomagnification, it is necessary to understand the interaction that mercury has with the benthic oligochaetes, *T. tubifex*. Through understanding the bioaccumulation occurring, it is possible to determine the capacity of passive DGT sampling of porewater and bulk solid samplings to predict bioavailability of mercury to macroorganisms. While simultaneously studying sediment biogeochemistry, it is also possible to understand the impact that the organisms have on mercury speciation.

For total mercury bioaccumulation, it can be concluded that DGTs show promise as a beneficial sampling technique employed to measure total mercury concentrations in porewater. Within depositional environments and across depositional environments, DGTs perform similarly to traditional bulk solid sampling of total mercury, given the variability within the systems, and thus can be applied to understand bioaccumulation of total mercury in benthic oligochaetes of freshwater systems. Bulk solid concentrations also serve as a good predictor of bioaccumulation of total mercury in *T. tubifex* within the South River sediment matrix.

Despite variability and low relative methylmercury concentrations, DGT measured total mercury in porewater is also capable of predicting methylmercury bioaccumulation in a variable depositional environment. However, this technique is less consistent when applied within a singular depositional environment. Within the South River sediment matrix, bulk solid measured total mercury is also a feasible means to predict bioaccumulation of methylmercury. Although this result was not expected, it is likely linked to biogeochemistry of the sediment which does not prevent bioavailability of mercury for methylation.

Through comparison of DGT measured total mercury and bulk solid methylmercury, it can be seen that DGTs are a good estimator of the bioavailable fractions of mercury which are capable of being methylated. For this reason, DGTs are representative of methylation potential and thus can be utilized when methylmercury cannot be directly sampled. However, it is notable that mercury available to microbes does not directly correlate to mercury available for bioaccumulation in benthic oligochaetes, and thus the DGT measured total mercury correlates to bioaccumulation with some variability.

Although organic matter is likely a factor in mercury bioaccumulation, it is difficult to measure in environments of which only a fraction of particles are available for consumption. In sediment matrices where organic carbon has a greater influence, this will diminish the capacity of bulk solids to predict bioaccumulation. Therefore, the use of

bulk solids as a bioaccumulative indicator is dependent on the sediment matrix. However, conceptually, the role of organic matter should not detract from the utilization of DGTs.

Bioturbation of organisms on sediment can have important implications for mercury fate and transport. Within sediments of little initial oxygen diffusion, bioturbation can increase transfer of oxygen and solutes across the sediment water interface ultimately leading to greater microbial productivity and lower overall reducing conditions. This in turn, can cause mercury complexes to occur and decrease overall toxicity, or can allow for mercury to flux into the overlying water further distributing risk of exposure. As this can have direct implications for remediative strategies, it should be assessed further.

5.2 RECOMMENDATIONS FOR FUTURE WORK

For a greater understanding of DGT application in prediction of bioaccumulation, it would be beneficial to repeat the experiment utilizing a test organism which is more likely to bioaccumulate methylmercury relative to total mercury. This will allow for clearer correlations to be made with methylmercury bioaccumulation, and thus can be applied for prediction of methylmercury bioaccumulation in higher trophic levels. It would also be beneficial to apply DGTs in a different freshwater sediment matrix. As geochemistry can influence mercury bioavailability for methylation, a sediment matrix which has higher capacity for complexation and immobilization onto solids should be used. This will further assess if bulk solids are good indicators of total mercury and

methylmercury bioaccumulation, or if this correlation was specific to the South River sediment matrix due to the low reduction occurring.

Finally, the research of bioturbation's impact on mercury fate and transport can be further expanded to encompass the governing factors in lowering methylmercury in porewater. It would be beneficial to more continually sample if there is a flux of mercury into the overlying water column in order to determine if additional considerations need to be taken for bioturbators when designing remedial strategies.

Appendix

APPENDIX A.

Concentration and salts used for artificial pond water:

0.5 mM NaCl

0.2 mM NaHCO₃

0.5 mM KCl

0.4 mM CaCl₂

References

- American Society for Testing and Materials International. (2010). *Standard Guide for Determination of the Bioaccumulation of Sediment- Associated Contaminants by Benthic Invertebrates*. West Conshohocken, PA. doi:10.1520/E1688-10.and
- Amirbahman, A., Massey, D. I., Lotufo, G., Steenhaut, N., Brown, L. E., Biedenbach, J. M., & Magar, V. S. (2013). Assessment of mercury bioavailability to benthic macroinvertebrates using diffusive gradients in thin films (DGT). *Environmental Science Processes & Impacts*, 15(11), 2104–14. doi:10.1039/c3em00355h
- Binnerup, S. J., Jensen, K., Revsbech, N. P., Jensen, M. H., & Sørensen, J. (1992). Denitrification, Dissimilatory Reduction of Nitrate to Ammonium, and Nitrification in a Bioturbated Estuarine Sediment as Measured with N and Microsensor Techniques. *Applied and Environmental Microbiology*, 58(1), 303–313.
- Bligh, E. G., & Dyer, W. J. (1959). A Rapid Method of Total Lipid Extraction and Purification. *Canadian Journal of Biochemistry and Physiology*, 37(8), 911–917.
- Bloom, N. S., Preus, E., Katon, J., & Hiltner, M. (2003). Selective extractions to assess the biogeochemically relevant fractionation of inorganic mercury in sediments and soils. *Analytica Chimica Acta*, 479, 233–248. doi:10.1016/S0003-2670(02)01550-7
- Bouché, M. L., Habets, F., Biagianti-Risbourg, S., & Vernet, G. (2000). Toxic Effects and Bioaccumulation of Cadmium in the Aquatic Oligochaete Tubifex tubifex. *Ecotoxicology and Environmental Safety*, 46, 246–251. doi:10.1006/eesa.2000.1919
- Brendel, P. J., & Luther, G. W. (1995). Development of a Gold Amalgam Voltammetric Microelectrode for the Determination of Dissolved Fe, Mn, O₂, and S(-II) in Porewaters of Marine and Freshwater Sediments. *Environmental Science & Technology*, 29(3), 751–61. Retrieved from <http://www.ncbi.nlm.nih.gov/pubmed/22200285>
- Bystrom, E. (2008). *Assessment of Mercury Methylation and Demethylation with Focus on Chemical Speciation and Biological Processes*. Georgia Institute of Technology.
- Cammen, L. M. (1980). Ingestion rate: An empirical model for aquatic deposit feeders and detritivores. *Oecologia*, 44(3), 303–310.
- Chapman, P. M., Wang, F., Janssen, C., Persoone, G., & Allen, H. E. (1998). Ecotoxicology of metals in aquatic sediments: binding and release , bioavailability ,

- risk assessment , and remediation. *Canadian Journal of Fisheries and Aquatic Sciences*, 55(10), 2221–2243. doi:10.1139/f98-145
- Chemaly, S. M. (2002). The link between vitamin B12 and methylmercury : a review. *South African Journal of Science*, 98(December), 568–572.
- Chen, C. Y., Dionne, M., Mayes, B. M., Ward, D. M., Sturup, S., & Jackson, B. P. (2009). Mercury Bioavailability and Bioaccumulation in Estuarine Food Webs in the Gulf of Maine. *Environmental Science & Technology*, 43(6), 1804–1810.
- Chess, T. (2010). *Laboratory Optimization and Field Demonstration of Diffusive Gradient in Thin Films for In-Situ Mercury Measurements of River Sediments*. The University of Texas at Austin.
- Choi, S., Chase, T., & Bartha, R. (1994). Metabolic Pathways Leading to Mercury Methylation in *Desulfovibrio desulfuricans* LS. *Applied and Environmental Microbiology*, 60(11), 4072–4077.
- Clarisse, O., & Hintlemann, H. (2006). Measurements of dissolved methylmercury in natural waters using diffusive gradients in thin film (DGT). *Journal of Environmental Monitoring*, 8, 1242–1247. doi:10.1039/B614560D
- Clarisse, O., Lotufo, G., Hintelmann, H., & Best, E. P. H. (2012). Biomonitoring and assessment of monomethylmercury exposure in aqueous systems using the DGT technique. *Science of the Total Environment*, 416, 449–454.
- Dallinger, R., Prosi, F., Segner, H., & Back, H. (1987). Contaminated Food and Uptake of Heavy Metals by Fish: a Review and a Proposal for Further Research. *Oecologia*, 73(1), 91–98.
- De Jonge, M., Dreesen, F., De Paepe, J., Blust, R., & Bervoets, L. (2009). Do Acid Volatile Sulfides (AVS) Influence the Accumulation of Sediment-Bound Metals to Benthic Invertebrates under Natural Field Conditions? *Environmental Science & Technology*, 43(12), 4510–4516.
- DeWild, J. F., Olund, S. D., Olson, M. L., & Tate, M. T. (2004). Method for the Preparation and Analysis of Solids and Suspended Solids for Methylmercury.
- Divis, P., Skandera, R., Brulik, L., Docekalova, H., Matus, P., & Bujdos, M. (2009). Application of new resin gels for measuring mercury by diffusive gradients in a thin-films technique. *Analytical Sciences*, 25, 575–578.

- Ekstrom, E. B., Morel, F. M. M., & Benoit, J. M. (2003). Mercury Methylation Independent of the Acetyl-Coenzyme A Pathway in Sulfate-Reducing Bacteria. *Applied and Environmental Microbiology*, *69*(9), 5414–5422. doi:10.1128/AEM.69.9.5414-
- Environment Canada. (2013). *Mercury in the Food Chain* (pp. 4–6).
- Gao, S., Davis, U. C., & Tanji, K. K. (2003). Incorporating Straw May Induce Sulfide Toxicity in Paddy Rice. *California Agriculture*, *57*(2), 55–59. doi:10.3733/ca.v057n02p55.
- Gilmour, C. C., Podar, M., Bullock, A. L., Graham, A. M., Brown, S. D., Somenahally, A. C., ... Elias, D. a. (2013). Mercury Methylation by Novel Microorganisms from New Environments. *Environmental Science & Technology*, *47*, 11810–20. Retrieved from <http://www.ncbi.nlm.nih.gov/pubmed/24024607>
- Gribsholt, B., & Kristensen, E. (2002). Effects of bioturbation and plant roots on salt marsh biogeochemistry: a mesocosm study. *Marine Ecology Progress Series*, *241*(2002), 71–87.
- Guthrie, R. K., Davis, E. M., Cherry, D. S., & Murray, H. E. (1979). Biomagnification of Heavy Metals by Organisms in a Marine Microcosm. *Bulletin of Environmental Contamination and Toxicology*, *21*, 53–61.
- Herbes, S. E., & Allen, C. P. (1983). Lipid Quantification of Freshwater Invertebrates: Method Modification for Microquantitation. *Canadian Journal of Fisheries and Aquatic Sciences*, *40*(8), 1315–1317.
- Hintelmann, H., & Nguyen, H. T. (2005). Extraction of methylmercury from tissue and plant samples by acid leaching. *Analytical and Bioanalytical Chemistry*, *381*, 360–365. doi:10.1007/s00216-004-2878-5
- Hsieh, Y., Chung, S., Tsau, Y., & Sue, C. (2002). Analysis of sulfides in the presence of ferric minerals by diffusion methods. *Chemical Geology*, *182*(2-4), 195–201.
- Hsu-Kim, H., Kucharzyk, K. H., Zhang, T., & Deshusses, M. a. (2013). Mechanisms Regulating Mercury Bioavailability for Methylating Microorganisms in the Aquatic Environment: A Critical Review. *Environmental Science & Technology*, *47*, 2441–56. Retrieved from <http://www.ncbi.nlm.nih.gov/pubmed/23384298>
- Jay, J. A., Murray, K. J., Gilmour, C. C., Mason, R. P., Morel, F. M. M., Roberts, a L., & Hemond, H. F. (2002). Mercury methylation by *Desulfovibrio desulfuricans* ND132

in the presence of polysulfides. *Applied and Environmental Microbiology*, 68(11), 5741–5745. doi:10.1128/AEM.68.11.5741-

Johnson, N. W. (2009). *Mercury Methylation Beneath an In-Situ Sediment Cap*. The University of Texas at Austin.

Kampalath, R. A., Lin, C.-C., & Jay, J. A. (2013). Influences of Zero-Valent Sulfur on Mercury Methylation in Bacterial Cocultures. *Water, Air, & Soil Pollution*, 224(1399), 1–14. doi:10.1007/s11270-012-1399-7

Kristensen, E., & Holmer, M. (2001). Decomposition of plant materials in marine sediment exposed to different electron accepters (O₂, NO₃⁻, and SO₄⁻), with emphasis on substrate origin, degradation kinetics, and the role of bioturbation. *Geochimica et Cosmochimica Acta*, 65(3), 419–433.

Lawrence, a. L., & Mason, R. P. (2001). Factors controlling the bioaccumulation of mercury and methylmercury by the estuarine amphipod *Leptocheirus plumulosus*. *Environmental Pollution*, 11(1), 217–231.

Liu, J., Feng, X., Qiu, G., Anderson, C. W. N., & Yao, H. (2012). Prediction of Methyl Mercury Uptake by Rice Plants (*Oryza sativa* L.) Using the Diffusive Gradient in Thin Films Technique. *Environmental Science & Technology*, 46(20), 11013–11020. doi:10.1021/es302187t

Mason, R., Bloom, N., Cappellino, S., Gill, G., Benoit, J., & Dobbs, C. (1998). Investigation of Porewater Sampling Methods for Mercury and Methylmercury. *Environmental Science & Technology*, 32(24), 4031–4040. doi:10.1021/es980377t

Mason, R. P., Laporte, J., & Andres, S. (2000). Factors Controlling the Bioaccumulation of Mercury, Methylmercury, Arsenic, Selenium, and Cadmium by Freshwater Invertebrates and Fish. *Archives of Environmental Contamination and Toxicology*, 38, 283–297. doi:10.1007/s002449910038

Morel, F. M. M., Kraepiel, A. M. L., Amyot, M., & Morel, F. M. M. (1998). The Chemical Cycle and Bioaccumulation of Mercury. *Annual Review of Ecology and Systematics*, 29, 543–566.

Navel, S., Mermillod-Blondin, F., Montuelle, B., Chauvet, E., & Marmonier, P. (2012). Sedimentary context controls the influence of ecosystem engineering by bioturbators on microbial processes in river sediments. *Oikos*, 121(7), 1134–1144. doi:10.1111/j.1600-0706.2011.19742.x

- Parkerton, T., Maruya, K., Lydy, M., Landrum, P., Peijnenburg, W., Mayer, P., ... Chapman, P. (2012). *Guidance on Passive Sampling Methods to Improve Management of Contaminated Sediments: Summary of a SETAC Technical Workshop Edited by Upal Ghosh* (pp. 1–20). Costa Mesa, California.
- Parks, J., Johs, A., Podar, M., Bridou, R., Hurt, R., Smith, S., ... Elias, D. (2013). The Genetic Basis for Bacterial Mercury Methylation. *Science*, 339(6125), 1332–1335. doi:10.1038/220173a0
- Pasteris, A., Vecchi, M., Reynoldson, T. B., & Bonomi, G. (2003). Toxicity of copper-spiked sediments to *Tubifex tubifex* (Oligochaeta, Tubificidae): A comparison of the 28-day reproductive bioassay with a 6-month cohort experiment. *Aquatic Toxicology*, 65(3), 253–265. doi:10.1016/S0166-445X(03)00136-X
- Patton, G. W., & Crecelius, E. A. (2001). *Simultaneously Extracted Metals / Acid-Volatile Sulfide and Total Metals in Surface Sediment from the Hanford Reach of the Columbia River and the Lower Snake River* (pp. 1–34). Richland, Washington.
- Peijnenburg, W. J., Teasdale, P. R., Reible, D., Mondon, J., Bennett, W. W., & Campbell, P. G. (2014). Passive sampling methods for contaminated sediments: State of the science for metals. *Integrated Environmental Assessment and Management*, 10(2), 179–96. doi:10.1002/ieam.1502
- Phillips, E. J. P., & Lovely, D. (1987). Determination of Fe(III) and Fe(II) in Oxalate Extracts of Sediment. *Soil Science Society of America Journal*, 51, 938–941.
- Pirrone, N., Cinnirella, S., Feng, X., Finkelman, R. B., Friedli, H. R., Leaner, J., ... Telmer, K. (2010). Global mercury emissions to the atmosphere from anthropogenic and natural sources. *Atmospheric Chemistry and Physics*, 10, 5951–5964. doi:10.5194/acp-10-5951-2010
- Rathore, R. S., & Khangarot, B. S. (2003). Effects of water hardness and metal concentration on a freshwater *Tubifex tubifex* Muller. *Water Air and Soil Pollution*, 142(1-4), 341–356. Retrieved from <Go to ISI>://000181303900021
- Redeker, E. S., Bervoets, L., & Blust, R. (2004). Dynamic Model for the Accumulation of Cadmium and Zinc from Water and Sediment by the Aquatic Oligochaete, *Tubifex tubifex*. *Environmental Science & Technology*, 38(23), 6193–6200. doi:10.1021/es0496470

- Rosenberg, R., Nilsson, H. C., & Diaz, R. J. (2001). Response of Benthic Fauna and Changing Sediment Redox Profiles over a Hypoxic Gradient. *Estuarine, Coastal and Shelf Science*, 53, 343–350. doi:10.1006/ecss.2001.0810
- Salonen, J. T., Seppanen, K., Nyyssonen, K., Korpela, H., Kauhanen, J., & Marjatta Kantola. (1995). Intake of mercury from fish, lipid peroxidation, and the risk of myocardial infarction and coronary, cardiovascular, and any death in eastern Finnish men. *Circulation*, 92(8), 2355–6. Retrieved from <http://www.ncbi.nlm.nih.gov/pubmed/7554224>
- Schaefer, J. K., Rocks, S. S., Zheng, W., Liang, L., Gu, B., & Morel, F. M. M. (2011). Active transport, substrate specificity, and methylation of Hg(II) in anaerobic bacteria. *Proceedings of the National Academy of Sciences of the United States of America*, 108(21), 8714–8719. doi:10.1073/pnas.1105781108
- Schartup, A. T., Mason, R. P., Balcom, P. H., Hollweg, T. a, & Chen, C. Y. (2013). Methylmercury Production in Estuarine Sediments: Role of Organic Matter. *Environmental Science & Technology*, 47, 695–700. Retrieved from <http://www.ncbi.nlm.nih.gov/pubmed/23194318>
- South River Science Team. (2014a). South River Conceptual Model. Unpublished Work.
- South River Science Team. (2014b). South River Science Team. *Historical Timeline*. Retrieved April 15, 2014, from <http://southriverscienceteam.org/>
- United Nations Environmental Programme. (2002). *Global Mercury Assessment. Mercury* (Vol. 3, pp. 1–16). United Nations Environment Programme. Retrieved from <http://www.chem.unep.ch/mercury/report/GMA-report-TOC.htm>
<http://www.chem.unep.ch/MERCURY/Report/revdraft-afterWG/assessment-report-4Oct02.pdf>
- United States Environmental Protection Agency. (2001a). *Appendix to Method 1631 Total Mercury in Tissue, Sludge, Sediment, and Soil by Acid Digestion and BrCl Oxidation* (pp. 1–13). Washington, DC.
- United States Environmental Protection Agency. (2001b). *Method 1630 Methyl Mercury in Water by Distillation, Aqueous Ethylation, Purge and Trap, and CVAFS*. Washington, DC.
- United States Environmental Protection Agency. (2002). *Method 1631, Revision E: Mercury in Water by Oxidation, Purge and Trap, and Cold Vapor Atomic Fluorescence Spectrometry* (pp. 1–38). Washington, DC.

- United States Food and Drug Administration. (2000). *Food Guidance for Industry: Action Levels for Poisonous or Deleterious Substances in Human Food and Animal Feed*. College Park, MD.
- Van De Bund, W., Goedkoop, W., & Johnson, R. (1994). Effects of deposit-feeder activity in bacterial production and abundance in profundal lake sediment. *Journal of the North American Benthological Society*, 13(4), 532–539.
- Vidal, D. E., & Horne, A. J. (2003). Inheritance of mercury tolerance in the aquatic oligochaete *Tubifex tubifex*. *Environmental Toxicology and Chemistry*, 22(9), 2130–2135.
- Watras, C. J., Back, R. C., Halvorsen, S., Hudson, R. J. M., Morrison, K. a., & Wente, S. P. (1998). Bioaccumulation of mercury in pelagic freshwater food webs. *Science of the Total Environment*, 219, 183–208.
- Watras, C. J., & Bloom, N. (1992). Mercury and methylmercury in individual zooplankton: Implications for bioaccumulation. *Limnology and Oceanography Journal*, 37(6), 1313–1318.
- Winfrey, M., & Rudd, J. W. M. (2009). Environmental factors affecting the formation of methylmercury in low pH lakes. *Environmental Toxicology and Chemistry*, 9(7), 853–869. doi:10.1002/etc.v9
- Zhang, H., & Davison, W. (1995). Performance Characteristics of Diffusion Gradients in Thin Films for the in Situ Measurement of Trace Metals in Aqueous Solution. *Analytical Chemistry*, 67(19), 3391–3400.
- Zhang, H., & Davison, W. (1999). Diffusional characteristics of hydrogels used in DGT and DET techniques. *Analytica Chimica Acta*, 398(2-3), 329–340.
- Žižek, S., Horvat, M., Gibičar, D., Fajon, V., & Toman, M. J. (2007). Bioaccumulation of mercury in benthic communities of a river ecosystem affected by mercury mining. *Science of the Total Environment*, 377, 407–415. doi:10.1016/j.scitotenv.2007.02.010